AD NUMBER

ADB267654

NEW LIMITATION CHANGE

TO

Approved for public release, distribution unlimited

FROM

Distribution authorized to U.S. Gov't. agencies only; Proprietary Information; Oct 2000. Other requests shall be referred to US Army Medical Research and Materiel Command, 504 Scott Street, Fort Detrick, MD 21702-5012

AUTHORITY

U.S. Army Medical Research and Materiel Command and Fort Detrick ltr., dtd October 17, 2001.

AD_____

Award Number: DAMD17-96-1-6323

TITLE: Role of the EGF-related Growth Factor *cripto* in Murine Mammary Tumorigenesis

PRINCIPAL INVESTIGATOR: Michael M. Shen, Ph.D.

CONTRACTING ORGANIZATION: University of Medicine and Dentistry of New Jersey
Robert Wood Johnson Medical School
Piscataway, New Jersey 08854

REPORT DATE: October 2000

TYPE OF REPORT: Final

PREPARED FOR: U.S. Army Medical Research and Materiel Command
Fort Detrick, Maryland 21702-5012

20010620 130

NOTICE

USING GOVERNMENT DRAWINGS, SPECIFICATIONS, OR OTHER DATA INCLUDED IN THIS DOCUMENT FOR ANY PURPOSE OTHER THAN GOVERNMENT PROCUREMENT DOES NOT IN ANY WAY OBLIGATE THE U.S. GOVERNMENT. THE FACT THAT THE GOVERNMENT FORMULATED OR SUPPLIED THE DRAWINGS, SPECIFICATIONS, OR OTHER DATA DOES NOT LICENSE THE HOLDER OR ANY OTHER PERSON OR CORPORATION; OR CONVEY ANY RIGHTS OR PERMISSION TO MANUFACTURE, USE, OR SELL ANY PATENTED INVENTION THAT MAY RELATE TO THEM.

LIMITED RIGHTS LEGEND

Award Number: DAMD17-96-1-6323
Organization: University of Medicine and Dentistry of New Jersey
            Robert Wood Johnson Medical School
Location of Limited Rights Data (Pages):

Those portions of the technical data contained in this report marked as limited rights data shall not, without the written permission of the above contractor, be (a) released or disclosed outside the government, (b) used by the Government for manufacture or, in the case of computer software documentation, for preparing the same or similar computer software, or (c) used by a party other than the Government, except that the Government may release or disclose technical data to persons outside the Government, or permit the use of technical data by such persons, if (i) such release, disclosure, or use is necessary for emergency repair or overhaul or (ii) is a release or disclosure of technical data (other than detailed manufacturing or process data) to, or use of such data by, a foreign government that is in the interest of the Government and is required for evaluational or informational purposes, provided in either case that such release, disclosure or use is made subject to a prohibition that the person to whom the data is released or disclosed may not further use, release or disclose such data, and the contractor or subcontractor or subcontractor asserting the restriction is notified of such release, disclosure or use. This legend, together with the indications of the portions of this data which are subject to such limitations, shall be included on any reproduction hereof which includes any part of the portions subject to such limitations.

THIS TECHNICAL REPORT HAS BEEN REVIEWED AND IS APPROVED FOR PUBLICATION.

REPORT DOCUMENTATION PAGE

Public reporting burden for this collection of information is estimated to average 1 hour per response, including the time for reviewing instructions, searching existing data sources, gathering and maintaining the data needed, and completing and reviewing this collection of information. Send comments regarding this burden estimate or any other aspect of this collection of information, including suggestions for reducing this burden to Washington Headquarters Services, Directorate for Information Operations and Reports, 1215 Jefferson Davis Highway, Suite 1204, Arlington, VA 22202-4302, and to the Office of Management and Budget, Paperwork Reduction Project (0704-0188), Washington, DC 20503

1. AGENCY USE ONLY (Leave blank)	2. REPORT DATE October 2000	3. REPORT TYPE AND DATES COVERED Final (23 Sep 96 - 22 Sep 00)

4. TITLE AND SUBTITLE

Role of the EGF-related Growth Factor *cripto* in Murine Mammary Tumorigenesis

5. FUNDING NUMBERS
DAMD17-96-1-6323

6. AUTHOR(S)
Michael M. Shen, Ph.D.

7. PERFORMING ORGANIZATION NAME(S) AND ADDRESS(ES)
University of Medicine and Dentistry of New Jersey
Robert Wood Johnson Medical School
Piscataway, New Jersey 08854

E-MAIL:
mshen@cabm.rutgers.edu

8. PERFORMING ORGANIZATION REPORT NUMBER

9. SPONSORING / MONITORING AGENCY NAME(S) AND ADDRESS(ES)

U.S. Army Medical Research and Materiel Command
Fort Detrick, Maryland 21702-5012

10. SPONSORING / MONITORING AGENCY REPORT NUMBER

11. SUPPLEMENTARY NOTES

Report contains color graphics.

12a. DISTRIBUTION / AVAILABILITY STATEMENT
Distribution authorized to U.S. Government agencies only (proprietary information, Oct 00 97). Other requests for this document shall be referred to U.S. Army Medical Research and Materiel Command, 504 Scott Street, Fort Detrick, Maryland 21702-5012.

12b. DISTRIBUTION CODE

13. ABSTRACT (Maximum 200 Words)

We have investigated the biological and biochemical functions of the *Cripto* gene, which encodes an extracellular protein that is a member of the *EGF-CFC* gene family, and which has been implicated in autocrine/paracrine signaling during human breast carcinogenesis. To elucidate the potential role of *Cripto* in mammary development and tumorigenesis, we have analyzed the *in vivo* activities of *Cripto* using transgenic mice that overexpress *Cripto* in the mammary gland, as well as the molecular mechanisms of CRIPTO protein function. In the past four years, we have generated molecular genetic and biochemical lines of evidence that *Cripto* acts as an essential co-factor for signaling by the divergent TGF-β factor *Nodal*. These findings provide a model for potential mechanisms of *Cripto* function through modulation of specific TGF-β-related signals in mammary development and tumorigenesis.

14. SUBJECT TERMS
(1) growth factor receptor, (2) mammary gland development, (3) transgenic mice, (4) in situ hybridization, (5) cell culture, (6) histochemical affinity reagent

15. NUMBER OF PAGES
43

16. PRICE CODE

17. SECURITY CLASSIFICATION OF REPORT Unclassified	18. SECURITY CLASSIFICATION OF THIS PAGE Unclassified	19. SECURITY CLASSIFICATION OF ABSTRACT Unclassified	20. LIMITATION OF ABSTRACT Unlimited

Table of Contents

Introduction:

Our work on breast development and tumorigenesis has focused on the *Cripto* gene, which encodes an extracellular protein that is a member of the *EGF-CFC* gene family. Previous studies have suggested that *Cripto* may be involved in autocrine or paracrine signaling during human breast carcinogenesis (reviewed in (Salomon et al., 1999)). Thus, *Cripto* is consistently overexpressed in a large percentage of human breast cancers, and is not expressed at high levels in normal breast tissue (Qi et al., 1994), and *Cripto* has transforming activity when overexpressed in NOG-8 mouse mammary epithelial cells (Ciardiello et al., 1991). To elucidate the potential role of *Cripto* in breast development and tumorigenesis, we have been investigating the activities of *Cripto* in mammary development using transgenic mice and cell culture systems, and have been investigating the molecular mechanisms of CRIPTO protein action, with the initial objective of identifying a putative CRIPTO receptor(s).

Body:

Over the past four years, we have made significant progress towards understanding the molecular mechanisms of *Cripto* function, which has led to an important revision of our initial view of *Cripto* encoding an EGF (epidermal growth factor)-related growth factor. Based on recent molecular genetic data from our lab and others, we now have strong evidence that *Cripto* is essential for signaling by a divergent member of the TGF-β (transforming growth factor-beta) superfamily, and may in fact encode a co-receptor rather than a ligand.

Review of recent work

To understand the biological and biochemical basis for *Cripto* function, we have been investigating its role in normal development. We initially identified the *EGF-CFC* family through studies of mesoderm formation during mouse gastrulation, in which we isolated a novel gene that we named *Cryptic* (Shen et al., 1997), based on its similarity to murine and human *Cripto* (Ciccodicola et al., 1989; Dono et al., 1993). Mammalian *Cryptic* and *Cripto,* frog *FRL-1,* and zebrafish *oep* encode proteins that share an N-terminal signal sequence, a variant EGF-like motif, a novel conserved cysteine-rich domain (that we named the CFC (*Cripto,* *Frl-1,* and *Cryptic*) motif), and a C-terminal hydrophobic region (reviewed in (Shen and Schier, 2000); see appendix). Members of the *EGF-CFC* family encode extracellular proteins that are localized to the surface of transfected cells (Shen et al., 1997; Zhang et al., 1998). This association is mediated by the C-terminal hydrophobic domain, which in the case of CRIPTO is required for glycosyl-phosphatidylinositol (GPI) linkage to the cell membrane (Minchiotti et al., 2000). Although the overall level of sequence conservation is relatively low (approximately 30% identity), all *EGF-CFC* family members appear to have functionally similar activities in assays for phenotypic rescue of *oep* mutant fish embryos by mRNA microinjection (Gritsman et al., 1999).

In our studies, we have gained essential insights into the biological functions and potential biochemical activities of EGF-CFC proteins through analysis of knock-out mice for *Cripto* and *Cryptic* (reviewed in (Shen and Schier, 2000); see appendix). We have found that the roles of *EGF-CFC* genes in axis formation are neatly divided in the mouse embryo, so that *Cripto* is required for correct orientation of the A-P (anterior-posterior) axis, while *Cryptic* is necessary for determination of the L-R (left-right) axis ((Ding et al., 1998; Yan et al., 1999); see appendices). These recent studies have led to a revised model for the biochemical activities of EGF-CFC proteins.

Thus, in contrast to previous models for CRIPTO having growth factor activity (Salomon et al., 1999), recent lines of evidence from molecular genetic studies indicate that EGF-CFC proteins

act as essential co-factors for a signaling factor known as NODAL (reviewed in (Schier and Shen, 2000); see appendix). The *Nodal* gene encodes a divergent member of the TGF-β superfamily, and displays a mutant phenotype similar to that for *Cripto* (Conlon et al., 1994; Zhou et al., 1993). The downstream signaling pathway for *Nodal* has primarily been suggested by our current understanding of TGF-β signal transduction pathways (Massague and Chen, 2000), and by gene targeting experiments in mice that have demonstrated similar and/or synergistic phenotypes for targeted disruption of *Nodal,* the type II activin receptor *ActRIIB,* the type I receptor *ActRIB,* and the cytoplasmic signal transducer *Smad2* (Collignon et al., 1996; Conlon et al., 1994; Gu et al., 1998; Nomura and Li, 1998; Oh and Li, 1997; Waldrip et al., 1998); however, there is no biochemical evidence at present that NODAL protein directly binds to and activates activin receptors.

Recent work has led to the proposal that NODAL and EGF-CFC proteins are inactive by themselves, while in combination their activity is similar to that of activin (Gritsman et al., 1999). Moreover, the phenotypes of both *Cripto* and *Cryptic* mutant mice can be readily interpreted as resulting from defects in *Nodal* signaling ((Ding et al., 1998; Yan et al., 1999); see appendices). These data can be summarized in terms of a possible regulatory pathway for *Nodal* and *EGF-CFC* activities (Fig. 1).
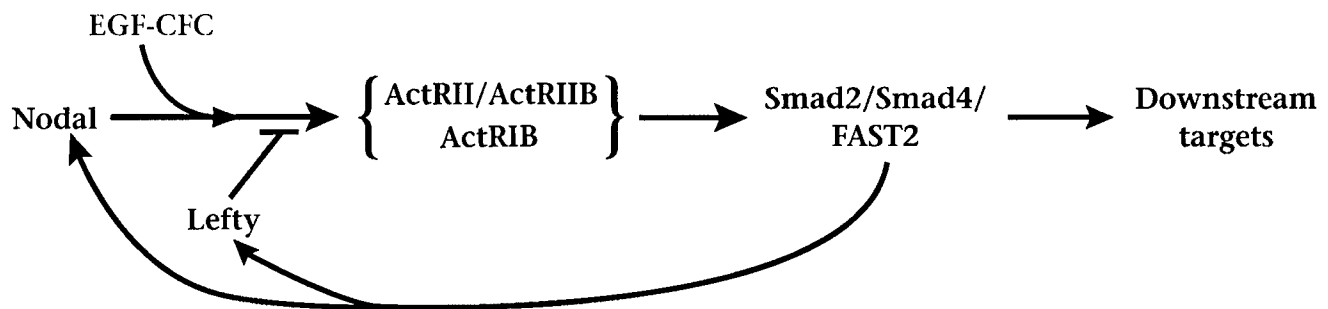

Figure 1. Model for EGF-CFC function in the Nodal signaling pathway. The activity of EGF-CFC proteins as essential co-factors for Nodal results in signaling through the Activin receptors ActRIIA/ActRIIB and ActRIB, leading to activation of Smad2 and subsequent effects on downstream target genes mediated by interaction with the transcription factor FAST2. FAST2 also activates autoregulatory loops that up-regulate Nodal itself as well as the competitive inhibitor Lefty, another member of the TGF-β family (Saijoh et al., 2000). It is important to note, however, that this pathway does not exclude the possibilities that EGF-CFC proteins could act as co-factors for other members of the TGF-β superfamily, or could also act through an unrelated signaling pathway.

These apparently discrepant findings can be resolved by a simple model in which EGF-CFC proteins form membrane-associated components of a receptor complex, and mediate *Nodal* signaling through signal-transducing partner(s) that may include activin receptors (Gritsman et al., 1999; Shen and Schier, 2000). Based on the requirement of *EGF-CFC* activity for Nodal signaling, the cell-autonomy of *oep* function in zebrafish, and the localization of EGF-CFC proteins at the cell surface, EGF-CFC proteins may function similarly to GFRα, IL-6Rα or CTNFRα. These proteins act as co-factors that mediate the binding of signaling molecules to signal-transducing receptors. For instance, GFRα is tethered to the membrane via a GPI linkage and together with the c-RET tyrosine kinase receptor forms a receptor for GDNF, a distant member of the TGF-β superfamily (Jing et al., 1996; Treanor et al., 1996); similarly, IL-6Rα interacts with gp130 to form a receptor complex for IL-6 (Hirano, 1998). Similar to EGF-CFC proteins, these factors are normally membrane-associated, and can also act as diffusible co-factors by binding to their ligands and associating with the transmembrane receptors. By analogy, EGF-CFC proteins might interact with Nodal proteins to form a complex that binds to Activin-like receptors. Alternatively, EGF-CFC

factors could modify or induce conformational changes in either Nodal signals and/or Activin-like receptors that allow them to interact.

In principle, release of EGF-CFC proteins from the membrane might result in a freely diffusible protein, which could form part of a receptor complex on a neighboring cell that may not itself express the *EGF-CFC* gene, in effect acting as a signal. Such a mechanism has been shown to be the case with the GFRα protein (Jing et al., 1996; Treanor et al., 1996). Moreover, the downstream signaling effects documented for CRIPTO protein might represent cross-talk between EGF receptor and SMAD2 signaling pathways, which has been previously documented (de Caestecker et al., 1998; Kretzschmar et al., 1999).

Technical Objective I: Generation and analysis of *Cripto* transgenic mice

Rationale: To investigate the effects of *Cripto* on mammary development and oncogenesis, we generated transgenic mice that overexpress *Cripto* in the mammary epithelium. Our previous studies had shown that *Cripto* is expressed at extremely low levels throughout mammary development, with slightly elevated expression during pregnancy and lactation. To overexpress *Cripto*, we produced a modified *Cripto* transgene that should direct high-level secretion. We had previously shown that EGF-CFC proteins, including CRIPTO, are poorly secreted from transfected cells in culture, probably because the endogenous signal sequence is unconventional and directs inefficient secretion (Shen et al., 1997). Moreover, CRIPTO protein appears to be membrane-associated due to the presence of the C-terminal hydrophobic region (Minchiotti et al., 2000). Since the biological activity of a *Cripto* transgene should depend upon the levels of protein secretion attained *in vivo*, we constructed a transgene expression vector containing a heterologous efficient signal sequence and encoding a C-terminally truncated protein.

Results: To direct expression of CRIPTO transgenes to the mammary epithelium of transgenic mice, we utilized the *MMTV-SVPA* vector (Wang et al., 1994), which contains a mouse mammary tumor virus (MMTV) long terminal repeat (LTR) enhancer/promoter. We have subcloned a modified mouse *Cripto* cDNA (sec-*Cripto*) into this vector, and successfully established five stable lines carrying this MMTV-sec-*Cripto* transgene. As described in our 1999 annual report, we examined transgene expression and phenotype at different stages of mammary development, thereby accomplishing tasks 1-5 of our Statement of Work. Analysis of whole-mounts of mammary fat pads from adult transgenic females from four independent expressing lines revealed no phenotypic abnormalities in virgin, pregnant, lactating, or involuting animals at up to one year of age (data not shown). The absence of any detectable phenotype suggests that *Cripto* expression alone is not sufficient to alter mammary epithelial differentiation.

These results are consistent with our model that EGF-CFC proteins act as essential co-factors for *Nodal* signaling, and with the finding that broad ectopic overexpression of *oep* in zebrafish does not result in embryonic phenotypes (Zhang et al., 1998). Our current interpretation is that the ectopic expression of *Cripto* in human breast tumors may reflect a cooperative interaction with overexpressed members of the TGF-β family, perhaps including *Nodal* or related genes.

Technical Objective II: Expression of *Cripto* in cell culture model systems

Rationale: To examine the role of *Cripto* in cellular proliferation, differentiation and transformation, we utilized retroviral gene transfer as a strategy to efficiently transfect *Cripto* into relevant cell lines. In studies reported in our 1998 update, we focused on cell lines that have been reported to respond to exogenous human CRIPTO protein, such as the HC-11 mammary epithelial cells (De Santis et al., 1997; Kannan et al., 1997), and made significant progress towards tasks 8-10.

Based on our revised model for *Cripto* function as well as the apparent lack of phenotype of MMTV-sec-*Cripto* transgenic mice, we decided not to continue our experiments on mammary cell lines until we acquired a better understanding of the biochemical basis of CRIPTO protein function. In future studies, we intend to test the hypothesis that co-expression of *Cripto* with specific TGF-β factors may play a critical role in mammary differentiation and/or tumorigenesis.

Technical Objective III: Biochemical analysis of CRIPTO function

Rationale: Despite the present lack of understanding as to the potential mechanism(s) by which *EGF-CFC* and *Nodal* activities might interact at the molecular level, understanding the biochemical basis of this interaction is of fundamental importance. Therefore, we have undertaken to *(i)* characterize the cellular localization of CRIPTO protein, *(ii)* produce and purify active CRIPTO protein for biochemical analyses, and *(iii)* examine potential interactions between CRIPTO and NODAL proteins. These experiments form the basis for elucidating the biochemical mechanism of CRIPTO function.

Results: Previous studies have suggested that members of the *EGF-CFC* family encode extracellular proteins that are localized to the surface of transfected cells, with this association mediated by the C-terminal hydrophobic domain (Shen et al., 1997; Zhang et al., 1998). As documented in our 1999 annual report, we have found that CRIPTO is in fact a secreted protein that is membrane-associated, using immunofluorescence and cell-fractionation approaches. These studies have been confirmed by another laboratory (Minchiotti et al., 2000). Our results support the idea that full-length EGF-CFC proteins are associated with the cell membrane, while C-terminal truncated proteins can be secreted into culture supernatants.

To purify CRIPTO protein, we employed a baculovirus expression strategy to produce CRIPTO protein into the culture supernatant of infected insect cells. As shown in our 1999 annual report, we have successfully expressed and purified CRIPTO protein from insect cell supernatants. To express NODAL protein, we made constructs that express secreted processed NODAL protein in transfected mammalian cells. We found that processing of unmodified NODAL protein is dependent upon the cell line used for expression, which presumably reflects differential expression of the specific pro-protein convertase(s) required for NODAL processing (Constam and Robertson, 1999). As shown in our 1999 report, cleaved mature Nodal protein can be produced in the culture supernatants of certain mammalian cell lines.

Using our purified CRIPTO protein as well as epitope-tagged CRIPTO and NODAL proteins produced in culture supernatants of transfected 293T cells, we obtained evidence from co-immunoprecipitation experiments for a direct binding interaction between CRIPTO and NODAL, as documented in our 1999 update. These data suggest that CRIPTO acts as a co-factor for NODAL signaling by a direct protein binding interaction, which presumably mediates signaling through activin receptors. In ongoing studies, we are pursuing biochemical cross-linking experiments to further investigate this interaction, as well as potential interactions with activin receptors. Taken together, our results imply that CRIPTO may not have a cell-surface receptor, but instead is itself a co-receptor for a ligand of the TGF-β family. Thus, we have essentially fulfilled Tasks 13-18 of our Statement of Work.

Key Research Accomplishments:

- We have generated mice carrying targeted gene disruptions of *Cripto* and *Cryptic*, two related members of the *EGF-CFC* family. Our analysis of these mice has revealed the complementary requirements of *Cripto* and *Cryptic* in embryonic anterior-posterior axis formation and left-right axis formation, respectively. These mice display significant phenotypic similarities to mutants for the TGF-β related factor Nodal and for activin receptor IIB. Thus, the analysis of *Cripto* and *Cryptic* mutant phenotypes supports an interaction of *EGF-CFC* genes with the *Nodal* signaling pathway, and support the hypothesis that EGF-CFC proteins are essential for Nodal in signaling through activin receptors.

- We have generated transgenic mice overexpressing *Cripto* in the mammary gland. These transgenic mice do not display an overt morphological phenotype, consistent with the lack of activity of *EGF-CFC* genes in isolation, and their function in *Nodal* signaling.

- We have expressed CRIPTO and NODAL proteins in cell culture for analyses of their activities and potential biochemical interactions. Purification of these proteins has led to the preliminary identification of a potential binding interaction.

- Our findings raise the possibility that *Cripto* overexpression in human breast cancer may result in de-regulation of TGF-β signaling pathways. In contrast, our results are not consistent with a role for EGF-CFC proteins as ligands for ErbB receptors.

Reportable Outcomes:

Published manuscripts (included in appendices):

Ding, J., Yang, L., Yan, Y.-T., Chen, A., Desai, N., Wynshaw-Boris, A., and Shen, M. M. (1998). *Cripto* is required for correct orientation of the anterior-posterior axis in the mouse embryo. Nature *395*, 702-707.

Yan, Y.-T., Gritsman, K., Ding, J., Burdine, R. D., Corrales, J. D., Price, S. M., Talbot, W. S., Schier, A. F., and Shen, M. M. (1999). Conserved requirement for *EGF-CFC* genes in vertebrate left-right axis formation. Genes Dev. *13*, 2527-2537.

Schier, A. F., and Shen, M. M. (2000). Nodal signalling in vertebrate development. Nature *403*, 385-389.

Shen, M. M., and Schier, A. F. (2000). The *EGF-CFC* gene family in vertebrate development. Trends Genet. *16*, 303-309.

Meeting abstracts:

Shen, M. M., Yan, Y.-T., Ding, J., Yang, L., E, C., and Wang, H. (1997). Molecular analysis of a novel growth factor family in murine development. 62nd Cold Spring Harbor Symposium: Pattern Formation during Development (Cold Spring Harbor, NY).

E, C., Yang, L., Wang, H., and Shen, M. M. (1997). Molecular analysis of two EGF-related growth factors and their receptors in mouse development and oncogenesis. Annual Retreat on Cancer Research in New Jersey (Princeton, NJ).

Shen, M. M., E, C., Yang, L., Wang, H. (1997). Molecular analysis of two EGF-related growth factors and their receptors in mouse development and oncogenesis. Gordon Conference on Mammary Gland Biology (Plymouth, NH).

Ding, J., Yan, Y.-T., Yang, L., Wang, H., Chen, A., Wynshaw-Boris, T., and Shen, M. M. (1998). Essential role for *Cripto*, a member of the *EGF-CFC* gene family, in murine gastrulation and axial patterning. 57th Annual Meeting of the Society for Developmental Biology (Palo Alto, CA). Dev. Biol. *198*, 203.

Ding, J., Yang, L., Yan, Y.-T., Chen, A., Desai, N., Wynshaw-Boris, A., and Shen, M. M. (1998). *Cripto*, a member of the *EGF-CFC* gene family, is required for correct orientation of the anterior-posterior axis in the mouse embryo. Mouse Molecular Genetics (Cold Spring Harbor, NY).

Ding, J., Yang, L., Yan, Y.-T., Chen, A., Desai, N., Wynshaw-Boris, A., and Shen, M. M. (1999). *Cripto*, a member of the *EGF-CFC* gene family, is required for correct orientation of the anterior-posterior axis in the mouse embryo. 1999 Northeast Regional Meeting of the Society for Developmental Biology (Woods Hole, MA).

Ding, J., Yang, L., Yan, Y.-T., Chen, A., Desai, N., Wynshaw-Boris, A., and Shen, M. M. (1999). Molecular analysis of *Cripto*, a member of the EGF-CFC gene family, in development and cancer. Annual Retreat on Cancer Research in New Jersey (New Brunswick, NJ).

Yan, Y.-T., Ding, J., Yang, L., Price, S., and Shen, M. M. (1999). The *EGF-CFC* gene family and mammalian axis determination. 58th Annual Meeting of the Society for Developmental Biology (Charlottesville, VA).

Yan, Y.-T., Ding, J., Price, S., and Shen, M. M. (2000). *Cryptic* is essential for determination of the left-right axis in the mouse embryo. 59th Annual Meeting of the Society for Developmental Biology (Boulder, CO).

Shen, M. M., E, C., Saplakoglu, U., Yan, Y.-T., and Ding, J. (2000). Functional analysis of *EGF-CFC* genes in mouse development indicates their essential role in Nodal signaling. Era of Hope Department of Defense Breast Cancer Research Program Meeting. (Atlanta, GA).

E, C., Saplakoglu, U., and Shen, M. M. (2000). Role for Cripto as a cofactor in the Nodal signaling pathway. Era of Hope Department of Defense Breast Cancer Research Program Meeting. (Atlanta, GA).

Shen, M. M., Yan, Y.-T., Iratni, R., Ding, J., Price. S., and Reinberg, D. (2000). Regulation of the Nodal signaling pathway in embryonic patterning. Mouse Molecular Genetics (Cold Spring Harbor, NY).

Invited presentations:

October, 1997	11th Annual CABM Symposium, *Cell Signaling in Growth and Development*
December, 1997	Developmental Genetics Program, Skirball Institute for Biomolecular Medicine (New York, NY)
December, 1998	Developmental Genetics Programme, University of Sheffield (England)
June, 1999	58th Annual Meeting of the Society for Developmental Biology (Charlottesville, VA)

October, 1999	Department of Molecular Biology and Pharmacology, Washington University (St. Louis, MO)
October, 1999	Department of Biochemistry, UMDNJ–Robert Wood Johnson Medical School
October, 1999	Institute for Molecular and Cellular Biology, Osaka University (Japan)
November, 1999	3rd Aso Meeting on Vertebrate Body Plan (Aso, Japan)
February, 2000	Molecular Biology Program, Memorial-Sloan Kettering Cancer Center (New York, NY)
March, 2000	First NIH Meeting on Holoprosencephaly (Bethesda, MD)
June, 2000	Max-Planck Institute for Embryology (Tübingen, Germany)
June, 2000	Institute for Genetics, Forschungzentrum (Karlrühe, Germany)
June, 2000	Max Delbrück Institute for Molecular Medicine (Berlin, Germany)
August, 2000	Mouse Molecular Genetics (Cold Spring Harbor, NY)
September, 2000	Department of Cell and Developmental Biology, University of Pennsylvania (Philadelphia, PA)

Personnel supported by this grant:

Michael Shen, PI

Jinfeng Liu, Graduate Student

Qin Xu, Graduate Student

Lu Yang, Graduate Student

Yelena Folk, Laboratory Technician

Yaping Hu, Research Associate

Sally Marshall, Research Technician

Sandy Price, Research Teaching Specialist

Jeff Bush, Undergraduate Student Assistant

Brian Donovan, Undergraduate Student Assistant

Degrees obtained supported by this award:

Qin Xu, M.S. received 10/98

Lu Yang, M.S. received 12/98

Conclusions:

In the past four years, we have made important progress in investigating the molecular basis of *Cripto* function. We have generated several lines of evidence that *Cripto* acts as an essential co-factor for *Nodal* signaling, and conversely, that *Cripto* activity requires interaction with *Nodal* and possibly other divergent members of the TGF-β family. These results are supported by our preliminary data indicating a direct binding interaction between CRIPTO and NODAL proteins. Our continuing studies will further investigate these biochemical interactions, and will utilize these findings to examine how *Cripto* expression can affect cellular proliferation and differentiation. Taken together, our results have resulted in a substantial revision of views of *Cripto* function, and have provided fresh insights into potential mechanisms of *Cripto* activity in mammary development and tumorigenesis.

References:

Ciardiello, F., Dono, R., Kim, N., Persico, M. G., and Salomon, D. S. (1991). Expression of cripto, a novel gene of the epidermal growth factor gene family, leads to in vitro transformation of a normal mouse mammary epithelial cell line, Cancer Res *51*, 1051-1054.

Ciccodicola, A., Dono, R., Obici, S., Simeone, A., Zollo, M., and Persico, M. G. (1989). Molecular characterization of a gene of the "EGF family" expressed in undifferentiated human NTERA2 teratocarcinoma cells, EMBO J *8*, 1987-1991.

Collignon, J., Varlet, I., and Robertson, E. J. (1996). Relationship between asymmetric *nodal* expression and the direction of embryonic turning, Nature *381*, 155-158.

Conlon, F. L., Lyons, K. M., Takaesu, N., Barth, K. S., Kispert, A., Herrmann, B., and Robertson, E. J. (1994). A primary requirement for nodal in the formation and maintenance of the primitive streak in the mouse, Development *120*, 1919-1928.

Constam, D. B., and Robertson, E. J. (1999). Regulation of bone morphogenetic protein activity by pro domains and proprotein convertases, J Cell Biol *144*, 139-149.

de Caestecker, M. P., Parks, W. T., Frank, C. J., Castagnino, P., Bottaro, D. P., Roberts, A. B., and Lechleider, R. J. (1998). Smad2 transduces common signals from receptor serine-threonine and tyrosine kinases, Genes Dev *12*, 1587-1592.

De Santis, M. L., Kannan, S., Smith, G. H., Seno, M., Bianco, C., Kim, N., Martinez-Lacaci, I., Wallace-Jones, B., and Salomon, D. S. (1997). Cripto-1 inhibits β-casein expression in mammary epithelial cells through a p21^{ras}- and phophatidylinositol 3'-kinase-dependent pathway, Cell Growth Diff *8*, 1257-1266.

Ding, J., Yang, L., Yan, Y. T., Chen, A., Desai, N., Wynshaw-Boris, A., and Shen, M. M. (1998). *Cripto* is required for correct orientation of the anterior-posterior axis in the mouse embryo, Nature *395*, 702-707.

Dono, R., Scalera, L., Pacifico, F., Acampora, D., Persico, M. G., and Simeone, A. (1993). The murine *cripto* gene: expression during mesoderm induction and early heart morphogenesis, Development *118*, 1157-1168.

Gritsman, K., Zhang, J., Cheng, S., Heckscher, E., Talbot, W. S., and Schier, A. F. (1999). The EGF-CFC protein one-eyed pinhead is essential for nodal signaling, Cell *97*, 121-132.

Gu, Z., Nomura, M., Simpson, B. B., Lei, H., Feijen, A., van den Eijnden-van Raaij, J., Donahoe, P. K., and Li, E. (1998). The type I activin receptor ActRIB is required for egg cylinder organization and gastrulation in the mouse, Genes Dev *12*, 844-857.

Hirano, T. (1998). Interleukin-6, in The Cytokine Handbook *Editor A. Thomson. 3rd Ed. Academic Press*, 197-228.

Jing, S., Wen, D., Yu, Y., Holst, P. L., Luo, Y., Fang, M., Tamir, R., Antonio, L., Hu, Z., Cupples, R., *et al.* (1996). GDNF-induced activation of the ret protein tyrosine kinase is mediated by GDNFR-alpha, a novel receptor for GDNF, Cell *85*, 1113-1124.

Kannan, S., De Santis, M., Lohmeyer, M., Riese II, D. J., Smith, G. H., Hynes, N., Seno, M., Brandt, R., Bianco, C., Persico, G., *et al.* (1997). Cripto enhances the tyrosine phosphorylation of Shc and activates mitogen-activated protein kinase (MAPK) in mammary epithelial cells, J Biol Chem *272*, 3330-3335.

Kretzschmar, M., Doody, J., Timokhina, I., and Massague, J. (1999). A mechanism of repression of TGFbeta/ Smad signaling by oncogenic Ras, Genes Dev *13*, 804-816.

Massague, J., and Chen, Y. G. (2000). Controlling TGF-beta signaling, Genes Dev *14*, 627-644.

Minchiotti, G., Parisi, S., Liguori, G., Signore, M., Lania, G., Adamson, E. D., Lago, C. T., and Persico, M. G. (2000). Membrane-anchorage of Cripto protein by glycosylphosphatidylinositol and its distribution during early mouse development, Mech Dev *90*, 133-142.

Nomura, M., and Li, E. (1998). Smad2 role in mesoderm formation, left-right patterning and craniofacial development, Nature *393*, 786-790.

Oh, S. P., and Li, E. (1997). The signaling pathway mediated by the type IIB activin receptor controls axial patterning and lateral asymmetry in the mouse, Genes Dev *11*, 1812-1826.

Qi, C. F., Liscia, D. S., Normanno, N., Merlino, G., Johnson, G. R., Gullick, W. J., Ciardiello, F., Saeki, T., Brandt, R., Kim, N., *et al.* (1994). Expression of transforming growth factor alpha, amphiregulin and cripto-1 in human breast carcinomas, Br J Cancer *69*, 903-910.

Saijoh, Y., Adachi, H., Sakuma, R., Yeo, C. Y., Yashiro, K., Watanabe, M., Hashiguchi, H., Mochida, K., Ohishi, S., Kawabata, M., *et al.* (2000). Left-right asymmetric expression of lefty2 and nodal is induced by a signaling pathway that includes the transcription factor FAST2, Molec Cell *5*, 35-47.

Salomon, D. S., Bianco, C., and De Santis, M. (1999). Cripto: a novel epidermal growth factor (EGF)-related peptide in mammary gland development and neoplasia, Bioessays *21*, 61-70.

Schier, A. F., and Shen, M. M. (2000). Nodal signalling in vertebrate development, Nature *403*, 385-389.

Shen, M. M., and Schier, A. F. (2000). The *EGF-CFC* gene family in vertebrate development, Trends Genet *16*, 303-309.

Shen, M. M., Wang, H., and Leder, P. (1997). A differential display strategy identifies *Cryptic,* a novel EGF-related gene expressed in the axial and lateral mesoderm during mouse gastrulation, Development *124*, 429-442.

Treanor, J. J., Goodman, L., de Sauvage, F., Stone, D. M., Poulsen, K. T., Beck, C. D., Gray, C., Armanini, M. P., Pollock, R. A., Hefti, F., *et al.* (1996). Characterization of a multicomponent receptor for GDNF, Nature *382*, 80-83.

Waldrip, W. R., Bikoff, E. K., Hoodless, P. A., Wrana, J. L., and Robertson, E. J. (1998). Smad2 signaling in extraembryonic tissues determines anterior-posterior polarity of the early mouse embryo, Cell *92*, 797-808.

Wang, T. C., Cardiff, R. D., Zukerberg, L., Lees, E., Arnold, A., and Schmidt, E. V. (1994). Mammary hyperplasia and carcinoma in MMTV-cyclin D1 transgenic mice, Nature *369*, 669-671.

Yan, Y.-T., Gritsman, K., Ding, J., Burdine, R. D., Corrales, J. D., Price, S. M., Talbot, W. S., Schier, A. F., and Shen, M. M. (1999). Conserved requirement for *EGF-CFC* genes in vertebrate left-right axis formation, Genes Dev *13*, 2527-2537.

Zhang, J., Talbot, W. S., and Schier, A. F. (1998). Positional cloning identifies zebrafish *one-eyed pinhead* as a permissive EGF-related ligand required during gastrulation, Cell *92*, 241-251.

Zhou, X., Sasaki, H., Lowe, L., Hogan, B. L., and Kuehn, M. R. (1993). Nodal is a novel TGF-beta-like gene expressed in the mouse node during gastrulation, Nature *361*, 543-547.

The supernatants were pre-cleared with Sepharose-4BL beads and immuno-precipitated with anti-Myc-epitope antibody (9E2.10). The immunoprecipitates were then washed twice with RIPA-DOC buffer, resolved by 4–20% SDS–PAGE, and quantified by phosphorimaging with subtraction of individual lane background.

Analysis of PS1-transgenic mice. Wild-type and mutant *PS1* cDNAs were cloned into a Thy-1 expression vector and transgenic mice were generated and bred as described[26]. We identified founders by Southern blotting of genomic DNA from tail biopsies. Transgene-positive offspring were identified by polymerase chain reaction and confirmed by western blotting of cortical homogenates for human PS1 fragments. Transgene expression was also monitored by *in situ* hybridization for the human PS1 messenger RNA.

Quantitative analysis of β-catenin in the human brain. Grey matter was dissected from the temporal cerebral cortex of control cases ($n = 10$, average age 59 years, age range 25–86 years), cases with sporadic Alzheimer's disease ($n = 7$, average age 71, age range 63–82), and cases with familial Alzheimer's disease with PS1 mutations (G209V; $n = 2$; C410Y, $n = 3$; M139I, $n = 2$; H163R, $n = 2$; average age 51, age range 41–59; one case with a C410Y mutation was 84 years old). The tissue was extracted in RIPA-DOC buffer supplemented with protease inhibitors and cleared by centrifugation (100,000g, 60 min, 4 °C), and protein-equivalent samples were resolved by 4–20% SDS–PAGE. For detection of β-catenin, samples were heated for 1 min at 90 °C before loading. For detection of PS1, samples were loaded without previous heating. The proteins were electrotransferred to Immobilon-P membrane and immunoblotted with anti-PS1-N (1 : 5,000) or anti-β-catenin (mAb14; 1 : 1,000), followed by incubation with ^{125}I-conjugated anti-rabbit or anti-mouse IgG and quantitative analysis by phosphorimaging.

Analysis of neuronal apoptosis. We established and transfected primary cultures of rat E18 hippocampal neurons as described[27]. We added fibrillar amyloid-β protein residues 1–40 (ref. 28) to 40 μM at 12 h after transfection, and incubated the cultures for a further 36 h. Transfected neurons were identified by double labelling for GFP and neuron-specific β-tubulin. Apoptotic neurons were identified by characteristic nuclear morphology after staining with Hoechst 33342 (1 μg ml^{-1}).

1. Sherrington, R. *et al.* Cloning of a gene bearing missense mutations in early-onset familial Alzheimer's disease. *Nature* **375**, 754–760 (1995).
2. Levy-Lahad, E. *et al.* Candidate gene for chromosome 1 familial Alzheimer's disease locus. *Science* **269**, 973–977 (1995).
3. Rogaev, E. I. *et al.* Familial Alzheimer's disease in kindreds with missense mutations in a gene on chromosome 1 related to the Alzheimer's disease type 3 gene. *Nature* **376**, 775–778 (1995).
4. Li, J., Ma, J. & Potter H. Identification and expression of a potential familial Alzheimer disease gene on chromosome 1 related to AD3. *Proc. Natl Acad. Sci. USA* **92**, 12180–12184 (1995).
5. Zhou, J. *et al.* Presenilin 1 interaction in the brain with a novel member of the Armadillo family. *Neuroreport* **8**, 1489–1494 (1997).
6. Yu, G. *et al.* The presenilin 1 protein is a component of a high molecular weight complex that contains β-catenin. *J. Biol. Chem.* **273**, 161–16475 (1998).
7. Busciglio, J. *et al.* Neuronal localization of presenilin-1 and association with amyloid plaques and neurofibrillary tangles in Alzheimer's disease. *J. Neurosci.* **17**, 5101–5107 (1997).
8. Thinakaran, G. *et al.* Endoproteolysis of presenilin 1 and accumulation of processed derivatives *in vivo*. *Neuron* **17**, 181–190 (1996).
9. Nusse, R. A versatile transcription effector of wingless signalling. *Cell* **89**, 321–323 (1997).
10. Kovacs, D. M. *et al.* Alzheimer-associated presenilins 1 and 2: neuronal expression in brain and localization to intracellular membranes in mammalian cells. *Nature Med.* **2**, 224–229 (1996).
11. Walter, J. *et al.* Alzheimer's disease-associated presenilins are differentially phosphorylated proteins located within the endoplasmic reticulum. *Mol. Med.* **2**, 673–691 (1996).
12. De Strooper, B. *et al.* Deficiency of presenilin-1 inhibits the normal cleavage of amyloid precursor protein. *Nature* **391**, 387–390 (1998).
13. Yankner, B. A. Mechanisms of neuronal degeneration in Alzheimer's disease. *Neuron* **16**, 921–932 (1996).
14. Molenaar, M. *et al.* Xtcf-3 transcription factor mediates β-catenin-induced axis formation in *Xenopus* embryos. *Cell* **86**, 391–399 (1996).
15. van de Wetering, M. *et al.* Armadillo coactivates transcription driven by the product of the *Drosophila* segment polarity gene dTCF. *Cell* **88**, 789–799 (1997).
16. Capell, A. *et al.* The proteolytic fragments of the Alzheimer's disease-associated presenilin-1 form heterodimers and occur as a 100–150-kDa molecular mass complex. *J. Biol. Chem.* **273**, 3205–3211 (1998).
17. Scheuner, D. *et al.* Secreted amyloid beta-protein similar to that in the senile plaques of Alzheimer's disease is increased *in vivo* by the presenilin 1 and 2 and APP mutations linked to familial Alzheimer's disease. *Nature Med.* **2**, 864–870 (1996).
18. Duff, K. *et al.* Increased amyloid-β42(43) in brains of mice expressing presenilin 1. *Nature* **383**, 710–713 (1996).
19. Borchelt, D. R. *et al.* Familial Alzheimer's disease-linked presenilin-1 variants elevate Aβ1-42/1-40 ratio *in vitro* and *in vivo*. *Neuron* **17**, 1005–1013 (1996).
20. Citron, M. *et al.* Mutant presenilins of Alzheimer's disease increase production of 42-residue amyloid beta-protein in both transfected cells and transgenic mice. *Nature Med.* **3**, 67–72 (1997).
21. Morin, P. J., Vogelstein, B. & Kinzler, K. W. Apoptosis and APC in colorectal tumorigenesis. *Proc. Natl Acad. Sci. USA* **93**, 7950–7954 (1996).
22. Ahmed, Y., Hayashi, S., Levine, A. & Wieschaus, E. Regulation of Armadillo by a *Drosophila* APC inhibits neuronal apoptosis during retinal development. *Cell* **93**, 1171–1182 (1998).
23. Wolozin, B. *et al.* Participation of presenilin 2 in apoptosis: enhanced basal activity conferred by an Alzheimer mutation. *Science* **274**, 1710–1713 (1996).
24. Guo, Q. *et al.* Alzheimer's presenilin mutation sensitizes neural cells to apoptosis induced by trophic factor withdrawal and amyloid β-peptide: involvement of calcium and oxyradicals. *J. Neurosci.* **17**, 4212–4222 (1997).
25. Guo, Q. *et al.* Par-4 is a mediator of neuronal degeneration associated with the pathogenesis of Alzheimer disease. *Nature Med.* **4**, 957–962 (1998).
26. Sturchler-Pierrat, C. *et al.* Two amyloid precursor protein transgenic mouse models with Alzheimer disease-like pathology. *Proc. Natl Acad. Sci. USA* **94**, 13287–13292 (1997).
27. Dudek, H. *et al.* Regulation of neuronal survival by the serine-threonine protein kinase Akt. *Science* **275**, 661–665 (1997).
28. Lorenzo, A. & Yankner, B. A. Beta-amyloid neurotoxicity requires fibril formation and is inhibited by Congo Res. *Proc. Natl Acad. Sci. USA* **91**, 12243–12247 (1994).

Cripto is required for correct orientation of the anterior–posterior axis in the mouse embryo

Jixiang Ding*, Lu Yang*, Yu-Ting Yan*, Amy Chen†,
Nishita Desai*, Anthony Wynshaw-Boris†
& Michael M. Shen*

* *Center for Advanced Biotechnology and Medicine and Dept of Pediatrics, UMDNJ-Robert Wood Johnson Medical School, 679 Hoes Lane, Piscataway, New Jersey 08854, USA*

† *Laboratory of Genetic Disease Resarch, National Human Genome Research Institute, 49 Convent Drive, Bethesda, Maryland 20892, USA*

....

The anterior–posterior axis of the mouse embryo is established by two distinct organizing centres in the anterior visceral endoderm and the distal primitive streak[1-7]. These organizers induce and pattern the head and trunk respectively, and have been proposed to be localized through coordinate cell movements that rotate a pre-existing proximal–distal axis[6,8]. Here we show that correct localization of both head- and trunk-organizing centres requires *Cripto*[9,10], a putative signalling molecule that is a member of the EGF-CFC gene family[11,12]. Before gastrulation, *Cripto* is asymmetrically expressed in a proximal–distal gradient in the epiblast, and subsequently is expressed in the primitive streak and newly formed embryonic mesoderm. A *Cripto* null mutation generated by targeted gene disruption results in homozygous *Cripto*$^{-/-}$ embryos that mostly consist of anterior neuroectoderm and lack posterior structures, thus resembling a head without a trunk. Notably, markers of the head organizer are located at the distal end of the embryo, whereas markers of the primitive streak are absent or localized to the proximal side. Our results indicate that Cripto signalling is essential for the conversion of a proximal–distal asymmetry into an orthogonal anterior–posterior axis.

Members of the EGF-CFC gene family, including *Cripto*, murine *Cryptic*[11], *Xenopus FRL-1*[13], and zebrafish *one-eyed pinhead*[12], encode secreted proteins that contain a divergent epidermal growth factor (EGF)-like motif and a novel cysteine-rich CFC motif[11,12]. EGF-CFC genes are expressed during gastrulation, with limited expression at later embryonic stages, and have been implicated in early development. For example, *FRL-1* has mesoderm and neural-inducing activities in *Xenopus* animal cap assays[13], and *one-eyed pinhead* is required for prechordal plate formation during zebrafish gastrulation[12]. Expression of *Cripto* can be detected in the epiblast

of pre-streak- and primitive-streak-stage embryos[9,10]; Cripto is necessary for cardiogenesis during embryonic stem cell differentiation in culture[14]. We demonstrate here that Cripto is required for early embryogenesis in the mouse, thus establishing an essential role for the EGF-CFC family in mammalian development.

We have found that the expression of Cripto during pregastrulation and gastrulation stages is dynamic and is associated with early signs of overt anterior–posterior asymmetry. Before gastrulation, at 5.5 days post coitum (d.p.c.), Cripto expression is initially symmetric and uniform in the epiblast, and is not found in the extraembryonic visceral endoderm (Fig. 1a, b). At 6.0 d.p.c., before primitive streak formation, Cripto becomes asymmetrically expressed in the epiblast, in a graded proximal–distal distribution (Fig. 1c–e). By the onset of gastrulation (6.5 d.p.c.), Cripto expression localizes to the region of the nascent primitive streak (Fig. 1f–h). In the early stages of gastrulation (6.75 d.p.c.), Cripto expression is found in the primitive streak and in the wings of embryonic mesoderm that spread rostrally, while regressing caudally in the epiblast (Fig. 1i, j). During the early neural plate stage (7.25 d.p.c.), expression of Cripto fades in the embryonic mesoderm and becomes increasingly confined to the primitive streak and head process (Fig. 1k, l). Cripto expression disappears completely by the late neural plate stage (7.75 d.p.c.), whereas a later phase of expression in cardiac progenitors initiates at the late head-fold stage (8.0 d.p.c.) (J.D., H. Wang and M.M.S., unpublished results).

To investigate whether Cripto activity is required for proper gastrulation, we generated a null mutation by targeted gene disruption, simultaneously 'knocking-in' a promoterless lacZ marker gene (Fig. 2a). The resulting heterozygous Cripto^{+/−} mice are phenotypically normal, and Cripto^{+/−} embryos display β-galactosidase staining patterns that resemble those obtained by in situ hybridization, albeit with a slight lag in developmental stage that probably reflects protein persistence (Fig. 1m–r). However, homozygosity for the Cripto targeted mutation results in embryonic lethality (Fig. 2b). Although no homozygous embryos were obtained after 10.5 d.p.c., Cripto homozygotes were recovered in the expected mendelian ratios at 6.75 d.p.c. through to 8.5 d.p.c. (Fig. 2c).

Morphological and histological analysis demonstrated that Cripto homozygotes have striking defects in embryonic mesoderm formation and axial organization. The earliest stage at which Cripto homozygotes can be reliably distinguished is 6.75 d.p.c., when wild-type littermates are at early-to-mid-streak stages of gastrulation. At this stage, Cripto mutants can be identified by the absence of a primitive streak and embryonic mesoderm, and by a thickened layer of visceral endoderm at the distal tip of the egg cylinder (Fig. 2d,h,i). In contrast, in wild-type embryos, the visceral endoderm is thin distally, but is thicker proximally towards the embryonic/extraembryonic constriction, particularly on the anterior side[2] (Fig. 2d, g). Later, at 7.5 and 8.5 d.p.c. Cripto mutants appear to be completely deficient for embryonic mesoderm derivatives such as somites and cardiac tissue, whereas extra-embryonic mesoderm is often formed, including the allantois and blood islands of the visceral yolk sac mesoderm (Fig. 2d–l). Notably, Cripto mutant
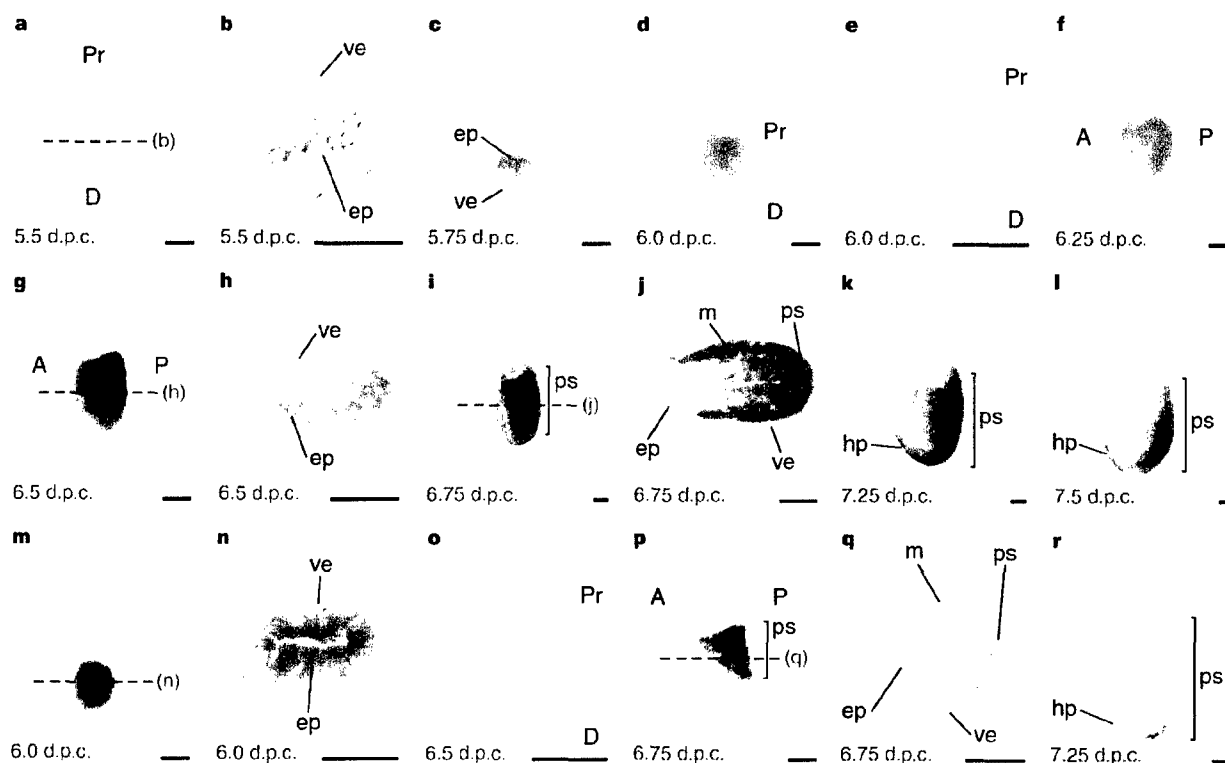

Figure 1 Expression of Cripto at pre-gastrulation and gastrulation stages. **a–l**, Whole-mount in situ hybridization analysis. **a**, Uniform symmetric staining in the epiblast at 5.5 d.p.c.; **b**, a cross section shows lack of expression in the visceral endoderm. **c, d**, Proximal–distal gradient of expression in the epiblast. **e**, Sagittal section of **d**. **f, g**, Expression shifts caudally before the onset of gastrulation at 6.5 d.p.c. **h**, Cross-section of **g** shows widespread expression in the epiblast and no expression in the visceral endoderm. **i**, Mid-streak stage; **j**, cross-section shows intense staining in the newly formed embryonic mesoderm. **k, l**, Expression persists in the primitive streak and head process at the neural plate stage. **m–r**, β-Galactosidase staining of Cripto heterozygotes. **m, n**, Uniform staining in the epiblast before gastrulation. **o**, Sagittal section shows proximal-distal graded staining just before gastrulation. **p**, Early-streak stage embryo, and **q**, cross-section. **r**, Early neural-plate-stage embryo: note more intense staining at distal end of the primitive streak. In all panels, anterior faces to the left when anterior-posterior orientation can be identified; staging before primitive streak formation is approximate. Scale bars, 0.05 mm. A, anterior; D, distal; ep, epiblast; hp, head process; m, mesoderm; P, posterior; Pr, proximal; ps, primitive streak (bar denotes extent of streak); ve, visceral extra-embryonic endoderm.
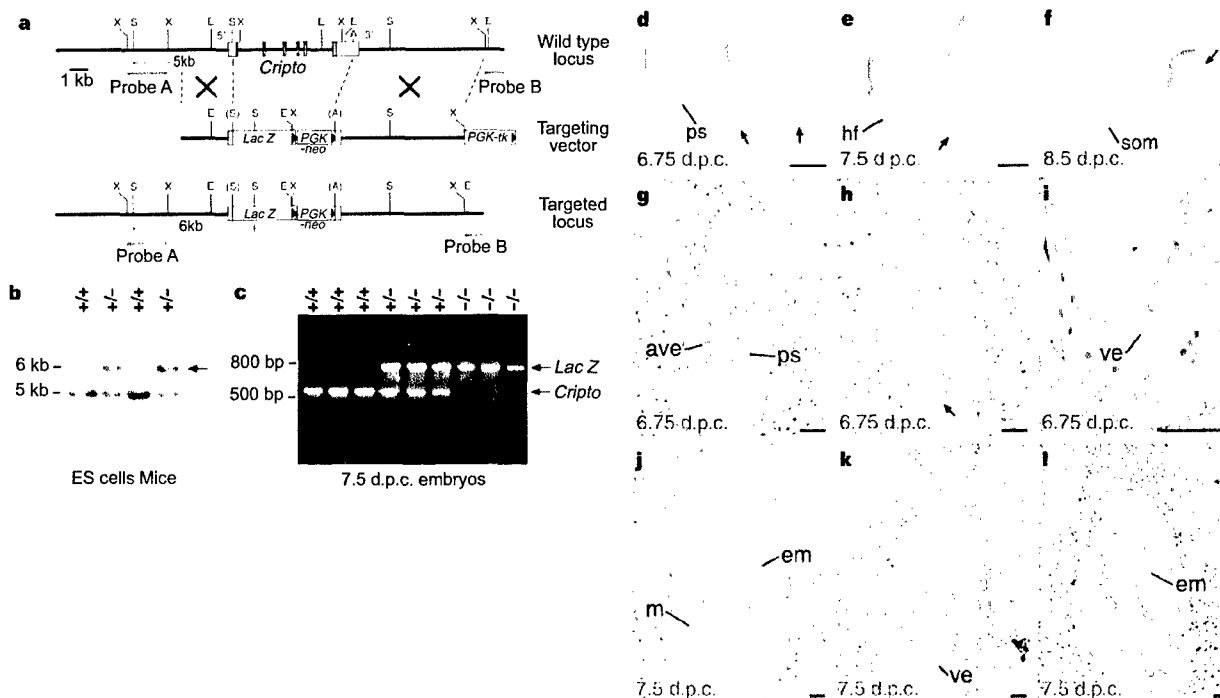
Figure 2 Targeted disruption of Cripto and characterization of the null phenotype. **a**, Homologous recombination with the targeting vector deletes the entire Cripto coding region (dark boxes), and inserts a promoter-less LacZ marker gene into the 5' untranslated region; triangles indicate orientation of PGK-neo, LacZ, and PGK-tk cassettes. A, ApaI, E, EcoRI; S, SspI; X, XbaI. **b**, Southern blotting using a 5' flanking probe (A) detects a 5-kb SspI fragment in wild-type genomic DNA and a 6-kb fragment (arrow) from the targeted allele in ES cells (lanes 1, 2) and in mice (lanes 3, 4). Targeted ES clones were confirmed using a LacZ probe and a 3' external probe (B) (not shown). **c**, PCR analysis of extra-embryonic tissues demonstrates recovery of wild-type (lanes 1-3), heterozygous (lanes 4-6), and homozygous mutant embryos (lanes 7-9) at 7.5 d.p.c.; the primers amplify a 751-bp LacZ fragment and a 536-bp Cripto genomic fragment deleted in the targeted allele. **d-f**, Morphology of dissected embryos; scale bars represent 0.2 mm. **d**, Wild-type mid-streak stage embryo at 6.75 d.p.c. (left) and two Cripto mutant littermates (centre, right), showing thickened visceral endoderm at the distal tip (arrows). **e**, Wild-type early head-fold embryo at 7.5 d.p.c. (left) and mutant littermate with ectopic ectodermal folds (arrow). **f**, Wild-type embryo at 8.5 d.p.c. (left) and mutant littermate (right), with an apparent blood island in the extra-embryonic region (arrow). **g-l**, Haematoxylin-eosin staining of paraffin sections of embryos within intact decidual tissue at 6.75 d.p.c. (**g-i**) and at 7.5 d.p.c. (**j-l**); scale bars represent 0.1 mm. **g-i**, Wild-type mid-streak embryo (**g**) and Cripto mutant littermate (**h**), showing lack of primitive streak and embryonic mesoderm and thickening of the visceral endoderm at the distal tip (arrow), also shown at higher power (**i**). **j-l**, Wild-type neural-plate-stage embryo (**j**) and two Cripto mutant littermates, one with no evidence of primitive streak or mesoderm formation (**k**), and the second showing formation of extra-embryonic mesoderm, but not embryonic mesoderm (**l**). Abbreviations: ave, anterior visceral endoderm; em, extra-embryonic mesoderm; hf, head folds; m, embryonic mesoderm; ps, primitive streak; som, somites; ve, visceral endoderm.

embryos have ectopic folds of ectodermal tissue that are located distally, and frequently lack an overt anterior–posterior axis (Fig. 2d–l).

We further characterized the Cripto mutant phenotype by examining expression of appropriate marker genes for specific tissues in embryos dissected at 7.5 d.p.c. and 8.5 d.p.c. Consistent with our histological findings, we observed no embryonic expression of HNF-3β and Sonic hedgehog (Shh), which are markers of axial mesoderm and definitive endoderm at these stages (Fig. 3a, b). We also found no evidence for formation of paraxial mesoderm using a Mox1 probe[15] (Fig. 3c). Similar results were obtained using a Lim1 probe for caudal lateral plate mesoderm (data not shown). To determine the identity of the ectopic ectodermal folds in Cripto mutants, we next investigated the expression of several neuro-ectoderm markers. In all Cripto homozygotes examined, we found widespread expression in the ectoderm layer for Otx2, which is initially expressed throughout the undifferentiated epiblast before gastrulation and then marks the prospective forebrain and midbrain at 7.5 d.p.c.[16] (Fig. 3d, e). In addition, expression of the forebrain marker BF1[17] was observed in four out of seven embryos at 7.5 d.p.c. and 8.5 d.p.c. (Fig. 3f). En1, a marker of prospective midbrain and anterior hindbrain, was expressed in every homozygous embryo examined, usually in an asymmetric patch (Fig. 3g, h). In contrast to

these anterior neuroectoderm markers, staining was not observed for Krox20, a marker for rhombomeres 3 and 5 of the posterior hindbrain (Fig. 3i). Similarly, expression of the more caudal neural and mesodermal markers HoxB1 and HoxB4 was completely absent (Fig. 3j; data not shown). To rule out the possibility that the tissues in Cripto mutant embryos correspond to undifferentiated epiblast, we examined expression of the epiblast marker Oct4 and found no evidence of expression at 7.5 d.p.c. (data not shown). Based on these data, we conclude that Cripto mutant embryos are severely deficient for production of embryonic mesoderm and endoderm, and instead largely consist of anterior neuroectoderm.

The absence of embryonic mesoderm and ectopic neuroectoderm in Cripto mutants suggested that formation and/or localization of the trunk and head organizing centres might be defective. To determine whether the trunk organizing centre is affected, we used Brachyury, an early marker of the primitive streak, and found that it was expressed in a proximal band near the embryonic/extraembryonic constriction at 6.75 d.p.c. (Fig. 3k, l), but was undetectable at 7.5 d.p.c. (data not shown). To confirm this finding, we examined the markers Fgf8 and Evx1, which mark the entire streak and caudal (proximal) primitive streak respectively[18], and obtained similar results at 6.75 d.p.c. (Fig. 3m; data not shown). We also examined expression of Lim1, which marks both the primitive
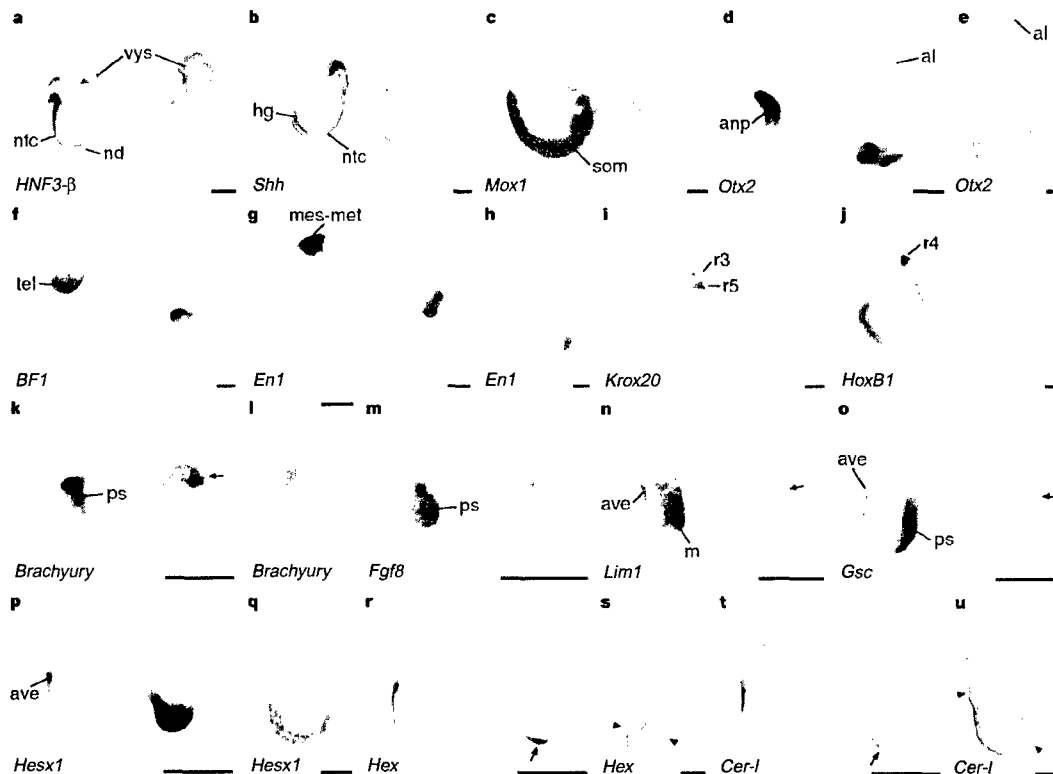
Figure 3 Analysis of marker gene expression. Panels show whole-mount *in situ* hybridization on a wild-type littermate control (left), with anterior facing to the left, and a *Cripto* mutant embryo (right). **a–j**, Analysis of embryos at 7.5 (**a, d, e**) and 8.5 d.p.c. (**b, c, f–j**). **a**, *HNF3-β* is not expressed in the embryonic region of a *Cripto* mutant; weak staining in extraembryonic endoderm of the visceral yolk sac is detected in both embryos. **b**, No expression of *Sonic hedgehog* in a *Cripto* mutant. **c**, *Mox1* expression is not observed in a mutant embryo. **d**, *Otx2* expression in the ectopic distal ectodermal folds of a *Cripto* mutant, also shown in sagittal section (**e**); note the presence of an allantois in the extra-embryonic region. **f**, *BF1* is expressed asymmetrically in a *Cripto* mutant. **g**, *En1* is expressed in the ectodermal folds of a *Cripto* mutant, also shown in sagittal section (**h**). **i**, No expression is detected in *Cripto* mutants for *Krox20*. **j**, No expression is detected in *Cripto* mutants for *HoxB1*, a marker for rhombomere 4 and the posterior neural tube and mesoderm. **k–u**, Analysis of embryos at 6.75 d.p.c. **k**, *Brachyury* is expressed in the primitive streak of the wild-type embryo, but in a proximal band in the mutant (arrows), also shown in frontal section (**l**). **m**, *Fgf8* is expressed proximally in a *Cripto* mutant. **n**, Limited proximal expression of *Lim1* in a *Cripto* homozygote (arrow); faint staining in the distal visceral endoderm can occasionally be observed in mutants (not shown). **o**, Faint proximal staining for *Goosecoid* in a *Cripto* mutant (arrow). **p**, Extensive expression of *Hesx1* is observed for all *Cripto* mutants in the ectoderm, as shown by a sagittal section (**q**); weak staining in the visceral endoderm can often be observed but is largely obscured by the ectoderm expression. **r**, *Hex* expression in the thickened visceral endoderm of a *Cripto* mutant; **s**, sagittal section shows the apparent limits of distal staining (arrowheads). **t**, *Cerberus-like* is expressed in the distal visceral endoderm of a mutant embryo (arrow); **u**, frontal section shows that the apparent distribution of staining is broad and asymmetric (arrowheads). Scale bars correspond to 0.2 mm. Abbreviations: al, allantois; anp, anterior neural plate; ave, anterior visceral endoderm; hg, hindgut; m, embryonic mesoderm; mes-met, mesencephalon-metencephalon; ntc, notochordal plate or notochord; nd, node; ps, primitive streak; som, somites; r, rhombomere; tel, telencephalon; vys, visceral yolk sac.

streak and the anterior visceral endoderm[4] (head organizing centre), and observed expression in the proximal epiblast (Fig. 3n). In contrast, expression of *Goosecoid* (*Gsc*), which marks the anterior visceral endoderm and the rostral (distal) region of the primitive streak[3], was absent or appeared in a faint proximal band (Fig. 3o). Similar results were obtained for *HNF-3β*, which is likewise expressed in the anterior visceral endoderm and rostral primitive streak[3] (data not shown). In addition, as *Cripto* expression marks the primitive streak, we performed β-galactosidase staining of mutant embryos at 6.75 d.p.c. and found that staining was always absent (data not shown).

Finally, we investigated whether head organizing activities are affected in *Cripto* mutants by examining several markers that are normally expressed in the anterior visceral endoderm during early gastrulation. Expression of *Hesx1* (also known as *Rpx*), which marks the anterior visceral endoderm and is subsequently induced in the adjacent neuroectoderm[1,19], was found throughout the ectodermal layer of the distal region of the egg cylinder at 6.75 d.p.c. (Fig. 3p, q); this ectopic expression significantly precedes the normal time at

which *Hesx1* expression appears in the anterior neural plate of wild-type embryos. This finding suggested that head organizer activity might be mislocalized distally in *Cripto* mutants, which may be consistent with the thickened visceral endoderm at the distal tip (Fig. 2d,h,i). To confirm this, we examined expression of *Cerberus-like* (*Cer-l*), which encodes a candidate head-inducing signal[3,5], and *Hex*, which is the earliest known marker of the prospective head organizer and of anterior–posterior polarity[6]. Both of these genes were expressed in the thickened region of visceral endoderm, with a broad distribution around the distal tip that was sometimes slightly askew (Fig. 3r–u).

In summary, our analysis of *Cripto* mutants indicates that early markers of a head-organizing centre (*Hex*, *Cerberus-like*) are mislocalized in the distal visceral endoderm and, as a result, anterior neuroectoderm is induced distally. In contrast, early markers of the primitive streak (*Brachyury*, *Fgf8*) are mislocalized proximally, whereas little or no expression is observed for later markers of the distal primitive streak (*Goosecoid*, *HNF-3β*), which corresponds to the position of the trunk organizing centre and future node. These
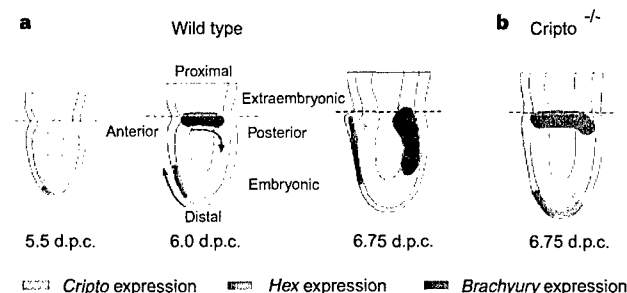
a Wild type   **b** Cripto $^{-/-}$

5.5 d.p.c.   6.0 d.p.c.   6.75 d.p.c.   6.75 d.p.c.

Cripto expression   Hex expression   Brachyury expression

Figure 4 Schematic interpretation of the Cripto mutant phenotype. **a**, Model for anterior–posterior axis formation proposed by Beddington et al. (adapted from refs 6, 8). Expression of Hex (red) and Brachyury (blue) correspond to the position of prospective anterior and posterior organizing centres, respectively; orange arrows represent putative head-inducing activities. Also shown is the expression of Cripto (hatched) at these stages, based on Fig. 1. Dashed lines indicate the embryonic/extra-embryonic boundary. **b**, Deduced locations of anterior and posterior organizing centres in Cripto mutant embryos. We propose that mislocalization of head-organizing activities accounts for the ectopic generation of anterior neuroectoderm in a distal position. Note that loss of Cripto activity results in a phenotype in the visceral endoderm, where it is not expressed, consistent with its putative role as a signalling factor, although the basis for this effect may be indirect.

findings correlate with the failure to form embryonic mesoderm, but not extra-embryonic mesoderm, and demonstrate that anterior neural fates can arise in the absence of embryonic mesoderm. Moreover, the lack of posterior neuroectoderm in Cripto mutants is consistent with a lack of signals from paraxial mesoderm that are normally required to caudalize neuroectoderm[20]. Consequently, Cripto mutant embryos display a 'head-without-trunk' phenotype that is superficially the opposite of that found in mutants for Otx2 and Lim1, which have defects in head-organizing activities[21–23]. Mislocalized distal expression of Cerberus-like has been observed in Otx2 mutants[5], and mislocalized proximal expression of Goosecoid in Otx2[22] and Lim-1 mutants[21]; however, these mutants have at least partially intact trunk-organizing activities. Furthermore, the Cripto null phenotype also differs from that of Smad2, which results in a lack of anterior–posterior asymmetry and no localized expression of markers for both head and trunk organizing centres[7]. Thus, Smad2 is required for the generation of the anterior–posterior organizing centres, whereas Cripto is required for their correct localization.

Our results support a recent model proposed to explain the formation of the anterior–posterior axis in the mouse embryo. Beddington et al. have suggested that precursors of the head- and trunk-organizing centres originate on the distal and proximal ends of the pregastrulation embryo, and that vectorial cell movements convert this pre-existing distal–proximal asymmetry into an anterior–posterior axis before gastrulation[6,8] (Fig. 4a). Our findings agree with this model as we found that Cripto is required for the correct orientation of the anterior–posterior axis. In particular, our data indicate that rotation of the anterior–posterior axis fails to occur in the absence of Cripto activity, resulting in mislocalization of the head- and trunk-organizing centres (Fig. 4b). We suggest that Cripto signalling, possibly involving its proximal–distal gradient of expression, is required for the vectorial movements that correctly orient the anterior–posterior axis, and perhaps for coordinating these cell movements in two distinct tissue layers.

Relatively little is known about the signalling activities of EGF–CFC protein products and the molecular identities of their putative receptor(s), although recombinant Cripto protein activates the Ras/Raf/MAPK pathway in cultured mammary epithelial cells[24]. Our demonstration of an essential role for Cripto in anterior–posterior

axis formation underscores the importance of this newly identified family of signalling molecules in vertebrate development. □

Methods

Gene targeting. A partial cDNA corresponding to base pairs (bp) 41 to 985 of the published Cripto sequence[9] was amplified by RT-PCR from F9 teratocarcinoma cells, and used to screen a λFIXII library constructed from 129Sv/J genomic DNA (Stratagene). Positive phage clones were screened by PCR to distinguish the authentic Cripto locus from pseudogenes[25]. To construct a targeting vector for Cripto, a 6.5-kb ApaI to EcoRI fragment was cloned into the BamHI/EcoRI sites of pPNT[26] to create the 3′ flank. The 5′ flank was cloned as a 2.6-kb XhoI to SspI fragment cloned into the NotI site of pSDKlacZpA[27], excised as a NotI/XhoI fragment and cloned into the NotI/XhoI sites of pPNT containing the 3′ flank. Note that the SspI site of the 5′ arm is located at bp 175 of the Cripto cDNA sequence in the 5′ untranslated region. The linearized construct was electroporated into TC1 ES cells[28]; targeted clones were obtained at a frequency of 13% (19/145). ES cell culture and blastocyst injection were done as described[29]. Chimaeric males obtained following blastocyst injection were bred with Black Swiss females (Taconic), and germline transmission was obtained from one targeted ES clone. The targeted mutation has been maintained through backcrossing with outbred Black Swiss mice, and on an inbred 129/SvEv strain background; the phenotype of Cripto mutant embryos appears similar in both genetic backgrounds.

Embryo genotyping and phenotypic analysis. Staging of embryos was done according to standard criteria[30]; 0.5 d.p.c. is considered to be noon of the day of the copulatory plug. Embryos analysed at 7.5 d.p.c. and 8.5 d.p.c. were genotyped by PCR using extraembryonic tissues; for 6.75 d.p.c., over 50 embryos have been genotyped, with a strict correlation observed between the genotype and the phenotype described. PCR amplification for genotyping was done at an annealing temperature of 59 °C, using the following primers: for LacZ, 5′ CCGCGCTGTACTGGAGGCTGAAG 3′ and 5′ ATACTG-CACCGGGCGGGAAGGAT 3′; for Cripto, 5′ GCGCACGCTTCCAACTCTA-CAATC 3′ and 5′ TTCCAAGGCAACCAGGGCTACAC 3′ (corresponding to bp 2,464–2,999 of the genomic sequence[25]). Histological analysis of intact decidua was performed as described[29].

In situ hybridization and probes. Whole-mount in situ hybridization was carried out as previously described[11] using the indicated probes, except that embryos were processed in 0.74-μm mesh inserts (Costar) for ease of handling[6]. For each probe, at least five, and usually six or more, Cripto mutant embryos were examined at each developmental stage analysed. Whole-mount embryos were stained for β-galactosidase activity as described[27].

1. Thomas, P. & Beddington, R. S. P. Anterior primitive endoderm may be responsible for patterning the anterior neural plate in the mouse embryo. Curr. Biol. 6, 1487–1496 (1996).
2. Varlet, I., Collignon, J. & Robertson, E. J. nodal expression in the primitive endoderm is required for specification of the anterior axis during mouse gastrulation. Development 124, 1033–1044 (1997).
3. Belo, J. A. et al. Cerberus-like is a secreted factor with neutralizing activity expressed in the anterior primitive endoderm of the mouse gastrula. Mech. Dev. 68, 45–57 (1997).
4. Tam, P. P. & Behringer, R. R. Mouse gastrulation: the formation of a mammalian body plan. Mech. Dev. 68, 3–25 (1997).
5. Biben, C. et al. Murine cerberus homologue mCer-1: a candidate anterior patterning molecule. Dev. Biol. 194, 135–151 (1998).
6. Thomas, P. Q., Brown, A. & Beddington, R. S. P. Hex homeobox gene revealing peri-implantation asymmetry in the mouse embryo and an early transient marker of endothelial cell precursors. Development 125, 85–94 (1998).
7. Waldrip, W. R., Bikoff, E. K., Hoodless, P. A., Wrana, J. L. & Robertson, E. J. Smad2 signaling in extraembryonic tissues determines anterior–posterior polarity of the early mouse embryo. Cell 92, 797–808 (1998).
8. Beddington, R. S. P. & Robertson, E. J. Anterior patterning in mouse. Trends Genet. 14, 277–284 (1998).
9. Dono, R. et al. The murine cripto gene: expression during mesoderm induction and early heart morphogenesis. Development 118, 1157–1168 (1993).
10. Johnson, S. E., Rothstein, J. L. & Knowles, B. B. Expression of epidermal growth factor family gene members in early mouse development. Dev. Dyn. 201, 216–226 (1994).
11. Shen, M. M., Wang, H. & Leder, P. A differential display strategy identifies Cryptic, a novel EGF-related gene expressed in the axial and lateral mesoderm during mouse gastrulation. Development 124, 429–442 (1997).
12. Zhang, J., Talbot, W. S. & Schier, A. F. Positional cloning identifies zebrafish one-eyed pinhead as a permissive EGF-related ligand required during gastrulation. Cell 92, 241–251 (1998).
13. Kinoshita, N., Minshull, J. & Kirschner, M. W. The identification of two novel ligands of the FGF receptor by a yeast screening method and their activity in Xenopus development. Cell 83, 621–630 (1995).
14. Xu, C., Liguori, G., Adamson, E. D. & Persico, M. G. Specific arrest of cardiogenesis in cultured embryonic stem cells lacking Cripto-1. Dev. Biol. 196, 237–247 (1998).
15. Candia, A. F. et al. Mox-1 and Mox-2 define a novel homeobox gene subfamily and are differentially expressed during early mesodermal patterning in mouse embryos. Development 116, 1123–1136 (1992).

16. Ang, S. L., Conlon, R. A., Jin, O. & Rossant, J. Positive and negative signals from mesoderm regulate the expression of mouse Otx2 in ectoderm explants. *Development* **120**, 2979–2989 (1994).
17. Tao, W. & Lai, E. Telencephalon-restricted expression of BF-1, a new member of the HNF-3/fork head gene family, in the developing rat brain. *Neuron* **8**, 957–966 (1992).
18. Crossley, P. H. & Martin, G. R. The mouse Fgf8 gene encodes a family of polypeptides and is expressed in regions that direct outgrowth and patterning in the developing embryo. *Development* **121**, 439–451 (1995).
19. Hermesz, E., Mackem, S. & Mahon, K. A. Rpx: a novel anterior-restricted homeobox gene progressively activated in the prechordal plate, anterior neural plate and Rathke's pouch of the mouse embryo. *Development* **122**, 41–52 (1996).
20. Muhr, J., Jessell, T. M. & Edlund, T. Assignment of early caudal identity to neural plate cells by a signal from caudal paraxial mesoderm. *Neuron* **19**, 487–502 (1997).
21. Shawlot, W. & Behringer, R. R. Requirement for Lim1 in head-organizer function. *Nature* **374**, 425–430 (1995).
22. Ang, S. L. *et al.* A targeted mouse Otx2 mutation leads to severe defects in gastrulation and formation of axial mesoderm and to deletion of rostral brain. *Development* **122**, 243–252 (1996).
23. Rhinn, M. *et al.* Sequential roles for Otx2 in visceral endoderm and neuroectoderm for forebrain and midbrain induction and specification. *Development* **125**, 845–856 (1998).
24. Kannan, S. *et al.* Cripto enhances the tyrosine phosphorylation of Shc and activates mitogen-activated protein kinase (MAPK) in mammary epithelial cells. *J. Biol. Chem.* **272**, 3330–3335 (1997).
25. Liguori, G. *et al.* Characterization of the mouse Tdgf1 gene and Tdgf pseudogenes. *Mamm. Genome* **7**, 344–348 (1996).
26. Tybulewicz, V. L., Crawford, C. E., Jackson, P. K., Bronson, R. T. & Mulligan, R. C. Neonatal lethality and lymphopenia in mice with a homozygous disruption of the c-abl proto-oncogene. *Cell* **65**, 1153–1163 (1991).
27. Shalaby, F. *et al.* Failure of blood-island formation and vasculogenesis in Flk-1 deficient mice. *Nature* **376**, 62–66 (1995).
28. Deng, C., Wynshaw-Boris, A., Zhou, F., Kuo, A. & Leder, P. Fibroblast growth factor receptor 3 is a negative regulator of bone growth. *Cell* **84**, 911–921 (1966).
29. Deng, C.-X. *et al.* Murine FGFR-1 is required for early postimplantation growth and axial organization. *Genes Dev.* **8**, 3045–3057 (1994).
30. Downs, K. M. & Davies, T. Staging of gastrulating mouse embryos by morphological landmarks in the dissecting microscope. *Development* **118**, 1255–1266 (1993).

Sexually dimorphic development of the mammalian reproductive tract requires *Wnt-7a*

Brian A. Parr* & **Andrew P. McMahon**

Department of Molecular and Cellular Biology, The Biolabs, Harvard University, 16 Divinity Avenue, Cambridge, Massachusetts 02138, USA

An important feature of mammalian development is the generation of sexually dimorphic reproductive tracts from the Müllerian and Wolffian ducts. In females, Müllerian ducts develop into the oviduct, uterus, cervix and upper vagina, whereas Wolffian ducts regress. In males, testosterone promotes differentiation of Wolffian ducts into the epididymis, vas deferens and seminal vesicle. The Sertoli cells of the testes produce Müllerian-inhibiting substance, which stimulates Müllerian duct regression in males[1–4]. The receptor for Müllerian-inhibiting substance is expressed by mesenchymal cells underlying the Müllerian duct that are thought to mediate regression of the duct[5–7]. Mutations that inactivate either Müllerian-inhibiting substance or its receptor allow development of the female reproductive tract in males[8–12]. These pseudohermaphrodites are frequently infertile because sperm passage is blocked by the presence of the female reproductive system[9,10,12]. Here we show that male mice lacking the signalling molecule Wnt-7a fail to undergo regression of the Müllerian duct as a result of the absence of the receptor for Müllerian-inhibiting substance. *Wnt7a*-deficient females are infertile because of abnormal development of the oviduct and uterus, both of which are

Müllerian duct derivatives. Therefore, we propose that signalling by Wnt-7a allows sexually dimorphic development of the Müllerian ducts.

Wnt-7a is a member of the Wnt family of secreted glycoproteins, which function as signalling molecules in several developmental contexts[13]. We have described previously the generation of a mutant *Wnt-7a* allele by homologous recombination in mouse embryonic stem cells[14]. Mice homozygous for the targeted allele exhibit defects in limb patterning, but are otherwise fully viable[14,15]. However, we did not observe pregnancies when homozygous *Wnt-7a*-mutant males or females were mated.

To study the *Wnt-7a*-associated sterility, we dissected the reproductive tracts of postnatal mice. The Müllerian duct derivatives of homozygous *Wnt-7a*-mutant neonate or adult females, as compared with their wild-type or heterozygous littermates, failed to differentiate properly. At the neonatal stage, Müllerian ducts are present but there are no signs of coiled oviducts in homozygous *Wnt-7a*-mutant females (Fig. 1a–c). In addition, the uterine wall is thinner and notably less muscular than that of the wild-type mice (Fig. 1c). Adult *Wnt-7a*$^{-/-}$ females still lack visibly coiled oviducts,
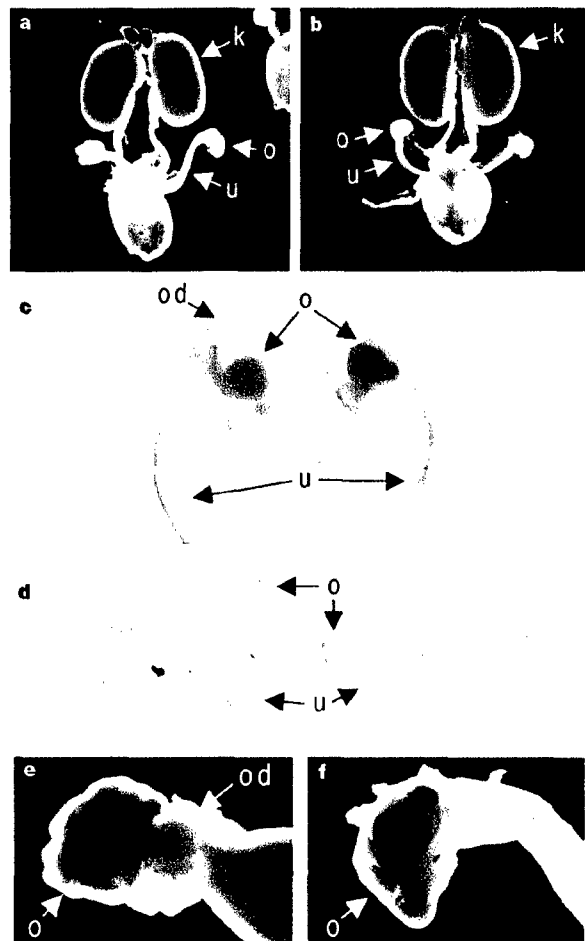
Figure 1 Development of female reproductive tracts in wild-type and *Wnt-7a*-mutant mice. **a, b,** The urogenital region of **a**, wild-type and **b**, mutant neonates. k, kidney; o, ovary; u, uterus. **c,** Coiled oviducts (od) are seen in wild-type (left) but not in mutant (right) neonatal mice. The uterus of the mutants is less muscular and more slender than the wild-type uterus. **d,** Adult reproductive tracts of wild-type (left) and homozygous *Wnt-7a*-mutant (right) females. The wild-type uterus is substantially larger and thicker than the mutant uterus. However, ovarian development is similar. **e, f,** The coiled oviduct, which is visible in wild-type mice (**e**), is not apparent in *Wnt-7a* mutants (**f**). Comparative photographs of wild-type and mutant siblings in all figures are taken at the same magnification.

* Present address: MCD Biology, University of Colorado, Campus Box 347, Boulder, Colorado 80309, USA.

Conserved requirement for *EGF–CFC* genes in vertebrate left–right axis formation

Yu-Ting Yan,[1,3] Kira Gritsman,[2,3] Jixiang Ding,[1] Rebecca D. Burdine,[2] JoMichelle D. Corrales,[2]
Sandy M. Price,[1] William S. Talbot,[2] Alexander F. Schier,[2,4] and Michael M. Shen[1,4]

[1]Center for Advanced Biotechnology and Medicine (CABM) and Department of Pediatrics, University of Medicine
and Dentistry of New Jersey–Robert Wood Johnson Medical School, Piscataway, New Jersey 08854 USA; [2]Developmental
Genetics Program, Skirball Institute of Biomolecular Medicine, Department of Cell Biology, New York University School
of Medicine, New York, New York 10016 USA

Specification of the left–right (L-R) axis in the vertebrate embryo requires transfer of positional information
from the node to the periphery, resulting in asymmetric gene expression in the lateral plate mesoderm. We
show that this activation of L-R lateral asymmetry requires the evolutionarily conserved activity of members
of the *EGF–CFC* family of extracellular factors. Targeted disruption of murine *Cryptic* results in L-R laterality
defects including randomization of abdominal situs, hyposplenia, and pulmonary right isomerism, as well as
randomized embryo turning and cardiac looping. Similarly, zebrafish *one-eyed pinhead* (*oep*) mutants that
have been rescued partially by mRNA injection display heterotaxia, including randomization of heart looping
and pancreas location. In both *Cryptic* and *oep* mutant embryos, L-R asymmetric expression of
Nodal/cyclops, *Lefty2/antivin*, and *Pitx2* does not occur in the lateral plate mesoderm, while in *Cryptic*
mutants *Lefty1* expression is absent from the prospective floor plate. Notably, L-R asymmetric expression of
Nodal at the lateral edges of the node is still observed in *Cryptic* mutants, indicating that L-R specification
has occurred in the node but not the lateral plate. Combined with the previous finding that *oep* is required for
nodal signaling in zebrafish, we propose that a signaling pathway mediated by *Nodal* and *EGF–CFC* activities
is essential for transfer of L-R positional information from the node.

[Key Words: Left–right asymmetry; isomerism; heterotaxia; node; lateral plate mesoderm; *Nodal*]

Of the three major body axes, the left–right (L-R) axis is the last to be determined during vertebrate embryogenesis. The initial specification of the L-R axis is likely to begin during late stages of gastrulation, but tissue-specific manifestations of morphological L-R asymmetry become apparent much later in development, throughout organogenesis into the late fetal period (for review, see Ramsdell and Yost 1998; Beddington and Robertson 1999). In all vertebrates, the first overt appearance of L-R asymmetry occurs during early somitogenesis, with an initial rightward bending of the linear heart tube that presages the direction of cardiac looping. In the mouse, another early sign of laterality is the direction of embryonic turning that inverts the three primary germ layers of the embryo. Most morphological L-R asymmetry arises at later stages of organogenesis, when unilateral tissues such as the stomach are positioned on one side, or when bilateral paired tissues such as the lung form asymmetrically. Defects in this process of L-R specification can lead to highly pleiotropic effects, including L-R reversals of organ position (inverted situs), mirror image symmetry of bilaterally asymmetric tissues (isomerism), and/or random and independent occurrence of laterality defects in different tissues (heterotaxia).

Recent molecular genetic studies performed in chick, frog, zebrafish, and mouse systems have shown that tissue-specific laterality decisions are mediated by a pathway of regulatory genes that acts during gastrulation and early postgastrulation stages of embryogenesis. These studies have led to a conceptual pathway for L-R axis determination, in which an initial event that breaks L-R symmetry is believed to occur in or around the embryonic node and its derivatives. The resulting L-R positional information is transferred outward to the lateral plate mesoderm, where it is interpreted to generate the situs of individual tissues (for review, see Harvey 1998; Ramsdell and Yost 1998; Beddington and Robertson 1999; King and Brown 1999). Notably, several members of this regulatory pathway are themselves expressed in a

[3]These authors contributed equally to this work.
[4]Corresponding authors.
E-MAIL schier@saturn.med.nyu.edu; FAX (212) 263-7760.
E-MAIL mshen@cabm.rutgers.edu; FAX (732) 235-5318.

L-R asymmetric pattern on the left side of the embryo, in particular the left lateral plate mesoderm.

Several genes in the L-R pathway have roles that appear evolutionarily conserved among vertebrates, including *Nodal* (Levin et al. 1995; Collignon et al. 1996; Lowe et al. 1996; Lustig et al. 1996; Lohr et al. 1997; Sampath et al. 1997; Rebagliati et al. 1998) and *Lefty2* (Meno et al. 1996,1997; Bisgrove et al. 1999; Thisse and Thisse 1999), which encode distant members of the transforming growth factorβ (TGF-β) superfamily, and are asymmetrically expressed in the left lateral plate mesoderm. Another conserved asymmetrically expressed gene is the *Pitx2* homeobox gene, which has been proposed to represent a primary regulator of tissue-specific L-R laterality because it is expressed on the left side of many tissues (Logan et al. 1998; Piedra et al. 1998; Ryan et al. 1998; Yoshioka et al. 1998; Campione et al. 1999). In contrast, there are several apparent differences between vertebrate systems that have complicated our understanding of the L-R pathway. For example, many genes that display transient asymmetry of expression in the chick are not asymmetrically expressed in the mouse, including *activin βB*, *activin receptor IIA*, and *Sonic hedgehog* (*shh*) (Harvey 1998; Ramsdell and Yost 1998; Beddington and Robertson 1999).

We show that L-R axis formation requires the evolutionarily conserved activity of members of the *EGF–CFC* gene family. The *EGF–CFC* family is comprised of mammalian *Cryptic* and *Cripto*, frog *FRL-1*, and zebrafish *one-eyed pinhead* (*oep*) and encodes extracellular proteins containing a divergent EGF-like motif and a novel cysteine-rich CFC motif (Shen et al. 1997; Zhang et al. 1998). We find that targeted disruption of mouse *Cryptic* results in L-R laterality defects including randomization of abdominal situs, pulmonary right isomerism, and vascular heterotaxia, as well as randomized embryo turning and cardiac looping. In parallel studies, we show that partial rescue of *oep* mutant embryos by *oep* mRNA injection results in randomization of the direction of heart looping and location of the pancreas, revealing that loss of *oep* function leads to heterotaxia. Notably, in both *Cryptic* and *oep* mutant embryos, L-R asymmetric gene expression does not occur in the lateral plate mesoderm. Based on recent studies indicating that EGF–CFC proteins act as essential cofactors for Nodal (Gritsman et al. 1999), we propose that a signaling pathway mediated by Nodal and EGF–CFC proteins is required for activation of L-R asymmetric gene expression in the lateral plate mesoderm.

Results

Targeted disruption of Cryptic

Previous mutational analyses have revealed that *oep* and *Cripto* have essential requirements prior to gastrulation (Schier et al. 1997; Ding et al. 1998; Gritsman et al. 1999), but it has been unclear if the later expression of *EGF–CFC* genes reflects a role in postgastrulation processes. In particular, *oep* is expressed in the lateral plate mesoderm and forebrain during early somitogenesis (Zhang et al. 1998), and *Cryptic* is expressed in the lateral plate mesoderm, node, notochordal plate, and prospective floor plate from head-fold stages through approximately the six to eight somite stage (Shen et al. 1997). The expression of *oep* and *Cryptic* is symmetric in the lateral plate and precedes the asymmetric expression of genes such as *Nodal/cyclops*, *Lefty2/antivin* and *Pitx2*.

To determine the biological function of *Cryptic*, we performed targeted gene disruption. The *Cryptic* targeting construct should result in a null mutation, because it deleted most of the third exon and the entire fourth and fifth exons of the gene, which encode two-thirds of the mature protein including the central EGF and CFC motifs (Fig. 1a–c). In addition, a second targeting construct that deleted the entire *Cryptic* coding region resulted in the identical homozygous mutant phenotype (Y.-T. Yan, S.M. Price, and M.M. Shen, unpubl.). Homozygosity for the targeted *Cryptic* mutation resulted in neonatal lethality in the first 2 weeks after birth, apparently because of cardiac defects (see below); to date, only five homozygotes (from >90) have survived past weaning. Our initial indication of a phenotypic defect in L-R laterality was that many newborn *Cryptic* homozygotes displayed a milk spot (corresponding to the stomach) on their right side, instead of the left (Fig. 1d).

L-R laterality defects in Cryptic mutant mice

To examine the L-R laterality defects of *Cryptic* homozygous mutant mice, we analyzed their gross anatomy at 18.5 days post coitum (dpc) and at neonatal stages (P0–P7) (Table 1). We found that *Cryptic* homozygotes displayed numerous laterality defects, including heterotaxia, randomization of organ situs, and isomerism of bilaterally asymmetric tissues. Thus, within the abdominal cavity, approximately half of the homozygotes (*n* = 22/49) displayed inverted situs of visceral organs including the stomach, spleen, and pancreas (Fig. 2a,b). In contrast, all homozygous animals displayed asplenia or severe hyposplenia (Fig. 2c–e); a significant proportion of homozygotes also displayed abnormal lobation or midline positioning of the liver (Table 1).

In the thoracic cavity, we found that all homozygotes showed right pulmonary isomerism (Fig. 2f,g); this phenotype is correlated frequently with hyposplenia in human patients with laterality defects (Kosaki and Casey 1998). Moreover, approximately half of the homozygotes (*n* = 24/50) displayed dextrocardia (cardiac apex pointing to the right) or mesocardia (pointing to the middle), as opposed to the normal levocardia (Fig. 2h–j). Regardless of cardiac situs, nearly all homozygotes displayed cardiac abnormalities, most notably transposition of the great arteries (Fig. 2k,l), as well as severe atrial septal defects (Fig. 2m–o). Finally, we observed numerous random and uncorrelated laterality defects within the vasculature, consistent with heterotaxia (Table 1). For example, the azygos vein could be located on the left side (as it is in the wild type), on the right, or bilaterally (Fig. 2p–r).

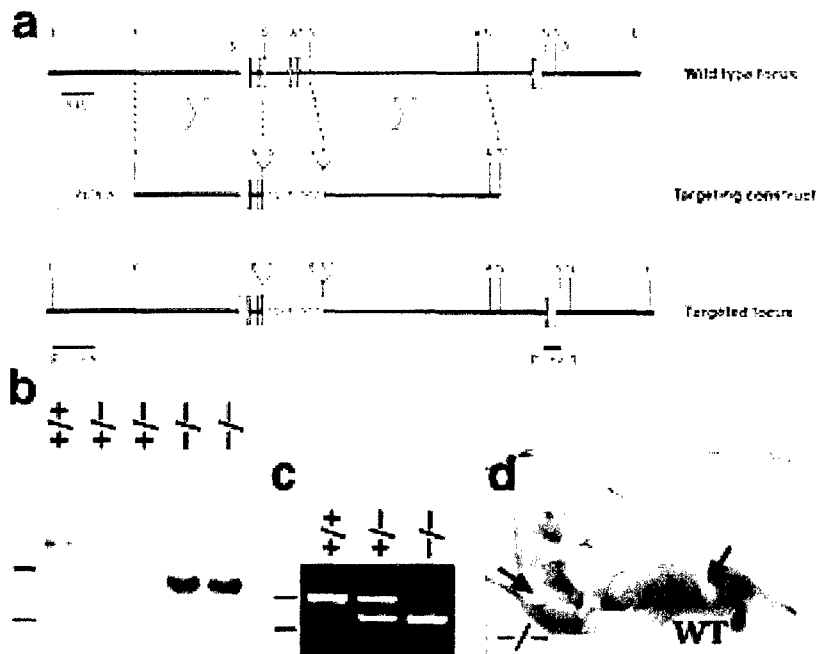The L-R laterality defects observed in neonatal *Cryptic*

Figure 1. Targeted disruption of *Cryptic*. (*a*) Homologous recombination with the targeting vector results in deletion of exons 4 and 5, as well as most of exon 3; exons are shown as boxes, with the coding region in dark gray. (A) *Avr*II; (E) *Eco*RI; (N) *Nhe*I; (S) *Sma*I; (X) *Xba*I. (*b*) Southern blotting using the 5'-flanking probe. A detects an 18-kb *Eco*RI fragment from the wild-type genomic locus and an 8.5-kb fragment from the targeted allele in progeny of F$_1$ heterozygous intercrosses; dashes (*left*) indicate positions of markers at 5 and 10 kb. (*c*) PCR analysis of visceral yolk sac DNA from 7.5-dpc embryos, showing amplification of an 860-bp band corresponding to *Cryptic* and a 735-bp fragment corresponding to *neo*; markers at 615 and 861 bp are indicated as above. (*d*) Neonatal mice with milk spots on the right side (–/–) and left side (WT).

homozygotes were paralleled by phenotypic defects observed in early embryogenesis. At 8.5–9.5 dpc, *Cryptic* homozygous embryos were indistinguishable from their wild-type littermates except for randomization of cardiac looping and embryo turning (*n* = 21/45), with these two phenotypes highly correlated (Fig. 2s–u). Because *Cryptic* is expressed in the notochordal plate and prospective floor plate, and laterality defects are frequently associated with node and notochord defects (e.g., Danos and Yost 1996; Dufort et al. 1998; King et al. 1998; Melloy et al. 1998), we investigated potential axial midline defects by skeletal staining of homozygous neonates (*n* = 6), histological sections at 10.5 dpc (*n* = 3), and in situ hybridization with *Shh*, followed by sectioning (*n* = 3). No evidence for axial midline defects was observed (data not shown).

Absence of lateral L-R asymmetric gene expression in Cryptic *mutant embryos*

To determine the basis for L-R patterning defects in *Cryptic* mutants, we performed in situ hybridization on gastrulation and early somite-stage embryos (up to 10 somites), using probes for *Nodal, Lefty1, Lefty2*, and *Pitx2*, which are asymmetrically expressed at these stages. First, we examined expression of *Lefty1* and *Lefty2*, which are asymmetrically expressed at 2–10 somites in the left prospective floor plate and left lateral plate mesoderm, respectively (Meno et al. 1997, 1998)(Fig. 3a,b,c,f). We found that *Cryptic* homozygous embryos lacked all expression of *Lefty1* (*n* = 12) and *Lefty2* (*n* = 9) at these stages (Fig. 3c,d,g,h); however, an earlier phase of symmetric *Lefty2* expression in newly formed mesoderm during primitive streak stages was un-

Table 1. *Phenotype of* Cryptic *homozygous mice*

Phenotype	Number of mutant/total (%)
Abdominal tissues	
Visceral situs	22/49 inverted (45%)
Spleen	49/49 asplenic/hyposplenic (100%)
Liver	11/27 abnormal (41%)
Abdominal vasculature	
Branching of inferior vena cava	16/25 abnormal (64%)
Position of renal veins	4/19 left anterior (21%)
Thoracic tissues	
Cardiac apex	18/50 dextrocardia, 6/50 mesocardia (48%)
Cardiac malformation	14/16 septal defects (88%); 11/11 transposition of great arteries (100%)
Atrial shape	23/34 right isomerism, 1/34 left (71%)
Lung bronchi	50/50 bilateral eparterial (100%)
Lung lobes	50/50 right isomerism (100%)
Thoracic vasculature	
Aorta relative to pulmonary artery	44/50 aorta ventral, 5/50 adjacent (98%)
Aortic arching	12/29 right (41%)
Position of azygos vein	5/30 right, 6/30 bilateral (37%)
Position of inferior vena cava	4/33 left, 19/33 bilateral (70%)

Phenotypes were scored in mice at 18.5 dpc (*n* = 6) and in neonates at <1 week of age (*n* = 44). Not all phenotypes were scored in each mouse. Unless indicated otherwise in the text, the occurrences of these phenotypes were not noticeably correlated with each other.
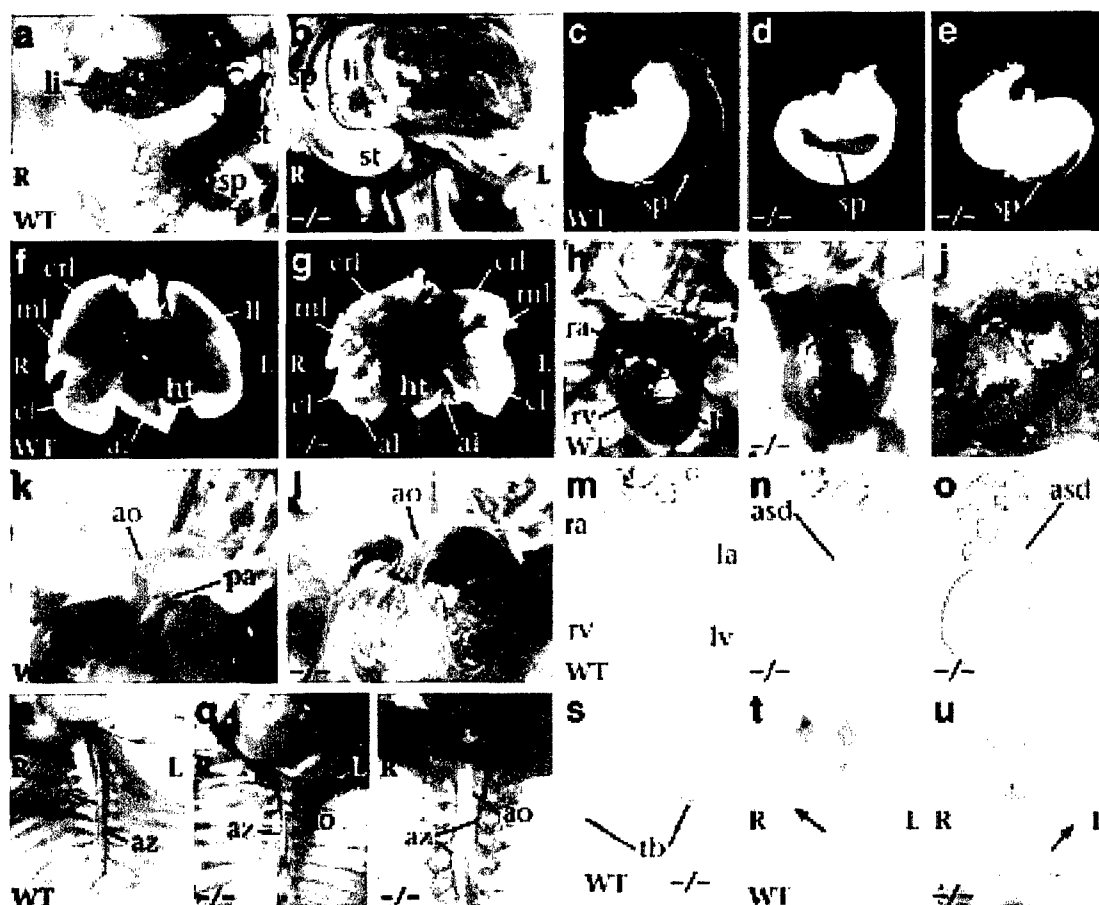
Figure 2. L-R laterality defects in *Cryptic* null mutants. (*a–r*) Ventral views of neonatal mice; in all panels, *left* (L) and *right* (R) are as indicated. Abdominal cavity of wild type (*a*) and mutant (*b*) with inverted situs and hyposplenia. Stomach and spleen from wild type (*c*), mutant with normal situs (*d*), and mutant with inverted abdominal situs (*e*). Heart and lung lobes of wild type (*f*) and mutant (*g*) with right pulmonary isomerism. Heart positions of wild type with normal levocardia (*h*), and mutants with mesocardia (*i*) and dextrocardia (*j*); note correlation with altered size of the atrial chambers. High-power view of cardiac arterial relationships. In the wild type (*k*), the aorta is dorsal to the pulmonary artery and connects to the left ventricle; in the mutant (*l*), the aorta is ventral and connects to the right ventricle, as shown following injection of blue dye into the right ventricle, consistent with transposition of the great arteries. Sections through hearts of wild type (*m*), and two mutants (*n,o*) that show an atrial septal defect. Position of the azygos vein and direction of aortic arching. In the wild type (*p*), the azygos vein is located on the *left*, and the aorta arches leftward; in the mutant (*q*), the azygos vein crosses over to the *right* and the aorta arches rightward; in the mutant (*r*), there is a bilateral azygos vein while the aorta arches leftward. (*s*) Lateral views of 8.5-dpc embryos, showing altered direction of embryo turning in the mutant. (*t,u*) Ventral views of 10-somite-stage embryos, with arrows indicating direction of cardiac looping in the wild type (*t*) and *Cryptic* mutant (*u*). (al) accessory lobe; (ao) aorta; (asd) atrial septal defect; (az) azygos vein; (cl) caudal lobe; (crl) cranial lobe; (ht) heart; (la) left atrium; (li) liver; (ll) left lung; (lv) left ventricle; (ml) medial lobe; (pa) pulmonary artery; (ra) right atrium; (rv) right ventricle; (sp) spleen; (st) stomach; (tb) tailbud.

affected (data not shown). Next, we examined expression of the homeobox gene *Pitx2*, which is found symmetrically in Rathke's pouch and asymmetrically in the left lateral plate mesoderm and left foregut endoderm from six to eight somites continuing through 9.5 dpc (Ryan et al. 1998; Yoshioka et al. 1998) (Fig. 3i,j). In *Cryptic* mutants at 8.5 and 9.5 dpc (*n* = 16), *Pitx2* expression was still observed in Rathke's pouch but not in the asymmetric domains (Fig. 3k,l).

Finally, we examined expression of *Nodal*, which is found at the lateral boundaries of the node at head-fold and early somite stages, with a transient phase of L-R asymmetry at four to eight somites, and in the left lateral plate mesoderm at approximately two to eight somites (Collignon et al. 1996; Lowe et al. 1996) (Fig. 3m,n). In *Cryptic* mutants (*n* = 41), *Nodal* expression was observed at the lateral boundaries of the node but was never detected in the lateral plate mesoderm (Fig. 3o,p). Notably, the markedly asymmetric expression of *Nodal* at the edges of the node at four to eight somites was still observed in the *Cryptic* mutant embryos (*n* = 29; Fig. 3q–s). Thus, our in situ hybridization results indicate that L-R
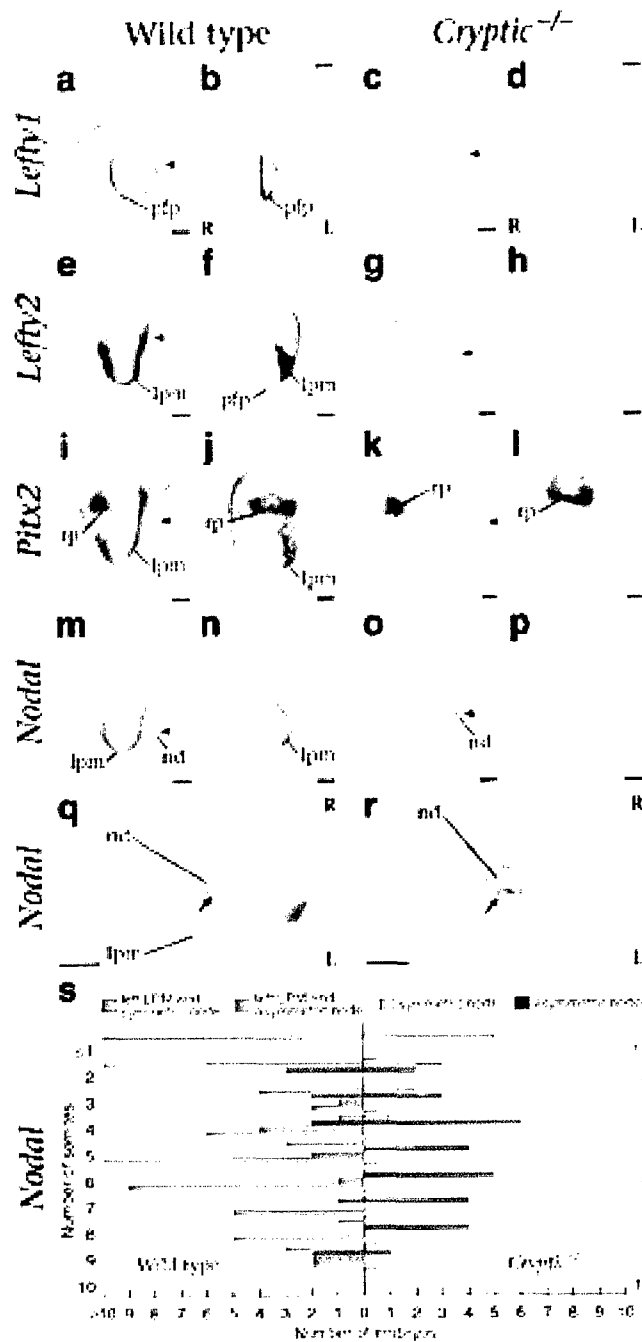
Figure 3. Expression of L-R pathway genes in *Cryptic* homozygous mutant embryos. (*a–p*) Lateral and frontal views of early somite stage mouse embryos following whole-mount in situ hybridization. Left (L) and right (R) are as shown, and the position of the node is indicated by an arrowhead. Expression of *Lefty1* is detected in the prospective floor plate of wild type (*a,b*) but not mutant embryos (*c,d*). Expression of *Lefty2* is detected in the left lateral plate mesoderm and weakly in the prospective floor plate of wild type (*e,f*) but not *Cryptic* homozygotes (*g,h*). *Pitx2* expression is observed symmetrically in Rathke's pouch in both wild type (*I,j*) and mutant (*k,l*) embryos, but asymmetric expression in the left lateral plate mesoderm is observed only in the wild type. *Nodal* expression is detected in the node of both wild-type (*m,n*) and mutant (*o,p*) embryos; left lateral plate expression is observed only in the wild type. High-power caudal views of the node in wild-type (*q*) and *Cryptic* homozygote (*r*) show asymmetric expression of *Nodal*. (*s*) Graphical representation of *Nodal* in situ hybridization results. The numbers of wild-type and *Cryptic* mutant embryos analyzed with the indicated *Nodal* expression patterns are graphed according to somite stage. (lpm) lateral plate mesoderm; (nd) node; (pfp) prospective floor plate; (rp) Rathke's pouch.

laterality has been initiated within the node but not in the lateral plate mesoderm.

Heterotaxia in oep mutant fish

To determine if the function of *EGF–CFC* genes in L-R determination is conserved in vertebrates, we studied the role of the zebrafish *oep* gene. Previous studies have shown that *oep* is required for formation of mesoderm,

endoderm, prechordal plate, and ventral neuroectoderm, correlating with the expression of *oep* in the progenitors of these cell types (Schier et al. 1997; Zhang et al. 1998; Gritsman et al. 1999). During somitogenesis, *oep* is also expressed in the left and right lateral plate, where progenitors of the heart and other organs are located in wild-type embryos (Serbedzija et al. 1998; Zhang et al. 1998). The potential role of *oep* in these territories cannot be analyzed in *oep* mutants, because mutant embryos lack

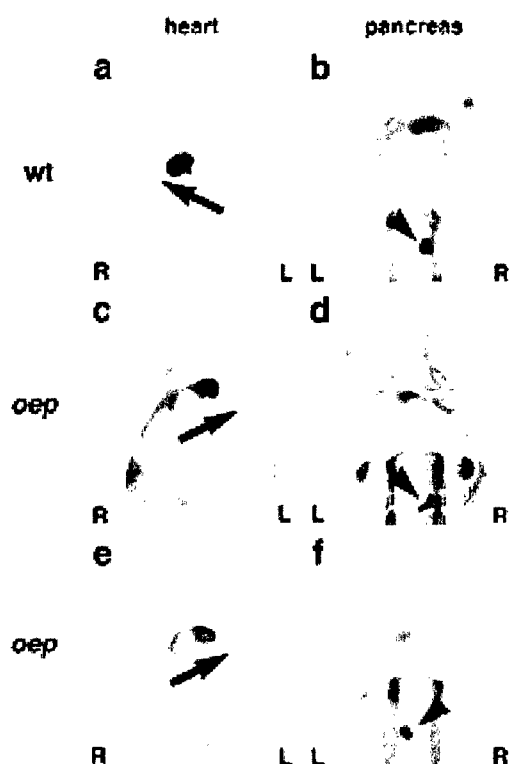**Figure 4.** Heart looping and location of the pancreas in *oep* mutants. Ventral (*a,c,e*) and dorsal views (*b,d,f*) of embryos upon immunohistochemistry with MF20 antibody (Bader et al. 1982) and RNA in situ hybridization with *insulin* probe (Milewski et al. 1998); anterior is up. (*a,b*) Wild-type embryo; (*c,d* and *e,f*) two examples of maternal-zygotic *oep* mutant embryos rescued by injection of *oep* mRNA. Note the normal development of eyes and trunk muscle (*d,f*) in rescued embryos [maternal–zygotic *oep* mutants show cyclopia and absence of trunk muscle (Gritsman et al. 1999)]. The arrow indicates heart looping from the atrium (weaker staining, posteriorly) to the ventricle (stronger staining, anteriorly); note right looping in *a* and left looping in *c* and *e*. The arrowhead indicates position of pancreas on *right* (*b,d*) or *left* (*f*) side. We note that the direction of cardiac looping in rescued mutants did not significantly affect their survival to adulthood [50/70 (71%) of right-looping embryos, 46/53 (87%) of left-looping embryos, and 2/6 (33%) of nonlooping embryos survived].

endodermal derivatives and heart (Schier et al. 1997; Gritsman et al. 1999). To circumvent this limitation, we examined the phenotype of maternal–zygotic *oep* (MZ*oep*) embryos whose early defects were rescued by *oep* mRNA injection (Fig. 4). Injected mRNA is present throughout gastrulation (data not shown) and is sufficient to completely rescue the formation of endoderm, mesoderm, axial midline, and ventral neuroectoderm (Fig. 4c–f), but is apparently insufficient to complement the loss of *oep* activity at later stages. Using morphological criteria and marker gene expression, we found that heart and pancreas form, but that the direction of heart looping and the location of the pancreas are randomized with respect to the L-R axis of the embryo (Fig. 4c–f;

Table 2). More than 81% (48/59) of *oep* mutant embryos that display abnormal heart asymmetry during embryogenesis survive to adulthood, demonstrating that mRNA injection rescues the development and function of all essential organs. Notably, there was no correlation between abnormal heart asymmetry and the location of the pancreas, revealing that loss of *oep* function leads to heterotaxia.

Absence of L-R asymmetric gene expression in oep mutants

To determine the onset of the L-R patterning defect in *oep* mutants, we performed in situ hybridization on somite-stage embryos using probes for *cyclops*, *antivin* (a member of the *lefty* family), and *pitx2*, which are all asymmetrically expressed in the lateral plate mesoderm (Rebagliati et al. 1998; Campione et al. 1999; Thisse and Thisse 1999). Analogous to *Cryptic* mouse mutants, we never detected the normal asymmetric expression of these markers, despite wild-type expression in other regions of the embryo (Fig. 5) . Importantly, asymmetric expression is not initiated, revealing a role for *oep* in the induction of lateral plate asymmetry.

Discussion

Our comparative mutational analyses have shown that homozygous *Cryptic* null mutant mice and partially res-

Table 2. *Direction of heart looping and location of pancreas in wild-type and* oep *mutants*

Genotype: *oep*/+ (+/+ female × ~/– male)
Injected mRNA: *lacZ*
Total no. embryos: 96

Pancreas (insulin)		Heart (MF20)		
		L	M	R
R	83 (86.5%)	2 (2.1%)	0	81 (84.3%)
M	6 (6.2%)	0	4 (4.2%)	2 (2.1%)
L	7 (7.3%)	4 (4.2%)	0	3 (3.1%)

Genotype: *oep*/+ (+/+ female × ~/– male)
Injected mRNA: *oep*
Total no. embryos: 108

Pancreas (insulin)		Heart (MF20)		
		L	M	R
R	90 (83.3%)	6 (5.5%)	3 (2.8%)	81 (75.0%)
M	4 (3.7%)	2 (1.9%)	0	2 (1.9%)
L	14 (13.0%)	9 (8.3%)	0	5 (4.6%)

Genotype: *oep*/*oep* (–/– female × –/– male)
Injected mRNA: *oep*
Total no. embryos: 106

Pancreas (insulin)		Heart (MF20)		
		L	M	R
R	48 (45.3%)	20 (18.9%)	1 (0.9%)	27 (25.5%)
M	7 (6.6%)	2 (1.9%)	1 (0.9%)	4 (3.8%)
L	51 (48.1%)	26 (24.5%)	1 (0.9%)	24 (22.7%)

wt   *oep*

pitx2

R **b**   R

L   L

R **d**   R

c

cyc

L   L

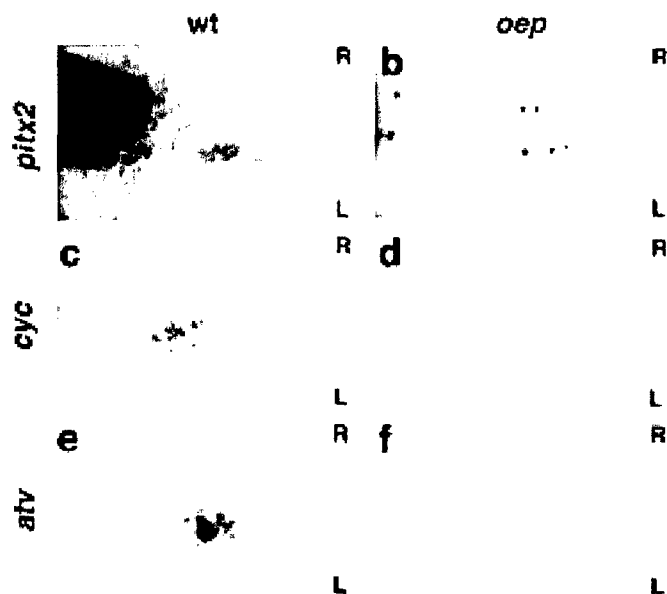**e**   R **f**   R

atv

L   L

Figure 5. Expression of L-R pathway genes in *oep* mutant embryos. Dorsal view (anterior to the *left*) of 22-somite-stage (*a–d*) and 24-somite-stage (*e,f*) embryos following whole-mount in situ hybridization with *pitx2* (*a,b*), *cyclops* (*c,d*), or *antivin* (*e,f*). Normal expression in the left lateral plate is only detected in wild-type (*a,c, oep/+* embryo injected with *oep* mRNA; *e, oep/+* embryo injected with *lacZ* mRNA) but not in maternal–zygotic *oep* mutants whose early patterning defects were rescued by *oep* mRNA injection (*b, n = 58* embryos analyzed between 14- and 24-somite stages; *d, n ≈ 67; f, n = 44*). Note the normal expression of *pitx2* in the spinal cord (*b*).

cued *oep* mutant fish both display highly penetrant L-R heterotaxia defects. Notably, in *Cryptic* as well as *oep* mutant embryos, *Nodal, Lefty2/antivin,* and *Pitx2* are not expressed in the lateral plate mesoderm, indicating that *EGF–CFC* activity is essential for asymmetric gene expression in the lateral mesoderm. Taken together, our findings with *oep* mutant fish are analogous to those for *Cryptic* mutant mice, and establish an evolutionarily conserved requirement for *EGF–CFC* genes in the establishment of L-R asymmetry in vertebrates. Interestingly, this evolutionary conservation of *EGF–CFC* activity in the L-R pathway markedly contrasts with the apparent non-conserved roles of *Fgf8* and *Shh* in the mouse and chick (Meyers and Martin 1999).

Essential function of EGF–CFC genes in L-R axis specification

Our results can be readily integrated with a general pathway for L-R axis determination in which initial L-R symmetry is broken in or around the node, and subsequent L-R positional information is transferred to the lateral plate mesoderm (Levin et al. 1995; Logan et al. 1998; Pagan-Westphal and Tabin 1998; Beddington and Robertson 1999). Given the requirement of *oep* activity for *nodal* signaling in zebrafish and the functional conservation of EGF–CFC proteins (Gritsman et al. 1999), we propose that *Cryptic* and *oep* are essential for *Nodal* signaling in L-R axis specification. Our findings indicate that *EGF–CFC* activity is required prior to the activation of L-R asymmetric gene expression in the periphery and may be involved in events downstream from an initial process that breaks L-R symmetry.

Specifically, our results are consistent with two possible models for *EGF–CFC* function in L-R axis forma-

tion (Fig. 6). In the first model, *Cryptic/oep* would be required in the lateral plate mesoderm to mediate the response to an asymmetric 'left'-determining signal emanating from the node (Fig. 6a,b). This signal might correspond to Nodal itself, as we have shown previously that EGF–CFC proteins are required for cells to respond to Nodal signals (Gritsman et al. 1999). In this scenario, Nodal signaling from the node or its derivatives cannot be received due to the absence of EGF–CFC activity in the lateral plate.

In the second model for *EGF–CFC* function, *Cryptic/oep* would be required at an earlier stage in the node or its derivatives for the generation or propagation of an asymmetric signal, which could either correspond to Nodal itself or be dependent on Nodal signaling (Fig. 6c). Defects in axial midline structures often result in L-R laterality defects and alterations in asymmetric gene expression, as seen for mouse mutations in *no turning, HNF-3β, Brachyury,* and *SIL* (Dufort et al. 1998; King et al. 1998; McIlloy et al. 1998; Izraeli et al. 1999) and for zebrafish mutations in *no tail* or *floating head* (Danos and Yost 1996; Chen et al. 1997). Although there are no apparent structural defects in the node or its derivatives in *Cryptic* and partially rescued *oep* mutants, absence of EGF–CFC activity might result in a block in Nodal signaling in the axial midline, indirectly leading to defects in the lateral plate (Fig. 6c). Of course, these models are not mutually exclusive, and *Cryptic/oep* may act in both the node and lateral plate. In either case, *EGF–CFC* activity would play an essential role in transferring L-R positional information from the node to the periphery, resulting in asymmetric *Nodal* and *Lefty2/antivin* expression in the lateral plate mesoderm, asymmetric *Lefty1* expression in the mouse floor plate, and subsequent asymmetric *Pitx2* expression, ultimately leading to specification of individual organ situs.
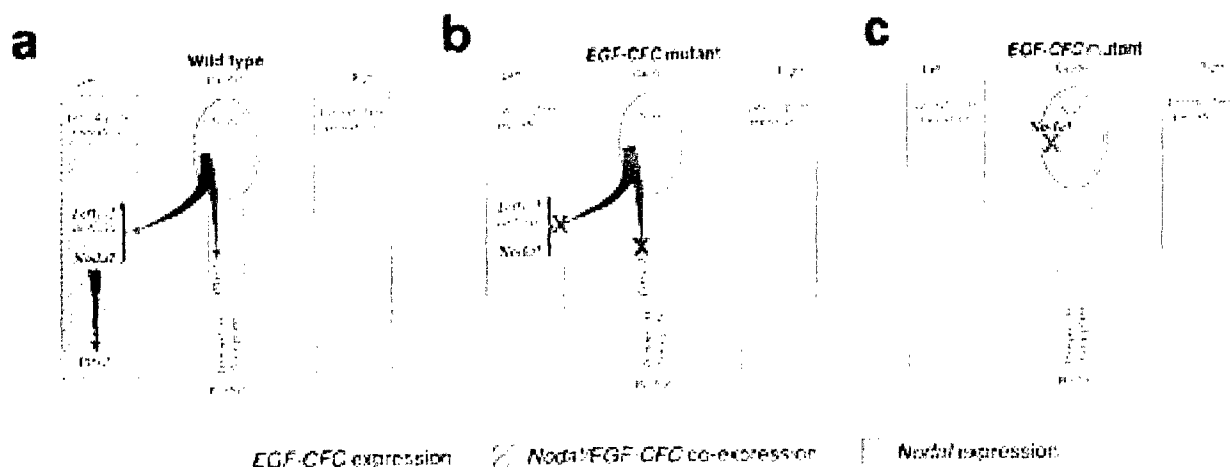
Figure 6. Schematic model for *EGF–CFC* function in L-R axis formation. (*a*) In wild-type embryos, a asymmetric signal emanating from the node activates expression of *Nodal/cyclops* and *Lefty2/antivin* in the left lateral plate mesoderm, as well as *Lefty1* in the left prospective floor plate, leading to subsequent activation of *Pitx2* and specification of organ situs. The node-derived signal could correspond to Nodal itself or to a hypothesized factor downstream of *Shh* signaling that conveys L-R positional information in the chick (Pagan-Westphal and Tabin 1998). (*b*) In this model, the response to the asymmetric node-derived signal is mediated by *Cryptic/oep*, which is symmetrically expressed in the lateral plate mesoderm. In the absence of *EGF–CFC* activity, the lateral plate and prospective floor plate do not respond to the node-derived signal, and asymmetric gene expression fails to occur, resulting in subsequent L-R laterality defects. (*c*) Here, *Cryptic/oep* is required to mediate a *Nodal* activity that is downstream of an initial L-R symmetry-breaking event in or around the node. As a consequence, L-R laterality is specified around the node but fails to be propagated to the lateral plate mesoderm.

Cryptic *mutants as a model for right isomerism/ asplenia syndrome*

In humans, the proper L-R situs of the visceral tissues is critical for their morphogenesis and/or physiological function, particularly in the cardiovascular system. In particular, children born with severe heterotaxia generally die shortly after birth, usually due to severe cardiac defects. In many cases, laterality defects in humans that result in heterotaxia can be classified into two primary categories: right isomerism associated with asplenia/hyposplenia and, conversely, left isomerism associated with polysplenia (Goldstein et al. 1998; Kosaki and Casey 1998). Our studies show that *Cryptic* mutant mice recapitulate many features of the right isomerism/asplenia syndrome, suggesting that the *Cryptic* mutant mice may represent a model for a major category of human L-R laterality defects.

Interaction of EGF–CFC genes with the Nodal signaling pathway

In contrast to the phenotype reported here for *oep*, mutations in the zebrafish *nodal* gene *cyclops* do not result in a significant incidence of heart looping defects (Chen et al. 1997). These differing laterality phenotypes of *oep* versus *cyclops* mutants may be due to redundant functions of zebrafish *nodal*-related genes in L-R axis determination. Moreover, a direct requirement for mouse *Nodal* in L-R patterning has also been difficult to establish, due to the early embryonic lethality of *Nodal* mutants, which precludes analysis of later defects. None-

theless, the L-R phenotypes of *Cryptic* and *oep* mutants, together with the phenotypes of $Nodal^{+/-}$; $HNF-3B^{+/-}$ and $Nodal^{+/-}$; $Smad2^{+/-}$ mutants (Collignon et al. 1996; Nomura and Li 1998), strongly suggest that Nodal signals are essential for L-R axis specification.

Although the Nodal signaling pathway has not been analyzed at the biochemical level, loss- and gain-of-function studies in mouse, frog, and fish suggest that during gastrulation Nodal signals may act via activin-like receptors (Hemmati-Brivanlou and Melton 1992; Armes and Smith 1997; Chang et al. 1997; New et al. 1997; Oh and Li 1997; Gu et al. 1998; Gritsman et al. 1999; Meno et al. 1999) and the transcription factor Smad2 (Baker and Harland 1996; Graff et al. 1996; Nomura and Li 1998; Waldrip et al. 1998; Weinstein et al. 1998). During germ-layer formation, Nodal signaling has also been shown to be dependent on EGF–CFC activity (Gritsman et al. 1999) and to be antagonized by members of the *Lefty* family (Bisgrove et al. 1999; Meno et al. 1999; Thisse and Thisse 1999). Therefore, it is thought that during gastrulation, Nodal signals are dependent on EGF–CFC proteins to activate activin-like receptors and Smad2, leading to the induction of *Lefty* genes and the attenuation of Nodal signaling.

Comparison of the L-R phenotypes of *Cryptic* and *oep* mutants with the defects found in *Lefty1* and *ActRIIB* mutant mice extends this model to L-R axis determination, raising the possibility that EGF–CFC proteins act universally as essential cofactors for Nodal signaling. First, mice lacking *Lefty1* (Meno et al. 1998) frequently display left pulmonary isomerism and bilateral expression of *Nodal*, *Lefty2*, and *Pitx2*. In contrast, *Cryptic*

mutants display right pulmonary isomerism and lack asymmetric gene expression in the lateral plate mesoderm. These opposing phenotypes support the notion that *Lefty1* acts by antagonizing EGF–CFC dependent *Nodal* activity during L-R determination. Secondly, the phenotype of *Cryptic* mutants superficially resembles that of *ActRIIB* mutant mice, which display right pulmonary isomerism and severe cardiac defects (Oh and Li 1997). Moreover, although *Smad2* homozygotes display early embryonic lethality due to defective specification of the anteroposterior (AP) axis (Nomura and Li 1998; Waldrip et al. 1998; Weinstein et al. 1998), a significant percentage of *Nodal*^{+/-}; *Smad2*^{+/-} compound heterozygotes display L-R laterality defects (Nomura and Li 1998), which are similar to those of *Cryptic* mutants. The greater severity of the laterality defects in *Cryptic* mice relative to those of *ActRIIB* mutants may reflect the ability of Nodal in conjunction with EGF–CFC proteins to signal through a type II receptor that is partially redundant with ActRIIB, perhaps ActRIIA (also known as ActRII). In summary, these findings indicate that Nodal signaling during L-R development is mediated by EGF–CFC proteins, activin receptors, and Smad2.

Conservation of EGF–CFC function in embryonic axis formation

The phenotypes of *Cripto* and *Cryptic* mutations in mice bear remarkable similarity to those of mutant zebrafish with different timing of *oep* activity. Specifically, complete removal of both maternal and zygotic *oep* activity (MZoep mutants) results in loss of head and trunk mesoderm, endoderm, and an incorrectly positioned AP axis (Gritsman et al. 1999), a phenotype similar to that of *Cripto* mutant mice (Ding et al. 1998). Conversely, restoration of early *oep* activity to MZoep embryos by *oep* mRNA injection rescues these defects, but the insufficient persistence of injected mRNA results in a subsequent L-R laterality defect that strongly resembles the phenotype of *Cryptic* mutants. Taken together, our results indicate that a Nodal and EGF–CFC signaling pathway is essential for both the AP and L-R axes in vertebrates, with the dual role for *oep* in both processes in fish being divided between the related genes *Cripto* and *Cryptic* in mice.

Materials and methods

Gene targeting

A murine *Cryptic* cDNA was used to screen a λFIXII library constructed from 129Sv/J genomic DNA (Stratagene), resulting in the isolation of a 21-kb genomic clone containing the entire coding region. To construct a targeting vector for *Cryptic*, a 3.5-kb *XbaI–SmaI* 5′ flank was subcloned into the *XbaI–SmaI* sites of pTKLNL (Mortensen 1999), followed by subcloning of a 5.0-kb *SmaI–NheI* 3′ flank, such that the PGK–neo and PGK–tk cassettes are in the opposite transcriptional orientation to *Cryptic*. Targeting was performed using TC1 ES cells (Deng et al. 1996), with targeted clones obtained at a frequency of 5% (4/88);

ES cell culture and blastocyst injection were performed as described previously (Ding et al. 1998). Chimeric males obtained following blastocyst injection were bred with Black Swiss females (Taconic), and germ-line transmission was obtained from one targeted ES clone; two independent lines were also derived using a different targeting vector (Y.-T. Yan, S.M. Price, and M.M. Shen, unpubl.). These targeted *Cryptic* mutations have been maintained through backcrossing with outbred Black Swiss mice; the phenotype appears similar in each line. In addition, the homozygous phenotype appears similar in a hybrid 129/SvEvTac-C57BL/6J strain background.

Mouse genotyping and phenotypic analysis

Genotyping was performed by Southern blotting or by PCR using genomic DNA prepared from tails or embryonic yolk sac. Primers for genotyping were as follows: for wild-type *Cryptic*, 5′GGAGATGGTGCCAGAGAAGTCAGC3′ and 5′AATAGGCAGGGCACACGCAGAAAC3′; for *neo*, 5′CTGCCGCGCTGTTCTCCTCTTCCT3′ and 5′ACACCCAGCCGGCCACAGTCG3′. The presence of cardiac septal defects and transposition of the great arteries was scored by injection of bromphenol blue dye into the right ventricle (Oh and Li 1997), and ventriculoarterial alignment was confirmed by histological sectioning. Cardiac histology was performed by hematoxylin-eosin staining of paraffin sections, with attention given to L-R orientation of sections. Whole-mount in situ hybridization to mouse embryos was performed as described (Ding et al. 1998), using probes for murine *Lefty1* (Meno et al. 1997), *Lefty2* (Meno et al. 1997), *Nodal* (Lowe et al. 1996), and *Pitx2* (Lanctèt et al. 1999).

Zebrafish genetics and phenotypic analysis

Homozygous *oep*[tz57]/*oep*[tz57] adults were obtained by rescue of homozygous *oep*[tz57]/*oep*[tz57] embryos with *oep* mRNA (Zhang et al. 1998; Gritsman et al. 1999). To rescue the early patterning defects of *oep* mutants, maternal-zygotic *oep*[tz57]/*oep*[tz57] embryos were injected with 25–50 pg of *oep* mRNA at the one- to four-cell stage. Heart looping was scored in live embryos and by immunohistochemistry using the MF20 antibody (Bader et al. 1982) that recognizes a myosin heavy chain. Embryos were then processed for in situ hybridization using an *insulin* antisense RNA probe (Milewski et al. 1998). Whole-mount in situ hybridization for *cyclops*, *antivin*, and *Pitx2* was performed as described (Zhang et al. 1998). Zebrafish *pitx2* was cloned by screening of a cDNA library (kindly provided by B. Appel and J. Eisen, University of Oregon, Eugene) with a PCR-amplified *pitx2* homeobox probe (R.D. Burdine; A.F. Schier, and W.S. Talbot, GenBank accession nos. AF156905 and AF156906).

References

Armes, N.A. and J.C. Smith. 1997. The ALK-2 and ALK-4 activin receptors transduce distinct mesoderm-inducing signals during early Xenopus development but do not cooperate to establish thresholds. *Development* **124:** 3797–3804.

Bader, D., T. Masaki, and D.A. Fischman. 1982. Immunochemical analysis of myosin heavy chain during avian myogenesis in vivo and in vitro. *J. Cell Biol.* **95:** 763–770.

Baker, J.C. and R.M. Harland. 1996. A novel mesoderm inducer, Madr2, functions in the activin signal transduction pathway. *Genes & Dev.* **10:** 1880–1889.

Beddington, R.S.P. and E.J. Robertson. 1999. Axis development and early asymmetry in mammals. *Cell* **96:** 195–209.

Bisgrove, B.W., J.J. Essner, and H.J. Yost. 1999. Regulation of midline development by antagonism of *lefty* and *nodal* signaling. *Development* **126:** 3253–3262.

Campione, M., H. Steinbeisser, A. Schweickert, K. Deissler, F. van Bebber, L.A. Lowe, S. Nowotschin, C. Viebahn, P. Haffter, M.R. Kuehn et al. 1999. The homeobox gene *Pitx2*: Mediator of asymmetric left–right signaling in vertebrate heart and gut looping. *Development* **126:** 1225–1234.

Chang, C., P.A. Wilson, L.S. Mathews, and A. Hemmati-Brivanlou. 1997. A Xenopus type I activin receptor mediates mesodermal but not neural specification during embryogenesis. *Development* **124:** 827–837.

Chen, J.N., F.J. van Eeden, K.S. Warren, A. Chin, C. Nusslein-Volhard, P. Haffter, and M.C. Fishman. 1997. Left-right pattern of cardiac BMP4 may drive asymmetry of the heart in zebrafish. *Development* **124:** 4373–4382.

Collignon, J., I. Varlet, and E.J. Robertson. 1996. Relationship between asymmetric *nodal* expression and the direction of embryonic turning. *Nature* **381:** 155–158.

Danos, M.C. and H.J. Yost. 1996. Role of notochord in specification of cardiac left–right orientation in zebrafish and Xenopus. *Dev. Biol.* **177:** 96–103.

Deng, C., A. Wynshaw-Boris, F. Zhou, A. Kuo, and P. Leder. 1996. Fibroblast growth factor receptor 3 is a negative regulator of bone growth. *Cell* **84:** 911–921.

Ding, J., L. Yang, Y.T. Yan, A. Chen, N. Desai, A. Wynshaw-Boris, and M.M. Shen. 1998. *Cripto* is required for correct orientation of the anterior-posterior axis in the mouse embryo. *Nature* **395:** 702–707.

Dufort, D., L. Schwartz, K. Harpal, and J. Rossant. 1998. The transcription factor HNF3beta is required in visceral endoderm for normal primitive streak morphogenesis. *Development* **125:** 3015–3025.

Goldstein, A.M., B.S. Ticho, and M.C. Fishman. 1998. Patterning the heart's left–right axis: From zebrafish to man. *Dev. Genet.* **22:** 278–287.

Graff, J.M., A. Bansal, and D.A. Melton. 1996. Xenopus Mad proteins transduce distinct subsets of signals for the TGF beta superfamily. *Cell* **85:** 479–487.

Gritsman, K., J. Zhang, S. Cheng, E. Heckscher, W.S. Talbot, and A.F. Schier. 1999. The EGF–CFC protein one-eyed pinhead is essential for nodal signaling. *Cell* **97:** 121–132.

Gu, Z., M. Nomura, B.B. Simpson, H. Lei, A. Feijen, J. van den

Eijnden-van Raaij, P.K. Donahoe, and E. Li. 1998. The type I activin receptor ActRIB is required for egg cylinder organization and gastrulation in the mouse. *Genes & Dev.* **12:** 844–857.

Harvey, R.P. 1998. Links in the left/right axial pathway. *Cell* **94:** 273–276.

Hemmati-Brivanlou, A. and D.A. Melton. 1992. A truncated activin receptor inhibits mesoderm induction and formation of axial structures in Xenopus embryos. *Nature* **359:** 609–614.

Izraeli, S., L.A. Lowe, V.L. Bertness, D.J. Good, D.W. Dorward, I.L. Kirsch, and M.R. Kuehn. 1999. The *SIL* gene is required for mouse embryonic axial development and left-right specification. *Nature* **399:** 691–694.

King, T., R.S.P. Beddington, and N.A. Brown. 1998. The role of the *brachyury* gene in heart development and left-right axis specification in the mouse. *Mech. Dev.* **79:** 29–37.

King, T. and N.A. Brown. 1999. Embryonic asymmetry: The left side gets all the best genes. *Curr. Biol.* **9:** R18–R22.

Kosaki, K. and B. Casey. 1998. Genetics of human left-right axis malformations. *Sem. Cell Dev. Biol.* **9:** 89–99.

Lanctèt, C., A. Moreau, M. Chamberland, M.L. Tremblay, and J. Drouin. 1999. Hindlimb patterning and mandible development require the Ptx1 gene. *Development* **126:** 1805–1810.

Levin, M., R.L. Johnson, C.D. Stern, M. Kuehn, and C. Tabin. 1995. A molecular pathway determining left-right asymmetry in chick embryogenesis. *Cell* **82:** 803–814.

Logan, M., S.M. Pagan-Westphal, D.M. Smith, L. Paganessi, and C.J. Tabin. 1998. The transcription factor Pitx2 mediates situs-specific morphogenesis in response to left-right asymmetric signals. *Cell* **94:** 307–317.

Lohr, J.L., M.C. Danos, and H.J. Yost. 1997. Left-right asymmetry of a nodal-related gene is regulated by dorsoanterior midline structures during Xenopus development. *Development* **124:** 1465–1472.

Lowe, L.A., D.M. Supp, K. Sampath, T. Yokoyama, C.V. Wright, S.S. Potter, P. Overbeek, and M.R. Kuehn. 1996. Conserved left-right asymmetry of nodal expression and alterations in murine situs inversus. *Nature* **381:** 158–161.

Lustig, K.D., K. Kroll, E. Sun, R. Ramos, H. Elmendorf, and M.W. Kirschner. 1996. A Xenopus nodal-related gene that acts in synergy with noggin to induce complete secondary axis and notochord formation. *Development* **122:** 3275–3282.

Melloy, P.G., J.L. Ewart, M.F. Cohen, M.E. Desmond, M.R. Kuehn, and C.W. Lo. 1998. No turning, a mouse mutation causing left-right and axial patterning defects. *Dev. Biol.* **193:** 77–89.

Meno, C., Y. Saijoh, H. Fujii, M. Ikeda, T. Yokoyama, M. Yokoyama, Y. Toyoda, and H. Hamada. 1996. Left-right asymmetric expression of the TGF beta-family member lefty in mouse embryos. *Nature* **381:** 151–155.

Meno, C., Y. Ito, Y. Saijoh, Y. Matsuda, K. Tashiro, S. Kuhara, and H. Hamada. 1997. Two closely-related left-right asymmetrically expressed genes, lefty-1 and lefty-2: Their distinct expression domains, chromosomal linkage and direct neuralizing activity in Xenopus embryos. *Genes Cells* **2:** 513–524.

Meno, C., A. Shimono, Y. Saijoh, K. Yashiro, K. Mochida, S. Ohishi, S. Noji, H. Kondoh, and H. Hamada. 1998. lefty-1 is required for left-right determination as a regulator of lefty-2 and nodal. *Cell* **94:** 287–297.

Meno, C., K. Gritsman, S. Ohishi, Y. Ohfuji, E. Heckscher, K. Mochida, A. Shimono, H. Kondoh, W.S. Talbot, E.J. Robertson et al. 1999. Mouse *Lefty-2* and zebrafish *antivin* are feed-

back inhibitors of *Nodal* signaling during vertebrate gastrulation. *Mol. Cell* (in press).

Meyers, E.N. and G.R. Martin. 1999. Differences in left–right axis pathways in mouse and chick: Functions of FGF8 and SHH. *Science* **285**: 403–406.

Milewski, W.M., S.J. Duguay, S.J. Chan, and D.F. Steiner. 1998. Conservation of PDX-1 structure, function, and expression in zebrafish. *Endocrinology* **139**: 1440–1449.

Mortensen, R. 1999. Gene targeting by homologous recombination. In *Current protocols in molecular biology* (ed. F.M. Ausubel, R. Brent, R.E. Kingston, D.D. Moore, J.G. Seidman, J.A. Smith, and K. Struhl), pp. 9.15.11–19.17.13. John Wiley & Sons, New York, NY.

New, H.V., A.L. Kavka, J.C. Smith, and J.B. Green. 1997. Differential effects on Xenopus development of interference with type IIA and type IIB activin receptors. *Mech Dev.* **61**: 175–186.

Nomura, M. and E. Li. 1998. Smad2 role in mesoderm formation, left–right patterning and craniofacial development. *Nature* **393**: 786–790.

Oh, S.P. and E. Li. 1997. The signaling pathway mediated by the type IIB activin receptor controls axial patterning and lateral asymmetry in the mouse. *Genes & Dev.* **11**: 1812–1826.

Pagan-Westphal, S.M. and C.J. Tabin. 1998. The transfer of left–right positional information during chick embryogenesis. *Cell* **93**: 25–35.

Piedra, M.E., J.M. Icardo, M. Albajar, J.C. Rodriguez-Rey, and M.A. Ros. 1998. Pitx2 participates in the late phase of the pathway controlling left–right asymmetry. *Cell* **94**: 319–324.

Ramsdell, A.F. and H.J. Yost. 1998. Molecular mechanisms of vertebrate left–right development. *Trends Genet.* **14**: 459–465.

Rebagliati, M.R., R. Toyama, C. Fricke, P. Haffter, and I.B. Dawid. 1998. Zebrafish nodal-related genes are implicated in axial patterning and establishing left–right asymmetry. *Dev. Biol.* **199**: 261–272.

Ryan, A.K., B. Blumberg, C. Rodriguez-Esteban, S. Yonei-Tamura, K. Tamura, T. Tsukui, J. de la Pena, W. Sabbagh, J. Greenwald, S. Choe et al. 1998. Pitx2 determines left–right asymmetry of internal organs in vertebrates. *Nature* **394**: 545–551.

Sampath, K., A.M. Cheng, A. Frisch, and C.V. Wright. 1997. Functional differences among Xenopus nodal-related genes in left–right axis determination. *Development* **124**: 3293–3302.

Schier, A.F., S.C.F. Neuhauss, K.A. Helde, W.S. Talbot, and W. Driever. 1997. The *one-eyed pinhead* gene functions in mesoderm and endoderm formation in zebrafish and interacts with *no tail*. *Development* **124**: 327–342.

Serbedzija, G.N., J.N. Chen, and M.C. Fishman. 1998. Regulation in the heart field of zebrafish. *Development* **125**: 1095–1101.

Shen, M.M., H. Wang, and P. Leder. 1997. A differential display strategy identifies *Cryptic*, a novel EGF-related gene expressed in the axial and lateral mesoderm during mouse gastrulation. *Development* **124**: 429–442.

Thisse, C. and B. Thisse. 1999. Antivin, a novel and divergent member of the TGFbeta superfamily, negatively regulates mesoderm induction. *Development* **126**: 229–240.

Waldrip, W.R., E.K. Bikoff, P.A. Hoodless, J.L. Wrana, and E.J. Robertson. 1998. Smad2 signaling in extraembryonic tissues determines anterior-posterior polarity of the early mouse embryo. *Cell* **92**: 797–808.

Weinstein, M., X. Yang, C. Li, X. Xu, J. Gotay, and C.X. Deng. 1998. Failure of egg cylinder elongation and mesoderm induction in mouse embryos lacking the tumor suppressor

smad2. *Proc. Natl. Acad. Sci.* **95**: 9378–9383.

Yoshioka, H., C. Meno, K. Koshiba, M. Sugihara, H. Itoh, Y. Ishimaru, T. Inoue, H. Ohuchi, E.V. Semina, J.C. Murray et al. 1998. Pitx2, a bicoid-type homeobox gene, is involved in a lefty-signaling pathway in determination of left–right asymmetry. *Cell* **94**: 299–305.

Zhang, J., W.S. Talbot, and A.F. Schier. 1998. Positional cloning identifies zebrafish *one-eyed pinhead* as a permissive EGF-related ligand required during gastrulation. *Cell* **92**: 241–251.

Nodal signalling in vertebrate development

Alexander F. Schier* & Michael M. Shen†

* Developmental Genetics Program, Skirball Institute of Biomolecular Medicine, Department of Cell Biology, New York University School of Medicine, New York, New York 10016, USA
† Center for Advanced Biotechnology and Medicine and Department of Pediatrics, UMDNJ-Robert Wood Johnson Medical School, 679 Hoes Lane, Piscataway, New Jersey 108854, USA

Communication between cells during early embryogenesis establishes the basic organization of the vertebrate body plan. Recent work suggests that a signalling pathway centering on Nodal, a transforming growth factor β-related signal, is responsible for many of the events that configure the vertebrate embryo. The activity of Nodal signals is regulated extracellularly by EGF-CFC cofactors and antagonists of the Lefty and Cerberus families of proteins, allowing precise control of mesoderm and endoderm formation, the positioning of the anterior–posterior axis, neural patterning and left–right axis specification.

The vertebrate body plan is laid down during early embryogenesis, when the primary axes and tissue layers form. During the 20th century, classical studies have shown that embryogenesis proceeds through inductive interactions that are mediated by intercellular signalling factors, including members of the Wnt, fibroblast growth factor (FGF), Hedgehog and transforming growth factor-β (TGFβ) families[1]. Here we discuss recent progress suggesting that the TGFβ-related factor Nodal may account for many of the roles attributed to TGFβ activities during embryogenesis. Based on genetic evidence, we propose that (1) Nodal signals represent the *in vivo* inducers of mesoderm; (2) Nodal activity is modulated by cofactors of the EGF-CFC family as well as inhibitors of the Lefty and Cerberus families; and (3) Nodal signalling is mediated by Activin-like receptors and transcription factors of the Smad family. The regulation of Nodal signalling allows precise temporal and spatial control of mesoderm formation and is employed in several other critical patterning events in early development, notably in the determination of left–right (L–R) asymmetry.

TGFβ-related activities induce mesoderm

The classic work of Nieuwkoop indicated that mesodermal cell types such as muscle and blood are induced by signals from neighbouring cells[1]. Subsequent studies in *Xenopus* suggested that Activin and Vg1, two members of the TGFβ family of signalling molecules, act as inducers of mesoderm *in vivo*[1]. Activin was the first TGFβ molecule shown to have mesoderm-inducing activity using *in vitro* explant assays. Another strong candidate for a mesoderm-inducing factor has been the TGFβ family member Vg1, on the basis of the localization of its messenger RNA to the vegetal hemisphere of the *Xenopus* embryo. This region has been implicated in inducing overlying cells to form mesoderm (Fig. 1). Moreover, processed and active Vg1 protein generated from bone morphogenetic protein (BMP)–Vg1 chimaeras can induce mesoderm in *Xenopus*. The identification of Vg1 and Activin suggested a relatively simple scenario in which maternally provided TGFβ signals activate Ser/Thr kinase receptors and thus regulate mesoderm-specific genes. However, it has been difficult to show unequivocally that Activin or Vg1 are required for the formation of vertebrate mesoderm[1]. For example, mouse mutants for both *Activin βA* and *Activin βB* form mesoderm and undergo normal gastrulation[2]. Furthermore, blocking of Activin activity with the inhibitor Follistatin or with dominant-negative versions of Activin does not consistently block mesoderm formation in *Xenopus*[3–6]. Although truncated activin receptors can inhibit mesoderm formation[7,8], these reagents are not fully specific for Activin as they can block BMP[9], Vg1[5] or Nodal[10] signalling as well. In addition, processed Vg1 has not been detected *in vivo* and Vg1 mutant derivatives thought to block endogenous Vg1 activity cause only variable disruption of dorsal mesoderm formation[11]. Similar experiments with the frog gene *Derriere*, which encodes a Vg1-related TGFβ molecule, have indicated that it might be
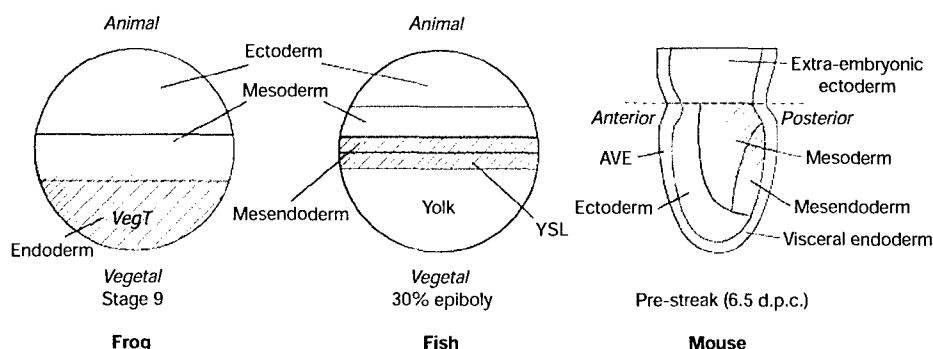
Figure 1 Schematic representation of Nodal signalling activities in frog, fish and mouse embryos before gastrulation. Expression patterns of *Nodal*-related genes (red hatching) are superimposed on simplified fate maps of embryos at the indicated stages. Mesoderm and endoderm are internalized through the primitive streak in mouse and the germ-ring in fish. Classical embryological studies have shown that the vegetal region in frog (presumptive endoderm) and fish (yolk syncytial layer; YSL) are sources of mesoderm-inducing factors. *Nodal*-related genes are expressed in these regions. AVE, anterior visceral endoderm; d.p.c., days *post coitum*.

involved in specifying posterior regions, but is not required for general mesoderm induction[6]. It thus remains to be established whether members of the Activin or Vg1 families represent primary inducers of mesoderm *in vivo*.

Nodal is required for mesoderm formation

Genetic studies in mouse and zebrafish have shown that TGFβ signals of the Nodal family are essential for mesoderm formation in vertebrates. Nodal was shown to be required for mesoderm formation by the isolation and cloning of a retroviral insertion mutation in the mouse *Nodal* gene[12,13], and the subsequent identification of a family of vertebrate *Nodal*-related TGFβ genes[14-20]. Mouse *Nodal* mutants lack a primitive streak (a thickening caused by ingression of mesoderm and endoderm progenitors) and most mesoderm, displaying only sporadic formation of some posterior mesoderm[13] (Table 1). Similarly, double mutants for the zebrafish *Nodal*-related genes *cyclops* and *squint* lack head and trunk mesoderm and fail to form the germ-ring, a structure analogous to the mouse primitive streak[21] (Table 1). *Nodal* genes are expressed in the vicinity of or overlapping with mesoderm progenitors (Fig. 1), including dorsal mesoderm precursors (also called the 'node' in mouse; hence the name *Nodal*). Moreover, mouse Nodal, zebrafish Cyclops and Squint and the frog homologues Xnr1, Xnr2 and Xnr4 can induce mesoderm formation in explant assays, similar to Activin and processed Vg1 (refs 15, 17, 19, 20, 22). Although additional signals (such as FGF and Derriere) may also be involved in (posterior) mesoderm induction, these genetic data establish that Nodal signals are central in the formation of vertebrate mesoderm.

Previous models have proposed that a maternal TGFβ signal is involved in *Xenopus* mesoderm induction[1,23]; however, *Nodal* genes are expressed zygotically during blastula stages (Fig. 1). This apparent contradiction appears to have been resolved by the recent identification of *Xenopus* VegT as a vegetally localized maternal T-box transcription factor. Depletion of *VegT* mRNA leads to a marked reduction in mesoderm and endoderm in *Xenopus*[24,25], and misexpression of *VegT* can induce *Nodal* gene expression[26,27]. These results do not exclude a role for a maternally provided TGFβ signal, but they suggest a revised model for mesoderm formation[23,25] wherein a localized transcription factor(s) activates *Nodal* gene expression, which in turn leads to the induction of mesoderm. Determining whether a similar mechanism

controls mesoderm formation in fish and mouse will require the isolation of factors that activate expression of *Nodal* in these species.

Extracellular regulation of Nodal signalling

Recent studies have revealed an unexpectedly complex regulation of the Nodal signalling pathway, as shown by the identification of EGF-CFC proteins as Nodal cofactors and Lefty and Cerberus proteins as Nodal antagonists. It is now apparent that cells can become competent to respond to Nodal by expressing EGF-CFC proteins, and can attenuate Nodal activity by expressing inhibitors of the Lefty and Cerberus families (Fig. 2).

EGF-CFC factors. Members of the *EGF-CFC* family such as zebrafish *one-eyed pinhead* (*oep*) and mouse *Cripto* and *Cryptic* encode extracellular proteins that share an amino-terminal signal sequence, a divergent epidermal growth factor (EGF)-like motif, a second conserved cysteine-rich domain (the CFC motif) and a carboxy-terminal hydrophobic region[28,29]. Although they were initially implicated in a receptor tyrosine kinase/ras pathway[30], genetic studies in zebrafish have shown that these extracellular proteins are essential for Nodal signalling[31]. Thus, embryos that lack both maternal and zygotic activity of *oep* display the same phenotype as double mutants for the *Nodal* factors *cyclops* and *squint*[31] (Table 1). Strikingly, whereas overexpression of *Nodal* in wild-type embryos induces ectopic mesoderm, overexpressed *Nodal* in maternal-zygotic *oep* mutants has no phenotypic effect[31]. Indeed, similar to *Nodal* mutants, *Cripto* mutant mice do not form a primitive streak and embryonic mesoderm[32] (Table 1). The cell-autonomous role[31,33,34] and membrane association[29] of Oep indicate that EGF-CFC proteins might represent components of Nodal receptor complexes or otherwise facilitate the response to Nodal signals. In particular, Nodal signals might act upon cells only in the presence of EGF-CFC proteins. In turn, cells might be protected from responding to Nodal signals by lack of expression of *EGF-CFC* genes, thereby creating an additional level of regulation of these potent inducers.

Lefty. Members of the Lefty subfamily of TGFβ molecules appear to act as antagonists of Nodal signalling. Lefty proteins are predicted to be structurally distinct from other TGFβ molecules, lacking a long α-helix and a critical cysteine residue involved in stabilizing TGFβ homodimers and heterodimers[35-37]. It is thus possible that Lefty proteins act as monomers. Initially, Lefty proteins were thought to

---

Table 1 Selected genes in the Nodal pathway and their mutant phenotypes in mouse and zebrafish

Genes and genotypes	Species	Role and phenotypes	References
Nodal		TGFβ-related factors; instructive signals	
Nodal	Mouse	Lack of primitive streak and most mesoderm; anterior neural truncations in chimaeras	12, 13
cyclops	Fish	Mild defects in prechordal mesoderm, lack of floor plate, cyclopia	17, 18, 20, 59
squint	Fish	Variable defects in axial mesoderm formation	17, 19, 21, 60
cyclops; squint	Fish	Lack of head and trunk mesoderm and endoderm, mispositioned anterior–posterior (A–P) axis	21
EGF-CFC		Extracellular cofactors for Nodal	
Cripto	Mouse	Lack of primitive streak, embryonic mesoderm and endoderm, mispositioned A–P axis	32
Cryptic	Mouse	Defective L–R axis formation (right isomerism and heterotaxia)	28, 53
zygotic *oep*	Fish	Lack of endoderm, prechordal mesoderm and floor plate, cyclopia	29, 33, 34, 57
maternal-zygotic *oep*	Fish	Lack of head and trunk mesoderm and endoderm, mispositioned A–P axis	31
partially rescued *oep*	Fish	Defective L–R axis formation (heterotaxia)	53
Lefty		TGFβ-related factors; inhibitors of Nodal signalling	
Lefty1	Mouse	Defective L–R axis formation (left isomerism)	35, 36, 54
Lefty2	Mouse	Enlarged primitive streak, excess of mesoderm progenitors	10, 35, 36
Lefty overexpression	Fish	Lack of head and trunk mesoderm and endoderm, mispositioned A–P axis	10, 37, 38
Activin receptors		Putative cell-surface receptors for Nodal	
ActRIIA	Mouse	No early embryonic phenotype	61
ActRIIB	Mouse	Defective L–R axis formation (right isomerism)	51, 55
ActRIIA−/−; ActRIIB+/−	Mouse	Variable defects in primitive streak formation, cyclopia, anterior neural truncations	51
ActRIIA−/−; ActRIIB−/−	Mouse	Lack of primitive streak, mesoderm and endoderm	51
ActRIB	Mouse	Lack of primitive streak, mesoderm and endoderm	50
Smad		Signal-transducing transcription factors	
Smad2	Mouse	Lack of primitive streak, embryonic mesoderm and endoderm	47–49
Smad2+/−; Nodal+/−	Mouse	Variable defects in anterior midline, cyclopia, anterior neural truncations, L–R patterning	49
Smad4	Mouse	Lack of primitive streak, embryonic mesoderm and endoderm; anterior neural truncations in chimaeras	62, 63

be instructive signals or inhibitors of BMP signalling[36]; however, recent studies in mouse and zebrafish indicate that these factors act as antagonists of Nodal, potentially by competing for binding to a common receptor (see below). In particular, the overexpression of mouse or zebrafish *Lefty* genes produces phenotypes in fish that are identical to those seen in *cyclops;squint* and maternal-zygotic *oep* mutants[10,37,38] (Table 1). The phenotypic effects induced by *Lefty* can be countered by overexpression of *cyclops* or *squint*, suggesting an antagonistic relationship between Nodal signals and Lefty proteins[10,38]. Similarly, *Lefty2* mutant mice have an enlarged primitive streak with more mesoderm progenitors (Table 1); this phenotype can be partially suppressed by decreasing Nodal activity, indicating that excess mesoderm formation may result from prolonged or hyperactivated Nodal signalling[10]. Interestingly, *Lefty2* expression temporally and spatially follows *Nodal* expression in mice, and studies in zebrafish indicate that Nodal signalling leads to the induction and maintenance of *Lefty* expression[10,38]. Recent results indicate that a similar pathway may also operate in *Xenopus*[39]. The negative feedback loop mediated by Lefty proteins effectively attenuates Nodal activity and renders it transient, allowing cells to respond to other signals after initial exposure to Nodal. This mechanism also blocks the positive autoregulation of *Nodal* expression[10], possibly restricting the spatial range of Nodal activity.
Cerberus. Overexpression studies in frogs have identified Cerberus as another molecule that can block Nodal signals[40–42]. *Cerberus* encodes an extracellular protein that belongs to a subclass of the cysteine-knot superfamily, which also includes DAN and Gremlin[41]. Biochemical analysis and structural modelling have revealed that Cerberus-like proteins act as trifunctional growth-factor antagonists, which bind and block not only Nodal but also Wnt and BMP ligands[41–43]. However, a truncated form of Cerberus (Cer-short) specifically blocks Nodal signals and, upon overexpression in *Xenopus*, induces phenotypes resembling *cyclops;squint* or maternal-zygotic *oep* mutants[42]. Although *Cerberus* expression does not

completely conform to Nodal signalling activity, it can be induced by Nodal signals in a subset of cells, thus potentially serving as a region-specific feedback inhibitor of Nodal signalling[42]. Nonetheless, an *in vivo* requirement for Cerberus-like proteins has not yet been established[44].

Transduction of Nodal signals

Although the *Nodal* signalling pathway has not yet been analysed biochemically, loss- and gain-of-function studies in mouse, frog and fish indicate that Nodal may utilize similar receptors and downstream effectors to those that have been identified for Activin (Fig. 2). Extensive studies have shown that Activin binds to the type II Ser/Thr kinase receptors ActRII (also known as ActRIIA) and ActRIIB, activating the type I receptor ActRIB, resulting in phosphorylation of Smad2. In turn, Smad2 forms a nuclear complex with Smad4 and members of the FAST family of forkhead domain transcription factors to regulate the expression of downstream target genes[1,45,46].

Several observations indicate that Nodal signals activate the same pathway as Activin or a highly related one. First, Nodal and Activin have similar activities as mesoderm inducers in explant assays and upon overexpression in whole embryos[15,17,19,20]. Second, misexpression of activated versions of Activin receptors, Smad2 or FAST-1 produce effects similar to those of overexpression of Nodal signals and Activin[1,46]. Third, maternal-zygotic *oep* mutants, which are defective in Nodal signalling, can be rescued by expression of activated forms of ActRIB and Smad2 (ref. 31). Strikingly, injection of *activin* mRNA can mimic this effect, indicating that forced activation of the Activin signalling pathway in *oep* mutants might recapitulate Nodal signalling *in vivo*, and that the combined activity of Nodal and EGF-CFCs may correspond to the activity of Activin alone[31]. Fourth, the extracellular domain of ActRIIB[7] blocks the effects of overexpression of Squint, as well as the antagonistic effects of Lefty[10]. These results indicate that Nodal and Lefty may compete for interaction with a type II Activin receptor. Consistent with this model, Lefty also blocks Activin signalling[37]. Finally, mouse *Smad2* and *ActRIB* mutants as well as *ActRIIA;ActRIIB* double mutants display gastrulation-defective phenotypes resembling those of mouse *Nodal* mutants[47–51] (Table 1). As these mutant phenotypes are not identical, it is conceivable that Activin receptors and Smad2 also mediate additional signals during early embryogenesis, and that some aspects of Nodal signalling are mediated by additional downstream components. Taken together, however, the current genetic data are consistent with a pathway in which Nodal, in conjunction with EGF-CFC proteins, activates Activin receptors or Activin-like receptors and Smad2 or related Smad proteins, resulting in the transcription of downstream genes as well as *Lefty*, *Cerberus* and other potential feedback inhibitors, leading to the attenuation of Nodal signalling (Fig. 2).

Nodal signalling in left–right axis formation

The Nodal signalling pathway described above has been implicated in several other processes (Box 1), notably the specification of the L–R axis (Table 1; Fig. 2). In particular, members of the *Nodal* gene family in each vertebrate species (mouse *Nodal*; chick *cNR-1*; frog *Xnr1*; zebrafish *cyclops*) are specifically expressed in the left, but not right, lateral plate during somitogenesis; asymmetric expression is also observed around the node in chick and mouse[52]. The presence of Nodal signals in the lateral plate mesoderm has thus been proposed to determine 'left-sidedness', and absence of Nodal to determine 'right-sidedness'. In support of this model, ectopic expression of Nodal on the right side can perturb the asymmetry of internal organs[52].

A requirement for Nodal signals in L–R asymmetry has been difficult to demonstrate, however, owing to the early embryonic lethality of *Nodal* mutants. Recent evidence for a direct role of Nodal signalling in L–R axis specification has been provided by analysis of

Figure 2 The putative Nodal signalling pathway. Loss- and gain-of-function studies indicate that Nodal signals may act with EGF-CFC cofactors to activate an Activin-like pathway. Lefty proteins act as feedback inhibitors during both mesoderm formation and L–R axis determination. Cerberus-related factors can bind directly to Nodal signals, but their role during development and their relationship with Nodal signalling is not clear. For instance, recent studies have identified a chick *Cerberus*-related gene, *Caronte*, which is expressed in the left paraxial and lateral-plate mesoderm[43,64,65]. Although Caronte binds to Nodal protein, it unexpectedly activates *Nodal* gene expression in the lateral plate by inhibiting BMP activity. Furthermore, ectopic Nodal activity is unable to induce *Caronte* (at least in the trunk, though it is reported to do so in the head[65]). Thus, in contrast to the proposed role of *Xenopus* Cerberus as an inhibitor of Nodal signalling during gastrulation, chick *Caronte* may not represent a downstream target or feedback inhibitor of Nodal signalling in L–R axis development.

the role of *EGF-CFC* genes in L–R axis formation in mouse and zebrafish. Mouse *Cryptic* and zebrafish *oep* are expressed in the lateral plate mesoderm, overlapping with *Nodal*, but are located symmetrically on both the left and right sides[28,29]. Mouse *Cryptic* mutants display numerous L–R laterality defects including right-sided mirror-image symmetry of the lungs (right pulmonary iso-merism), as well as loss of asymmetric gene expression in the lateral plate mesoderm[53] (Table 1). Moreover, zebrafish *oep* mutants that have been partially rescued by injection of *oep* mRNA show similar randomized laterality phenotypes and gene-expression patterns[53] (Table 1). These results are consistent with the idea that loss of Nodal signalling leads to 'right-sidedness' on both sides of the embryo.

Other genes implicated in the Nodal pathway are also required for L–R patterning. Mice lacking *Lefty1* often display left-sided mirror-image symmetry of the lungs (left pulmonary isomerism) and bilateral expression of genes that are normally expressed on the left[54]. This phenotype is the opposite of that of *Cryptic* mutants, supporting the notion that *Lefty1* antagonizes EGF-CFC-dependent Nodal activity during L–R determination. *ActRIIB* mutants and *Nodal*^{+/–}*;Smad2*^{+/–} compound heterozygotes display L–R laterality defects that resemble those of *Cryptic* mutants[49,55]. In summary, these findings indicate that during both mesoderm and L–R development, Nodal signalling is regulated by EGF-CFC and Lefty proteins and is mediated by ActRIIB and Smad2.

Future directions

We have discussed how a combination of instructive signals (Nodal), permissive cofactors (EGF-CFC) and feedback inhibitors (Lefty, Cerberus) regulates various aspects of vertebrate embryogenesis. The Nodal signalling pathway proposed above is based on genetic, not biochemical, evidence. First, therefore, it will be crucial to determine the molecular mechanisms by which Nodal signalling is regulated by EGF-CFC and Lefty factors and results in the activation of an Activin-like pathway. Second, *in vitro* studies on Activin have suggested that this TGFβ signal can act as a graded long-range morphogen that determines distinct cell types at different concentrations and distances[56]. Nodal signals can elicit concentration-dependent responses[15,57] but, in contrast to Activin, Nodal might act at a short range[58]. It is thus unclear whether Nodal signals pattern the embryo by acting as graded morphogens. Third, it remains a mystery how Nodal signalling controls development in different contexts. How is the identical pathway interpreted in distinct developmental processes, ranging from mesoderm induction to L–R patterning? Finally, overexpression of *Cripto* has been implicated in human carcinogenesis, particularly in the mammary gland[30]. This raises the possibility that Nodal or related TGFβ factors may be involved in human disease. More generally, the regulation of inductive signals by extracellular cofactors may be a general strategy employed during development and homeostasis. Extracellular cofactors such as EGF-CFC proteins may thus represent promising therapeutic targets for modulating the activity of signalling pathways. □

Box 1
Additional roles for the Nodal pathway

In addition to mesoderm formation and L–R axis specification, the Nodal signalling pathway has been implicated in several other processes in early vertebrate embryogenesis.

Endoderm formation. Mouse *Cripto* mutants lack definitive endoderm, similar to *cyclops;squint* double mutants and maternal-zygotic mutants for *oep*[21,31,32]. The lack of a primitive streak in mouse *Nodal* mutants also suggests endoderm defects. In addition, recent work in fish and frog has implicated Nodal signalling as an early component in the pathway for endoderm formation[26,27,66].

Anterior–posterior patterning. Differential Nodal signalling might be involved in anterior–posterior (A–P) patterning in both mesoderm and ectoderm. Modulation of Nodal signalling activity in zebrafish indicates that specification of anterior axial mesoderm fates requires higher Nodal signalling than posterior fates[57]. Increasing doses of zebrafish Lefty1 (Antivin) progressively delete posterior neural fates, whereas overexpression of Nodal-related factors leads to posterior transformations[67]. It is unclear whether high levels of Lefty1 specifically block Nodal or Activin signalling, but these results have led to the suggestion that Nodal-related signals and Activin specify fates along the A–P neural axis. Together, these results indicate that differential Nodal signalling in zebrafish may establish positional information along the animal–vegetal axis at blastula stages, which is then translated during gastrulation into distinct anterior-posterior mesodermal and ectodermal fates[57,67]. In addition, a role for the Nodal signalling pathway in anterior neural induction has been suggested in mouse by analysis of *Nodal* chimaeras, *Smad4* chimaeras and *ActRIIA*^{–/–}*;ActRIIB*^{+/–} compound mutants, and in *Xenopus* by phenotypes induced upon overexpression of dominant-negative *Xnr2* derivatives[51,62,68,69]. This analysis indicates that blocking Nodal signalling results in anterior truncations. However, this evidence for a role of Nodal in anterior neural induction is confounded by the observation that anterior neural tissue is present in *Cripto* mutant mice as well as maternal-zygotic *oep* and *cyclops;squint* mutant fish[21,31,32], and by the proposed role of the Nodal inhibitor Cerberus in head induction[40,42]. A partial resolution of these issues might be that Nodal signalling is essential at an earlier step for visceral endoderm differentiation in the mouse, leading to upregulation of Cerberus and consequent head formation[42].

Anterior–posterior axis positioning. Recent work in the mouse has suggested that the position of the A–P axis is established through a process of axial rotation involving morphogenetic movements of cells in the visceral endoderm and epiblast layers[70]. An unexpected role for Nodal signalling in this process has been suggested by the finding that *Cripto* mutants display an A–P axis that is displaced by nearly 90° compared to that of wild-type embryos, consistent with failure of axis rotation[32]. Similar phenotypes have been observed in maternal-zygotic *oep* and *cyclops;squint* mutants, as well as in zebrafish embryos following overexpression of *Lefty*[21,31,37]. These findings are consistent with the idea that an early Nodal signalling event is required to position the A–P axis in vertebrates.

Ventral midline formation. A role for Nodal signalling in formation of the ventral midline of the neural tube (including the floor plate) has been suggested by the phenotypes of *cyclops* and *oep* mutant fish[18,20,33,34,59]. The cell-autonomy of *oep* in floor-plate progenitors suggests that Nodal is directly involved in the specification of floor-plate cells during gastrulation[31,34], in a step that does not depend on *sonic hedgehog*[71]. A role for Nodal in ventral forebrain formation is also supported by the cyclopia defects that are variably observed in *Nodal*^{–/–}*;Smad2*^{+/–} and *Nodal*^{+/–}*;ActRIIA*^{–/–} as well as *ActRIIA*^{–/–}*;ActRIIB*^{+/–} compound mutants[49,51].

1. Harland, R. & Gerhart, J. Formation and function of Spemann's organizer. *Annu. Rev. Cell Dev. Biol.* **13**, 611–667 (1997).
2. Matzuk, M. M. *et al.* Functional analysis of activins during mammalian development. *Nature* **374**, 354–356 (1995).
3. Hawley, S. H. *et al.* Disruption of BMP signals in embryonic *Xenopus* ectoderm leads to direct neural induction. *Genes Dev.* **9**, 2923–2935 (1995).
4. Kessler, D. S. & Melton, D. A. Induction of dorsal mesoderm by soluble, mature Vg1 protein. *Development* **121**, 2155–2164 (1995).
5. Schulte-Merker, S., Smith, J. C. & Dale, L. Effects of truncated activin and FGF receptors and of follistatin on the inducing activities of BVg1 and activin: does activin play a role in mesoderm induction? *EMBO J.* **13**, 3533–3541 (1994).
6. Sun, B. I. *et al.* derriere: a TGF-β family member required for posterior development in *Xenopus*. *Development* **126**, 1467–1482 (1999).
7. Dyson, S. & Gurdon, J. B. Activin signalling has a necessary function in *Xenopus* early development. *Curr. Biol.* **7**, 81–84 (1997).
8. Hemmati-Brivanlou, A. & Melton, D. A. A truncated activin receptor inhibits mesoderm induction and formation of axial structures in *Xenopus* embryos. *Nature* **359**, 609–614 (1992).
9. Hemmati-Brivanlou, A. & Thomsen, G. H. Ventral mesodermal patterning in *Xenopus* embryos: expression patterns and activities of BMP-2 and BMP-4. *Dev. Genet.* **17**, 78–89 (1995).
10. Meno, C. *et al.* Mouse Lefty2 and zebrafish antivin are feedback inhibitors of Nodal signaling during vertebrate gastrulation. *Mol. Cell* **4**, 287–298 (1999).
11. Joseph, E. M. & Melton, D. A. Mutant Vg1 ligands disrupt endoderm and mesoderm formation in *Xenopus* embryos. *Development* **125**, 2677–2685 (1998).

12. Zhou, X., Sasaki, H., Lowe, L., Hogan, B. L. & Kuehn, M. R. Nodal is a novel TGF-β-like gene expressed in the mouse node during gastrulation. *Nature* **361**, 543–547 (1993).

13. Conlon, F. L. *et al.* A primary requirement for nodal in the formation and maintenance of the primitive streak in the mouse. *Development* **120**, 1919–1928 (1994).

14. Smith, W. C., McKendry, R., Ribisi, S. J. & Harland, R. M. A nodal-related gene defines a physical and functional domain within the Spemann organizer. *Cell* **82**, 37–46 (1995).

15. Jones, C. M., Kuehn, M. R., Hogan, B. L., Smith, J. C. & Wright, C. V. Nodal-related signals induce axial mesoderm and dorsalize mesoderm during gastrulation. *Development* **121**, 3651–3662 (1995).

16. Levin, M., Johnson, R. L., Stern, C. D., Kuehn, M. & Tabin, C. A molecular pathway determining left–right asymmetry in chick embryogenesis. *Cell* **82**, 803–814 (1995).

17. Rebagliati, M. R., Toyama, R., Fricke, C., Haffter, P. & Dawid, I. B. Zebrafish nodal-related genes are implicated in axial patterning and establishing left–right asymmetry. *Dev. Biol.* **199**, 261–272 (1998).

18. Rebagliati, M. R., Toyama, R., Haffter, P. & Dawid, I. B. *cyclops* encodes a nodal-related factor involved in midline signaling. *Proc. Natl Acad. Sci. USA* **95**, 9932–9937 (1998).

19. Erter, C. E., Solnica-Krezel, L. & Wright, C. V. Zebrafish nodal-related 2 encodes an early mesendodermal inducer signaling from the extraembryonic yolk syncytial layer. *Dev. Biol.* **204**, 361–372 (1998).

20. Sampath, K. *et al.* Induction of the zebrafish ventral brain and floorplate requires cyclops/nodal signalling. *Nature* **395**, 185–189 (1998).

21. Feldman, B. *et al.* Zebrafish organizer development and germ-layer formation require nodal-related signals. *Nature* **395**, 181–185 (1998).

22. Joseph, E. M. & Melton, D. A. Xnr4: a *Xenopus* nodal-related gene expressed in the Spemann organizer. *Dev. Biol.* **184**, 367–372 (1997).

23. Kimelman, D. & Griffin, K. J. Mesoderm induction: a postmodern view. *Cell* **94**, 419–421 (1998).

24. Zhang, J. *et al.* The role of maternal VegT in establishing the primary germ layers in *Xenopus* embryos. *Cell* **94**, 515–524 (1998).

25. Kofron, M. *et al.* Mesoderm induction in *Xenopus* is a zygotic event regulated by maternal VegT via TGF-β growth factors. *Development* **126**, 5759–5770 (1999).

26. Yasuo, H. & Lemaire, P. A two-step model for the fate determination of presumptive endodermal blastomeres in *Xenopus* embryos. *Curr. Biol.* **9**, 869–879 (1999).

27. Clements, D., Friday, R. V. & Woodland, H. R. Mode of action of VegT in mesoderm and endoderm formation. *Development* **126**, 4903–4911 (1999).

28. Shen, M. M., Wang, H. & Leder, P. A differential display strategy identifies Cryptic, a novel EGF-related gene expressed in the axial and lateral mesoderm during mouse gastrulation. *Development* **124**, 429–442 (1997).

29. Zhang, J., Talbot, W. S. & Schier, A. F. Positional cloning identifies zebrafish one-eyed pinhead as a permissive EGF-related ligand required during gastrulation. *Cell* **92**, 241–251 (1998).

30. Salomon, D. S., Bianco, C. & De Santis, M. Cripto: a novel epidermal growth factor (EGF)-related peptide in mammary gland development and neoplasia. *Bioessays* **21**, 61–70 (1999).

31. Gritsman, K. *et al.* The EGF-CFC protein one-eyed pinhead is essential for nodal signaling. *Cell* **97**, 121–132 (1999).

32. Ding, J. *et al.* Cripto is required for correct orientation of the anterior–posterior axis in the mouse embryo. *Nature* **395**, 702–707 (1998).

33. Schier, A. F., Neuhauss, S. C. F., Helde, K. A., Talbot, W. S. & Driever, W. The one-eyed pinhead gene functions in mesoderm and endoderm formation in zebrafish and interacts with no tail. *Development* **124**, 327–342 (1997).

34. Strähle, U. *et al.* one-eyed pinhead is required for development of the ventral midline of the zebrafish (*Danio rerio*) neural tube. *Genes Funct.* **1**, 131–148 (1997).

35. Meno, C. *et al.* Left-right asymmetric expression of the TGF β-family member lefty in mouse embryos. *Nature* **381**, 151–155 (1996).

36. Meno, C. *et al.* Two closely-related left-right asymmetrically expressed genes, lefty-1 and lefty-2: their distinct expression domains, chromosomal linkage and direct neuralizing activity in *Xenopus* embryos. *Genes Cell.* **2**, 513–524 (1997).

37. Thisse, C. & Thisse, B. Antivin, a novel and divergent member of the TGFβ superfamily, negatively regulates mesoderm induction. *Development* **126**, 229–240 (1999).

38. Bisgrove, B. W., Essner, J. J. & Yost, H. J. Regulation of midline development by antagonism of lefty and nodal signaling. *Development* **126**, 3253–3262 (1999).

39. Cheng, A., Thisse, B., Thisse, C. & Wright, C. V. E. The lefty-related factor Xatv acts as a feedback inhibitor of Nodal signaling in mesoderm induction and L–R axis development in *Xenopus*. *Development* (in the press).

40. Bouwmeester, T., Kim, S., Sasai, Y., Lu, B. & De Robertis, E. M. Cerberus is a head-inducing secreted factor expressed in the anterior endoderm of Spemann's organizer. *Nature* **382**, 595–601 (1996).

41. Hsu, D. R., Economides, A. N., Wang, X., Eimon, P. M. & Harland, R. M. The *Xenopus* dorsalizing factor Gremlin identifies a novel family of secreted proteins that antagonize BMP activities. *Mol. Cell* **1**, 673–683 (1998).

42. Piccolo, S. *et al.* The head inducer Cerberus is a multifunctional antagonist of Nodal, BMP and Wnt signals. *Nature* **397**, 707–710 (1999).

43. Rodriguez Esteban, C. *et al.* The novel Cer-like protein Caronte mediates the establishment of embryonic left–right asymmetry. *Nature* **401**, 243–251 (1999).

44. Simpson, E. H. *et al.* The mouse Cer1 (*Cerberus related* or *homologue*) gene is not required for anterior pattern formation. *Dev. Biol.* **213**, 202–206 (1999).

45. Massagué, J. TGF-β signal transduction. *Annu. Rev. Biochem.* **67**, 753–791 (1998).

46. Whitman, M. Smads and early developmental signaling by the TGFβ superfamily. *Genes Dev.* **12**, 2445–2462 (1998).

47. Waldrip, W. R., Bikoff, E. K., Hoodless, P. A., Wrana, J. L. & Robertson, E. J. Smad2 signaling in extraembryonic tissues determines anterior–posterior polarity of the early mouse embryo. *Cell* **92**, 797–808 (1998).

48. Weinstein, M. *et al.* Failure of egg cylinder elongation and mesoderm induction in mouse embryos lacking the tumor suppressor smad2. *Proc. Natl Acad. Sci. USA* **95**, 9378–9383 (1998).

49. Nomura, M. & Li, E. Smad2 role in mesoderm formation, left–right patterning and craniofacial development. *Nature* **393**, 786–790 (1998).

50. Gu, Z. *et al.* The type 1 activin receptor ActRIB is required for egg cylinder organization and gastrulation in the mouse. *Genes Dev.* **12**, 844–857 (1998).

51. Song, J. *et al.* The type II activin receptors are essential for egg cylinder growth, gastrulation, and rostral head development in mice. *Dev. Biol.* **213**, 157–169 (1999).

52. Ramsdell, A. F. & Yost, H. J. Molecular mechanisms of vertebrate left–right development. *Trends Genet.* **14**, 459–465 (1998).

53. Yan, Y.-T. *et al.* Conserved requirement for EGF-CFC genes in vertebrate left–right axis formation. *Genes Dev.* **13**, 2527–2537 (1999).

54. Meno, C. *et al.* lefty-1 is required for left–right determination as a regulator of lefty-2 and nodal. *Cell* **94**, 287–297 (1998).

55. Oh, S. P. & Li, E. The signaling pathway mediated by the type IIB activin receptor controls axial patterning and lateral asymmetry in the mouse. *Genes Dev.* **11**, 1812–1826 (1997).

56. Gurdon, J. B., Dyson, S. & St Johnston, D. Cells' perception of position in a concentration gradient. *Cell* **95**, 159–162 (1998).

57. Gritsman, K., Talbot, W. S. & Schier, A. F. Nodal signaling patterns the organizer. *Development* (in the press).

58. Jones, C. M., Armes, N. & Smith, J. C. Signalling by TGF-β family members: short-range effects of Xnr-2 and BMP-4 contrast with the long-range effects of activin. *Curr. Biol.* **6**, 1468–1475 (1996).

59. Hatta, K., Kimmel, C. B., Ho, R. K. & Walker, C. The cyclops mutation blocks specification of the floor plate of the zebrafish central nervous system. *Nature* **350**, 339–341 (1991).

60. Heisenberg, C. P. & Nüsslein-Volhard, C. The function of silberblick in the positioning of the eye anlage in the zebrafish embryo. *Dev. Biol.* **184**, 85–94 (1997).

61. Matzuk, M. M., Kumar, T. R. & Bradley, A. Different phenotypes for mice deficient in either activins or activin receptor type II. *Nature* **374**, 356–360 (1995).

62. Sirard, C. *et al.* The tumor suppressor gene Smad4/Dpc4 is required for gastrulation and later for anterior development of the mouse embryo. *Genes Dev.* **12**, 107–119 (1998).

63. Yang, X., Li, C., Xu, X. & Deng, C. The tumor suppressor SMAD4/DPC4 is essential for epiblast proliferation and mesoderm induction in mice. *Proc. Natl Acad. Sci. USA* **95**, 3667–3672 (1998).

64. Yokouchi, Y., Vogan, K. J., Pearse, R. V. 2nd & Tabin, C. J. Antagonistic signaling by Caronte, a novel Cerberus-related gene, establishes left–right asymmetric gene expression. *Cell* **98**, 573–583 (1999).

65. Zhu, L. *et al.* Cerberus regulates left–right asymmetry of the embryonic head and heart. *Curr. Biol.* **9**, 931–938 (1999).

66. Rodaway, A. *et al.* Induction of the mesendoderm in the zebrafish germ ring by yolk cell-derived TGF-β family signals and discrimination of mesoderm and endoderm by FGF. *Development* **126**, 3067–3078 (1999).

67. Thisse, B., Wright, C. V. E. & Thisse, B. Activin- and Nodal-related factors control antero–posterior patterning of the zebrafish embryo. *Nature* **403**, 425–428 (2000).

68. Varlet, I., Collignon, J. & Robertson, E. J. nodal expression in the primitive endoderm is required for specification of the anterior axis during mouse gastrulation. *Development* **124**, 1033–1044 (1997).

69. Osada, S. I. & Wright, C. V. *Xenopus* nodal-related signaling is essential for mesendodermal patterning during early embryogenesis. *Development* **126**, 3229–3240 (1999).

70. Beddington, R. S. P. & Robertson, E. J. Anterior patterning in mouse. *Trends Genet.* **14**, 277–284 (1998).

71. Schauerte, H. E. *et al.* Sonic hedgehog is not required for the induction of medial floor plate cells in the zebrafish. *Development* **125**, 2983–2993 (1998).

Acknowledgements

Correspondence should be addressed to A.F.S. (e-mail: schier@saturn.med.nyu.edu) or M.M.S. (e-mail: mshen@cabm.rutgers.edu).

The *EGF-CFC* gene family in vertebrate development

EGF-CFC genes encode extracellular proteins that play key roles in intercellular signaling pathways during vertebrate embryogenesis. Mutations in zebrafish and mouse *EGF-CFC* genes lead to defects in germ-layer formation, anterior–posterior axis orientation and left–right axis specification. In addition, members of the *EGF-CFC* family have been implicated in carcinogenesis. Although formerly regarded as signaling molecules that are distant relatives of epidermal growth factor (EGF), recent findings indicate that EGF-CFC proteins act as essential cofactors for Nodal, a member of the transforming growth factor β (TGF-β) family. Here, we review molecular genetic evidence from mouse and zebrafish on biological and biochemical roles of the *EGF-CFC* family, and discuss differing models for EGF-CFC protein function.

The *EGF-CFC* gene family is currently defined by four members: mammalian *Cripto* and *Cryptic*, frog *FRL-1* and zebrafish *one-eyed pinhead (oep)*. The first *EGF-CFC* gene, human *Cripto*, was serendipitously isolated in 1989 as a fusion transcript in a cDNA library screen[1]. Thereafter, mouse *Cripto* was isolated by homology[2]. For many years, these genes were regarded as being distantly related to EGF-like growth factors, such as TGF-α and amphiregulin[3]. Subsequently, functional similarity of EGF-CFC proteins to fibroblast growth factors (FGFs) was suggested by the identification of the *Cripto*-related factor *FRL-1* as a potential activator of the FGF receptor in *Xenopus*[4]. The recognition that *Cripto* and *FRL-1* are members of a distinct gene family resulted from studies of mesoderm formation during mouse gastrulation, which led to isolation of a novel *EGF-CFC* gene named *Cryptic*[5]. Shortly thereafter, positional cloning efforts identified the gene for zebrafish *one-eyed pinhead (oep)*[6], which had originally been identified in genetic screens[7-10].

All *EGF-CFC* genes encode extracellular proteins that share an N-terminal signal sequence, a variant EGF-like motif, a novel conserved cysteine-rich domain named the CFC (*C*ripto, *F*RL-1, and *C*ryptic) motif, and a C-terminal hydrophobic region[5,6] (Fig. 1). The EGF-like motifs possess a characteristic set of six cysteines and other conserved features of EGF motifs, so that they are believed to adopt an EGF-like fold[11]. However, these variant EGF-like motifs also have features unique to the *EGF-CFC* family. For instance, the first two cysteines are adjacent, eliminating the 'A-loop', and the spacing between the third and fourth cysteines is reduced. In addition, the positions of intron–exon boundaries in *EGF-CFC* genes appear to be well-conserved, with the EGF and CFC motifs occupying separate exons,

which suggests that these form distinct protein domains[6,12,13] (Y-T. Yan and M.M. Shen, unpublished).

The sequence conservation in the EGF-CFC family is relatively low, with most of the sequence similarity occurring in the central EGF and CFC motifs. Overall sequence identity is approximately 30% between members in different species, and remarkably low at 48% between the mouse and human Cryptic proteins (Fig. 1). Furthermore, there is no clear ortholog relationship between members of the family in different species – thus, the sequence of Oep appears equidistant from that of Cripto and Cryptic. Notably, no members of the *EGF-CFC* family have been identified in invertebrates thus far. The low overall sequence conservation might suggest that different EGF-CFC proteins have distinct activities, as observed for other gene families. Interestingly, however, all *EGF-CFC* family members appear to have functionally similar activities in assays for phenotypic rescue of *oep* mutants by mRNA microinjection[14] (J. Zhang, W.S. Talbot and A.F. Schier, unpublished).

Genetic analysis of *EGF-CFC* gene function

The essential roles of *EGF-CFC* genes have been established by genetic studies in mouse and zebrafish. In the mouse embryo, the functions of these genes in axis formation are divided, such that *Cripto* is required for germ-layer formation and the correct positioning of the anterior–posterior (A–P) axis, whereas *Cryptic* is necessary for determination of the left–right (L–R) axis[12,13,15,16]. In zebrafish, *oep* is required for all of these processes[13,14].

Cripto

The A–P axis in the mouse is thought to be established by two distinct signaling centers. These inducing regions correspond

Michael M. Shen
mshen@
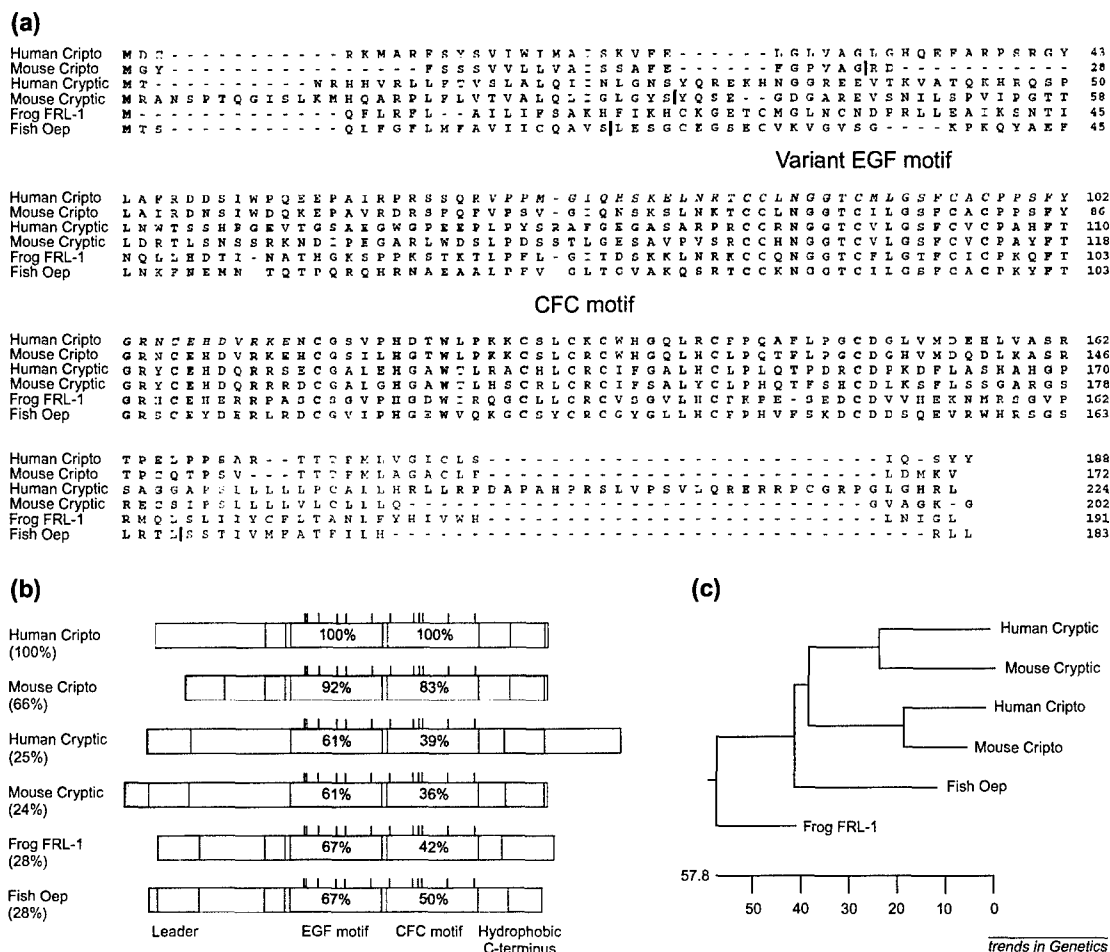cabm.rutgers.edu

Alexander F. Schier*
schier@
saturn.med.nyu.edu

Center for Advanced
Biotechnology and
Medicine and
Department of Pediatrics,
UMDNJ–Robert Wood
Johnson Medical School,
679 Hoes Lane,
Piscataway, NJ 08854,
USA.
*Developmental Genetics
Program, Skirball
Institute of Biomolecular
Medicine, Department of
Cell Biology, New York
University School of
Medicine, New York,
NY 10016, USA.

FIGURE 1. The EGF-CFC family

(a)

Variant EGF motif (top block)

Human Cripto	M D ? - - - - - - - - - - - R K M A R F S Y S V I W T M A ? S K V F F - - - - - - L G L V A G L G H Q E F A R P S R G Y	43
Mouse Cripto	M G Y - - - - - - - - - - - - - F S S S V V L L V A ? S S A F E - - - - - - F G P V A G|R E - - - - - - - - - - -	28
Human Cryptic	M T - - - - - - - - - - - W R H H V R L L F ? V S L A L Q I ? N L G N S Y Q R E K H N G G R E E V T K V A T Q K H R Q S P	50
Mouse Cryptic	M R A N S P T Q G I S L K M H Q A R P L F L V T V A L Q ? ? G L G Y S|Y Q S E - - G D G A R E V S N I L S P V I P G T T	58
Frog FRL-1	M - - - - - - - - - - - - - Q F L R F L - - A I L I F S A K H F I K H C K G E T C M G L N C N D F R L L E A I K S N T I	45
Fish Oep	M T S - - - - - - - - - - - Q I F G F L M F A V I I C Q A V S|L E S G C E G S E C V K V G V S G - - - - X P K Q Y A E F	45

CFC motif (second block)

Human Cripto	L A F R D D S I W P Q E E P A I R P R S S Q R V P P M - G I Q H S K E L N R T C C L N G G T C M L G S F C A C P P S F Y	102
Mouse Cripto	L A I R D N S I W D Q K E P A V R D R S P Q F V P S V - G ? Q N S K S L N K T C C L N G G T C I L G S F C A C P P S F Y	86
Human Cryptic	L N W T S S H P G E V T G S A E G W G P E E P L P Y S R A F G E G A S A R P R C C R N G G T C V L G S F C V C P A H F T	110
Mouse Cryptic	L D R T L S N S S R K N D ? P E G A R L W D S L P D S S T L G E S A V P Y S R C C H N G G T C V L G S F C V C P A Y F T	118
Frog FRL-1	N Q L L H D T I - N A T H G K S P P K S T K T I P F L - G ? T D S K K L N R K C C Q N G G T C F L G T F C I C P K Q F T	103
Fish Oep	L N K F N E M N T Q T P Q R Q H R N A E A A L P F V G L T C V A K Q S R T C C K N G G T C I I G S F C A C P K Y F T	103

CFC motif (third block)

Human Cripto	G R N ? E H D V R K E N C G S V P H D T N L P K K C S L C K C W H G Q L R C F P G A F L P G C D G L V M D E H L V A S R	162
Mouse Cripto	G R N C E H D V R K E H C G S I L H G T N L P K K C S L C R C W H G Q L H C L P Q T F L P G C D G H V M D Q D L K A S R	146
Human Cryptic	G R Y C E H D Q R R S E C G A L E H G A W ? L R A C H L C R C I F G A L H C L P L Q T P D R C D F K D F L A S K A H G P	170
Mouse Cryptic	G R Y C E H D Q R R R D C G A L G H G A W ? L H S C R L C R C I F S A L Y C L P H Q T F S H C D L K S F L S S G A R G S	178
Frog FRL-1	G R ? I C E H E R R P A S C S G V P H G D W ? R Q G C L L C R C V S G V L H C T K F E - S E D C D V V H E K N M R S G V P	162
Fish Oep	G R S C E Y D E R L R D C G V I P H G E W V Q K G C S Y C R C G Y G L L H C F P H V F S K D C D D S Q E V R W H R S G S	163

(fourth block)

Human Cripto	T P E L P P S A R - - T T ? F K I V G I C L S - I Q - S Y Y	188
Mouse Cripto	T P ? Q T P S V - - - T T ? F K L A G A C L F - L D M K V	172
Human Cryptic	S A S G A F ? L L L L L P C A I L H R L L R P D A P A H P R S L V P S V L Q R E R R P C G R P G L G H R L	224
Mouse Cryptic	R E ? S I P ? L L L L V L C L L L Q - G V A G K - G	202
Frog FRL-1	R M Q L S L I I Y C F L T A N L F Y H I V W H - L N I G L	191
Fish Oep	L R T L|S S T I V M F A T F I L H - R L L	183

(b)

	Leader	EGF motif	CFC motif	Hydrophobic C-terminus
Human Cripto (100%)		100%	100%	
Mouse Cripto (66%)		92%	83%	
Human Cryptic (25%)		61%	39%	
Mouse Cryptic (24%)		61%	36%	
Frog FRL-1 (28%)		67%	42%	
Fish Oep (28%)		67%	50%	

(c)

Phylogenetic tree:
- Human Cryptic
- Mouse Cryptic
- Human Cripto
- Mouse Cripto
- Fish Oep
- Frog FRL-1

57.8

Scale: 50 40 30 20 10 0
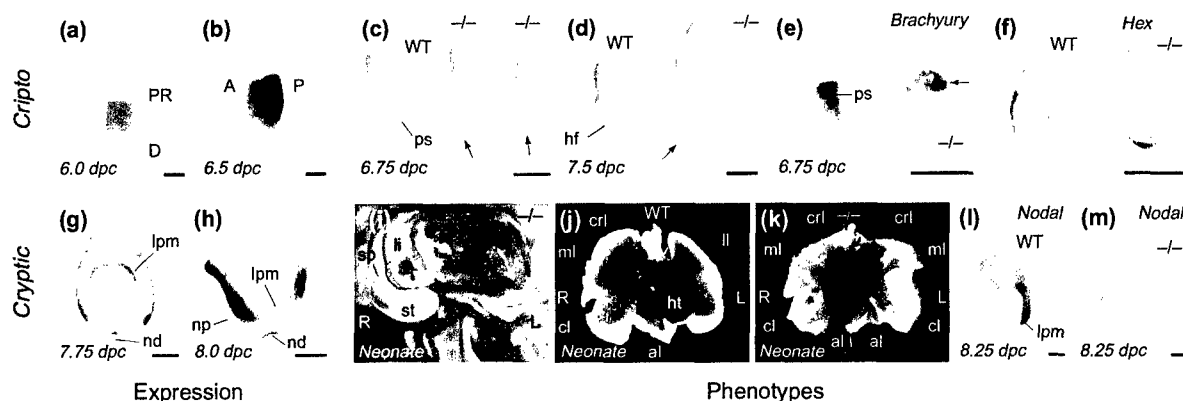
trends in Genetics

(a) Sequence alignment of family members, generated using the CLUSTAL algorithm of the MEGALIGN program (DNASTAR). Amino acid residues conserved among all family members are shaded in orange, while residues conserved among a majority are shaded in blue. The positions of the variant EGF-motif and the novel CFC motif are indicated, and the hydrophobic residues at the C terminus are shown in red. Locations of the predicted sites for N-terminal signal-sequence cleavage are indicated by vertical purple bars; the brown bar indicates the location of the stop codon generated by the *oep[m134]* mutation[6]. The sequence of the 47-mer peptide of human Cripto used in cell culture assays is shown in italics[27]. (b) Schematic illustration of domain structure, with the leader peptides shown in green, C-terminal hydrophobic region in blue, and a short poorly conserved region in pink. (c) Phylogenetic relationships of family members, with scale indicating the number of amino acid substitution events between sequences.

to the anterior visceral endoderm and the distal primitive streak and are required for formation of the head and trunk, respectively. These signaling centers have been proposed by Beddington and colleagues to be localized through coordinate cell movements that rotate a pre-existing proximal–distal axis[17]. The expression of *Cripto* during pre-gastrulation and gastrulation stages is highly dynamic, and is associated with early signs of overt A–P asymmetry (Fig. 2a, b). Prior to gastrulation, *Cripto* expression is initially symmetric and uniform in the epiblast, and then becomes asymmetrically expressed in a proximal–distal gradient, later shifting caudally to the region of the nascent primitive streak[12]. Targeted disruption of *Cripto* results in early post-gastrulation lethality, with homozygous mutants lacking a primitive streak, node and embryonic mesoderm (Fig. 2c, d)[12,16]. Despite the lack of embryonic mesoderm, homozygous mutants are mostly comprised of anterior neuroectoderm, as determined by expression of markers of forebrain and midbrain, but lack more posterior neural tissues[12].

In particular, markers of the presumptive head organizer (such as *Hex* and *Cerberus-like*) are located in the distal visceral endoderm, while markers of the prospective primitive streak (*Brachyury*, *FGF-8*) are localized in the proximal epiblast (Fig. 2e, f). These results provide support for a model of mouse A–P patterning in which the re-positioning of a pre-existing proximo-distal axis generates an orthogonal A–P axis[17].

Cryptic

Recent work has elucidated a L–R pathway starting with an initial symmetry-breaking event in or around the node, followed by propagation to the left lateral plate mesoderm, where *Nodal*, *Lefty2* and *Pitx2* are expressed and regulate subsequent asymmetric morphogenesis[18]. Notably, expression of *Cryptic* is L–R symmetrical in the lateral plate mesoderm, node, notochordal plate and prospective floor plate from head-fold stages through approximately the 6–8 somite stage, and overlaps the

FIGURE 2. Expression patterns and mutant phenotypes for mouse *Cripto* and *Cryptic*

Expression　　　　　　　　　　　　　　Phenotypes

trends in Genetics

(a, b) Expression of *Cripto* in a proximal-distal gradient prior to gastrulation (6.0 days *post coitum*, dpc), which shifts to a posterior-anterior gradient at the time of primitive-streak formation (6.5 dpc). (c) *Cripto* mutants at 6.75 dpc lack a primitive streak and display thickened visceral endoderm at the distal tip (arrows). (d) *Cripto* mutants at 7.5 dpc lack embryonic mesoderm and display ectodermal overproliferation (arrow) that corresponds to anterior neural tissue. (e, f) Marker analysis at 6.75 dpc shows proximal localization of caudal (streak) markers such as *Brachyury*, and distal localization of anterior visceral endoderm markers such as *Hex*. (g, h) Expression of *Cryptic* at head-fold (7.75 dpc) and early-somite stages (8.0 dpc) in the lateral plate mesoderm, node, and notochordal plate. (i) *Cryptic* mutants display randomized abdominal *situs* and hyposplenia. (j, k) Dissected lungs of wild-type littermate and *Cryptic* homozygote, showing right pulmonary isomerism. (l, m) Expression of *Nodal* in the left lateral plate mesoderm is abolished in *Cryptic* mutant embryos at early somite stages. Abbreviations: A, anterior; al, accessory lobe; cl, caudal lobe; crl, cranial lobe; D, distal; hf, head-fold; li, liver; ll, left lung; lpm, lateral plate mesoderm; ml, medial lobe; nd, node; np, notochordal plate; P, posterior; Pr, proximal; ps, primitive streak; sp, spleen; st, stomach.

asymmetric expression of genes in the L–R pathway (Fig. 2g, h)[5]. *Cryptic* mutant mice have defects in nearly all L–R asymmetric morphogenesis, displaying randomized abdominal *situs*, pulmonary right isomerism, and vascular heterotaxia, as well as randomized embryo turning and cardiac looping (Fig. 2i–k)[13,15]. In *Cryptic* mutant embryos, L–R asymmetric expression of *Nodal*, *Lefty2* and *Pitx2* does not occur in the lateral plate mesoderm, while *Lefty1* expression is absent from the prospective floor plate (e.g. Fig. 2l, m). Notably, the L–R asymmetric expression of *Nodal* at the lateral edges of the node is still observed in *Cryptic* mutants, suggesting that L–R specification has occurred in the node but not the lateral plate mesoderm[13,15].

Because *Cripto* and *Cryptic* have similar activities in zebrafish rescue assays[14] (J. Zhang, W.S. Talbot and A.F. Schier, unpublished), it is likely that the differences in biological function between *Cripto* and *Cryptic* are primarily due to their distinct expression patterns. In particular, there is relatively little overlap between the expression patterns of these genes except for the anterior primitive streak and axial mesendoderm (head process) at 6.75–7.25 days *post coitum* (dpc)[5,12]. Neither gene is broadly expressed in embryogenesis following the early somite stages. A potential later role for *Cripto* in cardiac development has been suggested by its expression in the developing outflow tract[2], and the lack of myocardial differentiation in embryoid bodies derived from *Cripto*-deficient embryonic stem cells[19]. The evaluation of such a role will require approaches such as tissue-specific gene targeting.

One-eyed pinhead

Following ubiquitous maternal and zygotic expression, highest levels of *oep* mRNA are found in the gastrula margin[6]. During later stages, *oep* is present in the forebrain, lateral plate and notochord (Fig. 3a, b, f, g). Four types of

oep mutants have been generated[9,10,13,14,20] (Fig 3c, d, h, i). These embryos lack: (i) maternal (M*oep*); (ii) zygotic (Z*oep*); (iii) maternal and zygotic (MZ*oep*); or (iv) late zygotic *oep* activity (LZ*oep*). Whereas maternal mutants develop normally[14], zygotic mutant embryos display cyclopia and lack prechordal mesoderm, endoderm and ventral neuroectoderm[9,10,20]. Loss of both maternal and zygotic *oep* activity results in severe defects in germ-layer formation and axis positioning[14]. These mutants lack head and trunk mesoderm, as well as endoderm, and display a vegetal shift of the A–P axis of the embryo with respect to the extraembryonic yolk. These results reveal that maternal *oep* activity is not required, but masks the early role of zygotic *oep* activity in germ-layer formation. A later role of *oep* is revealed by analysing *oep* mutant embryos whose gastrulation defects have been rescued by mRNA injection[13]. In these embryos, which are otherwise phenotypically normal, the direction of heart looping and the location of the pancreas are randomized with respect to the L–R axis, revealing that loss of late *oep* function leads to heterotaxia (Fig. 3c, j). Furthermore, asymmetric expression of genes on the left side is not established in these mutants, revealing a role for *oep* in the establishment of L–R laterality.

The *oep* mutant phenotypes described above bear remarkable similarity to the phenotypes of *Cripto* and *Cryptic* mutants in mice. The loss of mesoderm and endoderm in maternal-zygotic *oep* mutants (MZ*oep*) is similar to that of *Cripto* mutant mice[14]. Moreover, the A–P axis of these MZ*oep* mutants is displaced relative to the animal–vegetal axis, which supports the idea that *oep* and *Cripto* are both required for A–P axis orientation[12,14]. Conversely, the later role of *oep* in L–R development strongly resembles the requirement for *Cryptic* in the mouse[13]. Taken together, these results indicate that *EGF-CFC* activity is essential for germ-layer formation, and

(a) 1-cell
(b) shield
(c) wt
(d) M*oep*
(e) wt
(f) bud
(g) 8s
(h) Z*oep*
(i) MZ*oep*
(j) LZ*oep*

Expression   Phenotypes
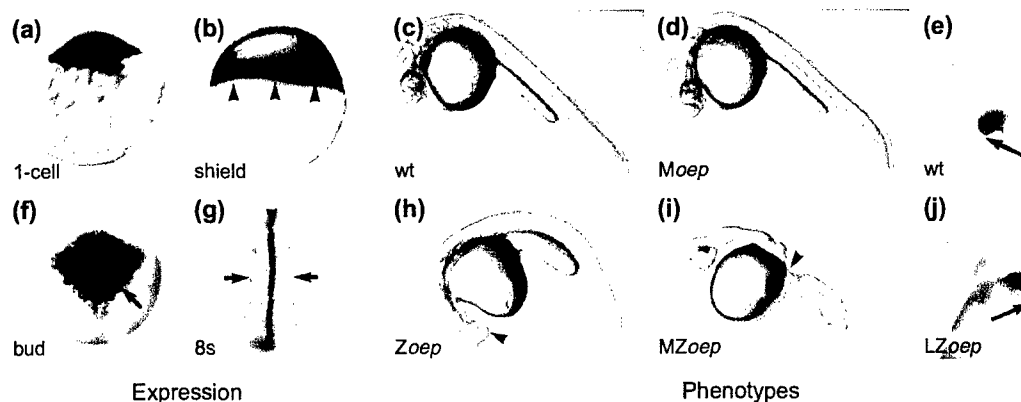
trends in Genetics

(a) Ubiquitous localization of maternal *oep* mRNA at 1-cell stage; lateral view. (b) *oep* expression in mesendodermal precursors in the marginal region (arrowheads) at shield stage; lateral view, dorsal to the right. (f) *oep* expression in presumptive forebrain (arrow) and underlying prechordal mesoderm at bud stage; animal-dorsal view, anterior up. (g) *oep* expression in lateral plate (arrow) and notochord (arrowhead) at 8-somite stage; dorsal view, anterior up. (c) Wild type. (d) Maternal *oep* mutant. (h) Zygotic *oep* mutant. (i) Maternal-zygotic *oep* mutant embryos at 30 hours postfertilization. Arrowheads point to cyclopic eye (h) and posterior border of head (i). (e, j) Heart looping in wild-type and late zygotic *oep* mutants; ventral view, anterior up. (e) Wild-type embryo with heart looping to the right (arrow). (j) Maternal-zygotic *oep* mutant embryos whose early defects were rescued by injection of *oep* mRNA display randomization of laterality. In the example shown, the heart loops to the left (arrow).

both A–P and L–R axis specification, with the roles for *oep* in these processes in fish being divided between the related genes *Cripto* and *Cryptic* in mice.

Cellular localization and cell-autonomous activity of *EGF-CFC* proteins

Members of the *EGF-CFC* family encode extracellular proteins that are localized to the surface of transfected cells[5,6,21]. This association is mediated by the C-terminal hydrophobic domain, which in the case of Cripto is required for glycosyl-phosphatidylinositol (GPI) linkage to the cell membrane[6,21]. Association with the cell surface appears to be important for EGF-CFC protein activity at physiological concentrations, as indicated by the finding that the *oep* mutant allele *oep^{m134}* contains a stop codon that results in truncation of 16 amino acids at the C-terminus[6]. Injection of mRNA corresponding to *oep^{m134}* can rescue the phenotype of *oep* mutants when injected in doses that are tenfold higher than that sufficient for wild type *oep* mRNA[6]. Moreover, injection of *oep^{m134}* mRNA into the extraembryonic yolk syncytial layer can rescue the defects of MZ*oep* mutant embryos, while full-length *oep* mRNA does not[14]. These results indicate that the C-terminal hydrophobic region of EGF-CFC proteins confers association with the cell membrane, most probably through GPI linkage, whereas mutant proteins lacking the C-terminus are diffusible and yet still possess activity.

Additional evidence for a local role of Oep protein comes from chimera analysis experiments. In such experiments, mutant cells are transplanted into wild-type hosts and *vice versa*, and examined for their ability to form cell types that are missing in mutants. These studies have shown that *oep* is required cell-autonomously in the progenitors for prechordal mesoderm, endoderm and floor plate[9,10,14]. Combined with the cellular-localization experiments, these results favor a local, cell-autonomous activity of Oep at the surface of expressing cells.

Potential role for EGF-CFC proteins as signaling factors

Although recent results suggest that EGF-CFC proteins act as cofactors for the TGF-β signal Nodal[14,22,23] (see below), a substantial body of work has previously indicated that Cripto protein can possess intrinsic signaling activity, behaving as a conventional growth factor-like molecule in cell culture assays (reviewed in Ref. 24). Activities of the human *Cripto* gene in tumor cell growth have been extensively studied, starting with the observation that transfection of human *Cripto* confers anchorage-independent growth to transfected NOG-8 mouse mammary epithelial cells[25]. Overexpression of *Cripto* has been found in approximately 80% of primary human breast carcinomas, but not in non-transformed mammary tissue[26]. These and other studies have documented *Cripto* overexpression in human breast, colorectal, gastric, and pancreatic carcinomas (reviewed in Ref. 24). In addition, mitogenic activity on human breast carcinoma cell lines has been shown for human Cripto protein secreted by transfected CHO cells, and for a refolded 47-mer peptide that contains the human Cripto EGF-like motif (but not the CFC motif)[27]. Taken together, these lines of evidence have suggested that *Cripto* is involved in the autocrine or paracrine stimulation of tumor cell growth.

Consistent with a signaling function of human Cripto in cell culture, mouse Cripto might function non-autonomously during development. Chimeric embryos consisting of *Cripto* mutant and wild-type cells display no phenotypic effects in mid-gestation embryos and in neonates, which suggests a non-cell autonomous activity of *Cripto*[16]. However, these experiments lacked a marker such as β-galactosidase to distinguish wild-type from mutant cells at cellular resolution.

Although Cripto was originally considered to represent an EGF-related signaling factor, Cripto protein is unable to bind to any of the four known members of the *ErbB*

receptor family (EGF receptor, c-*erbB-2/neu/HER-2*, c-*erbB-3*, and c-*erbB-4)*. In particular, the high-affinity binding of ^{125}I-labeled refolded Cripto peptide to HC-11 cells is not competed by *erbB* receptor ligands such as EGF, TGF-α, amphiregulin or heregulin β1, and does not stimulate receptor tyrosine phosphorylation in Ba/F3 cells stably transfected with single *erbB* receptor genes or with pair-wise combinations[28]. These results are consistent with the observation that the variant EGF-like motif of EGF-CFC proteins lacks residues essential for high-affinity binding to ErbB receptors, including the residues of the missing 'A loop' between the first two cysteines[11,29].

Despite their inability to bind to ErbB receptors, full-length Cripto and the 47-mer Cripto peptide can both bind with high affinity to a range of mammary epithelial cell lines, including murine HC-11 cells, and they can block HC-11 differentiation in response to lactogenic hormones[28]. Cripto binding results in tyrosine phosphorylation of the SH2-adaptor protein Shc, increased association of Shc with Grb2, and elevated p42/44 mitogen-activated protein kinase (MAPK) phosphorylation, indicating activation of components of the Ras signaling pathway[28]. Interestingly, an intact CFC motif does not appear to be required for activity in this assay, although it is required for rescue of *oep* mutants (J. Zhang, S. Cheng, W.S. Talbot and A.F. Schier, unpublished). More-recent studies have shown that Cripto binding to HC-11 cells results in a rapid tyrosine phosphorylation of the *ErbB4* receptor, which appears to be required for downstream MAPK activation[30]. However, the functional consequences of Cripto addition appear to result from activation of the phosphatidylinositol 3′-kinase (PI3K) pathway, which leads to downstream activation of the Akt protein kinase and inhibition of apoptosis, leading to the proposal that Cripto acts as a survival factor[31]. Finally, crosslinking studies have demonstrated Cripto binding to as yet unidentified 60 kDa and 130 kDa membrane proteins, which have been proposed to represent components of a receptor complex for Cripto[30].

Further complicating these issues, *FRL-1* was isolated on the basis of its ability to induce FGF receptor autophosphorylation in a heterologous yeast expression system[4]. *FRL-1* appears to possess mesoderm and neural-inducing activities in *Xenopus* animal cap assays. In addition, similar to secreted forms of FGF, FRL-1 overexpression induces caudalization of embryos, which can be blocked by expression of a truncated FGF receptor that acts in a dominant-negative manner[4]. Surprisingly, however, the activities of *FRL-1* can also be blocked by a mutant FGF receptor that has no effect *in vivo* or on FGF-mediated signaling, indicating that *FRL-1* does not act through upregulation of the endogenous FGF signaling pathway[4]. Although it has been proposed that FRL-1 represents a novel ligand for FGF receptors, there is no evidence that FRL-1 protein can bind directly to FGF receptors[4].

Interactions of *EGF-CFC* genes with the Nodal signaling pathway

Recently, strong genetic evidence has been provided for a relationship between *EGF-CFC* activity and Nodal signaling[14]. Nodal and its relatives encode members of the TGF-β superfamily and are essential for mesoderm development in mouse, zebrafish and frog[23,32–35]. EGF-CFC proteins appear to act as essential co-factors for Nodal
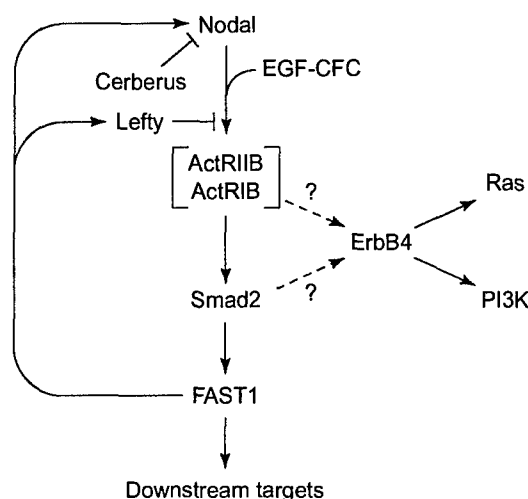
The activity of EGF-CFC proteins as essential co-factors for Nodal results in signaling through the Activin receptors ActRIIA/ActRIIB and ActRIB, leading to activation of Smad2 and subsequent effects on downstream target genes mediated by interaction with the transcription factor FAST1. In zebrafish, an activated form of the type I receptor TARAM-A can also rescue aspects of the zygotic *oep* mutant phenotype[50]. FAST1 also activates autoregulatory loops that upregulate Nodal itself as well as the competitive inhibitor Lefty[22], another member of the TGF-β family, whereas the tri-functional Nodal, BMP and Wnt inhibitor, Cerberus, appears to be largely independent of this autoregulation (reviewed in Ref. 23). The phosphorylation of ErbB4 and consequent activation of Ras and PI3K in response to Cripto could be owing to cross-talk at the level of Activin receptors or Smad2 (dashed arrows).

signaling, based in part on the similarity of phenotypes between MZ*oep* mutants and zebrafish Nodal mutants, and on the requirement of *oep* activity for Nodal signaling[14]. Thus, the phenotype of MZ*oep* mutant fish is virtually identical to that of double mutants for *cyclops (znr-1)* and *squint (znr-2)*[14,34], which encode *Nodal*-related genes[34,36,37]. In addition, the gain-of-function phenotypes induced by *cyclops* or *squint* overexpression are blocked by *oep* mutations[14]. Hence, *oep* is absolutely required for Nodal signaling during germ-layer formation. As all of the currently identified *EGF-CFC* genes can rescue MZ*oep* mutants upon mRNA injection, it is likely that Cripto, Cryptic and FRL-1 can also act as Nodal cofactors[14] (J. Zhang, W.S. Talbot and A.F. Schier, unpublished).

It has been proposed that the combined activity of Oep and Nodal is equivalent to the activity of Activin, another member of the TGF-β family[14]. Specifically, mRNA injection of constitutively activated forms of the Activin receptor ActRIB or the transcription factor Smad2 is able to rescue the MZ*oep* phenotype[14]. Furthermore, injection of mRNA encoding Activin also rescues MZ*oep* mutants, suggesting that Activin can bypass the requirement for *oep* by signaling through similar downstream components as the combination of Nodal and Oep[14]. Combined with the observation that overexpression of *oep* mRNA does not result in any detectable phenotype in fish embryos[6], these results have led to the model that Nodal and EGF-CFC proteins are inactive independently, while their combined activity is equivalent to that of Activin[14] (Fig. 4). A possible

TABLE 1. Expression patterns and functions of members of the *EGF-CFC* gene family

Gene	Species	Expression pattern	Function and mutant phenotype	Refs
Cripto	Mouse	Uniform, then proximal–distal graded expression in epiblast at pre-implantation stages (5.5–6.25 dpc[a]); caudal–rostral gradient in epiblast, newly formed mesoderm at streak stages (6.5–7.0 dpc); cardiac outflow tract at somite stages (8.5–9.5 dpc)	A–P axis positioning: mis-oriented A–P axis, with anterior visceral endoderm markers expressed distally, posterior primitive streak markers proximally; germ-layer formation: lack of primitive streak, embryonic mesoderm, and definitive endoderm.	2, 12
Cryptic	Mouse	Axial mesoderm and lateral plate mesoderm at neural plate stages (7.0–7.5 dpc); node, notochord, prospective floor plate, and lateral plate mesoderm at head-fold and early somite stages (7.5–8.25 dpc)	L–R axis specification: Randomized abdominal *situs*, right pulmonary isomerism, hyposplenia, transposition of the great arteries, vascular heterotaxia, no expression of left-side specific genes in lateral plate mesoderm.	5, 13, 15
FRL-1	Frog	RT–PCR analysis detects low level maternal expression and ubiquitous expression during gastrula stages	Unknown.	4
oep	Fish	Maternal message persists from the one-cell stage to approximately sphere stage (four hours postfertilization). Zygotic expression is uniform until 40% epiboly. Shield stage (six hours): slight dorsal to ventral gradient, predominantly in mesendodermal progenitors at the margin. Gastrulation: axial and paraxial hypoblast, including notochord and prechordal plate, and more weakly in the remainder of the embryo. End of gastrulation (bud stage): highest levels are found in the anlage of the forebrain and axial midline. Somitogenesis: notochord, lateral plate, dorsal diencephalic region including the anlage of the epiphysis.	Maternal *oep* mutants: no phenotype. Zygotic *oep* mutants: lack of endoderm, prechordal plate and ventral neuroectoderm, including floor plate; prechordal plate progenitors transformed into notochord progenitors. Maternal–zygotic *oep* mutants: lack of endoderm and mesoderm of head and trunk; abnormal positioning of the anterior–posterior axis with respect to extraembryonic yolk. Late zygotic *oep* mutants: randomized heart looping and location of pancreas, no expression of left-side specific genes in lateral plate mesoderm.	6, 9, 10, 13, 14, 20

[a]Days *post coitum*.

involvement of Activin receptors and Smad2 in Nodal signaling is also suggested by the phenotype of mouse mutants. Thus, gene targeting experiments have demonstrated similar and/or synergistic phenotypes for targeted gene disruptions of *Nodal*, the type II Activin receptors *ActRIIB* and *ActRIIA*, the type I Activin receptor *ActRIB*, and *Smad2* (reviewed in Ref. 23). Recent work using a *Xenopus* assay system has provided additional support for a combinatorial activity of Nodal and EGF-CFC proteins that leads to the activation of an Activin-like pathway[22]. A putative autoregulatory element in the mouse *Nodal* gene can be efficiently activated by Activin in *Xenopus* animal caps and is bound by an activin response factor (ARF) that consists of Smad2, Smad4 and FAST1. In the presence of the EGF-CFC factors Cripto or Cryptic, Nodal efficiently activates this promoter element and induces ARF formation. These findings lend further support for the signaling pathway model shown in Fig. 4.

Additional evidence for a role of EGF-CFC proteins in Nodal signaling comes from the requirement of both *oep* and *Cryptic* in L–R development. Members of the *Nodal* family have previously been implicated in the pathway for L–R axis formation[38–41] and the laterality defects observed in *EGF-CFC* mutants are consistent with a lack of Nodal signaling[13,15]. Moreover, *Cryptic* mutants have several L–R laterality defects similar to those of *ActRIIB* mutant mice, including right pulmonary isomerism and cardiac defects[42].

Cripto and *Nodal* mutants share common phenotypes, including the absence of embryonic mesoderm and definitive endoderm, consistent with a role for Cripto in Nodal signaling. However, there are also clear differences between the *Cripto* and *Nodal* mutant phenotypes. In particular, chimera studies in mice have indicated a role for extraembryonic *Nodal* in inducing head formation[43]. In contrast, *Cripto* mutants readily form anterior neural tissue[12]. These results suggest that some aspects of Nodal signaling could be independent of the activity of EGF-CFC genes such as *Cripto*. Alternatively, other *EGF-CFC* family

members such as *Cryptic* (or entirely different *EGF-CFC* genes) might partially compensate for lack of *Cripto*, masking the general dependence of Nodal signaling on EGF-CFC co-factors.

Models for EGF-CFC biochemical activity

Based on the requirement of *EGF-CFC* activity for Nodal signaling, the cell autonomy of *oep* function, and the localization of EGF-CFC proteins at the cell surface, it has been suggested that EGF-CFC proteins function in a similar manner to GFRα, IL-6Rα or CTNFRα (Ref. 14). These proteins act as cofactors that mediate the binding of signaling molecules to signal-transducing receptors. For instance, GFRα is tethered to the membrane via a GPI linkage and, together with the c-RET tyrosine kinase receptor, forms a receptor for GDNF, a distant member of the TGF-β superfamily[44,45]. Similarly, IL-6Rα interacts with gp130 to form a receptor complex for IL-6 (Ref. 46). Similar to Oep, these factors are normally membrane associated, and can also act as diffusible co-factors by binding to their ligands and associating with the transmembrane receptors. By analogy, EGF-CFC proteins might interact with Nodal proteins to form a complex that binds to Activin-like receptors. Alternatively, EGF-CFC factors could modify or induce conformational changes in either Nodal signals and/or Activin-like receptors that allow them to interact. Thus, EGF-CFC proteins offer an interesting paradigm to study extracellular factors that allow the functional interaction between a TGF-β signal and its receptors.

How can the role of EGF-CFC proteins in Nodal signaling be reconciled with the suggestion that these factors might be involved in Ras or PI3K signaling pathways? It is conceivable that the cell culture assays using Cripto reveal an additional, Nodal-independent function of EGF-CFC proteins. For instance, many of the effects seen with full-length Cripto protein are also elicited using the isolated EGF motif, perhaps revealing a role of the EGF-related domain in a Ras signaling pathway. However, no evidence

exists for a role of *oep* in *ras* signaling in fish[14]. Moreover, the isolated EGF domain is inactive in the *oep* mutant rescue assay (J. Zhang, W.S. Talbot and A.F.Schier, unpublished). An alternative possibility is that the downstream signaling effects documented for Cripto protein in mammary epithelial cells might represent cross-talk between TGF-β and EGF receptor signaling pathways; some evidence for such cross-talk in the opposite direction has been documented (see model in Fig. 4)[47,48]. Whether such indirect effects represent functional outputs of *EGF-CFC* activity *in vivo* remains to be determined. In the light of the strong genetic evidence that *oep* is essential for Nodal signaling, it is also possible that exposure to Cripto renders mammary epithelial cells responsive to TGF-β signals secreted by the cells or present in the culture medium. In this case, the potential involvement of *Cripto* in cancer formation might be regarded as activation of a TGF-β signaling pathway.

Prospects

The discovery and functional analysis of *EGF-CFC* genes have led to the identification of a hitherto unrecognized role of extracellular co-factors for TGF-β signaling. Further studies will undoubtedly focus on the detailed developmental roles and biochemical interactions of EGF-CFC proteins, Nodal and Activin-like receptors. It will also be important to investigate the possible links between this pathway and the effects that have been documented for Cripto protein in cell-culture assays. Although TGF-β-related factors have been implicated in virtually all aspects of human development and disease, the molecular basis of receptor interaction and activation of downstream signal-transduction pathways for many of these factors has not yet been elucidated[49]. Understanding how EGF-CFC proteins act as co-factors for Nodal signaling will be of broad and fundamental importance for understanding TGF-β signal transduction in general, with potential implications for molecular mechanisms of human disease.

References

1 Ciccodicola, A. *et al.* (1989) Molecular characterization of a gene of the 'EGF family' expressed in undifferentiated human NTERA2 teratocarcinoma cells. *EMBO J.* 8, 1987–1991

2 Dono, R. *et al.* (1993) The murine *cripto* gene: expression during mesoderm induction and early heart morphogenesis. *Development* 118, 1157–1168

3 Riese, D.J. and Stern, D.F. (1998) Specificity within the EGF family/ErbB receptor family signaling network. *BioEssays* 20, 41–48

4 Kinoshita, N. *et al.* (1995) The identification of two novel ligands of the FGF receptor by a yeast screening method and their activity in *Xenopus* development. *Cell* 83, 621–630

5 Shen, M.M. *et al.* (1997) A differential display strategy identifies *Cryptic*, a novel EGF-related gene expressed in the axial and lateral mesoderm during mouse gastrulation. *Development* 124, 429–442

6 Zhang, J. *et al.* (1998) Positional cloning identifies zebrafish *one-eyed pinhead* as a permissive EGF-related ligand required during gastrulation. *Cell* 92, 241–251

7 Driever, W. *et al.* (1996) A genetic screen for mutations affecting embryogenesis in zebrafish. *Development* 123, 37–46

8 Haffter, P. *et al.* (1996) The identification of genes with unique and essential functions in the development of the zebrafish, *Danio rerio. Development* 123, 1–36

9 Schier, A.F. *et al.* (1997) The *one-eyed pinhead* gene functions in mesoderm and endoderm formation in zebrafish and interacts with *no tail. Development* 124, 327–342

10 Strahle, U. *et al.* (1997) one-eyed pinhead is required for development of the ventral midline of the zebrafish (*Danio rerio*) neural tube. *Genes Funct.* 1, 131–148

11 Lohmeyer, M. *et al.* (1997) Chemical synthesis, structural modeling, and biological activity of the epidermal growth factor-like domain of human *Cripto. Biochemistry* 36, 3837–3845

12 Ding, J. *et al.* (1998) *Cripto* is required for correct orientation of the anterior–posterior axis in the mouse embryo. *Nature* 395, 702–707

13 Yan, Y-T. *et al.* (1999) Conserved requirement for *EGF-CFC* genes in vertebrate left–right axis formation. *Genes Dev.* 13, 2527–2537

14 Gritsman, K. *et al.* (1999) The EGF-CFC protein one-eyed pinhead is essential for nodal signaling. *Cell* 97, 121–132

15 Gaio, U. *et al.* (1999) A role of the *cryptic* gene in the correct establishment of the left–right axis. *Curr. Biol.* 9, 1339–1342

16 Xu, C. *et al.* (1999) Abrogation of the Cripto gene in mouse leads to failure of postgastrulation morphogenesis and lack of differentiation of cardiomyocytes. *Development* 126, 483–494

17 Beddington, R.S.P. and Robertson, E.J. (1999) Axis development and early asymmetry in mammals. *Cell* 96, 195–209

18 Burdine, R.D. and Schier, A.F. (2000) Conserved and divergent mechanisms in left–right axis formation. *Genes Dev.* 14, 763–776

19 Xu, C. *et al.* (1998) Specific arrest of cardiogenesis in cultured embryonic stem cells lacking Cripto-1. *Dev. Biol.* 196, 237–247

20 Gritsman, K. *et al.* (2000) Nodal signaling patterns the organizer. *Development* 127, 921–932

21 Minchiotti, G. *et al.* (2000) Membrane-anchorage of Cripto protein by glycosylphosphatidylinositol and its distribution during early mouse development. *Mech. Dev.* 90, 133–142

22 Saijoh, Y. *et al.* (2000) Left–right asymmetric expression of *lefty2* and *nodal* is induced by a signaling pathway that includes the transcription factor FAST2. *Mol. Cell.* 5, 35–47

23 Schier, A.F. and Shen, M.M. (2000) Nodal signalling in vertebrate development. *Nature* 403, 385–389

24 Salomon, D.S. *et al.* (1999) Cripto: a novel epidermal growth factor (EGF)-related peptide in mammary gland development and neoplasia. *BioEssays* 21, 61–70

25 Ciardiello, F. *et al.* (1991) Expression of *cripto*, a novel gene of the epidermal growth factor gene family, leads to *in vitro* transformation of a normal mouse mammary epithelial cell line. *Cancer Res.* 51, 1051–1054

26 Qi, C.F. *et al.* (1994) Expression of transforming growth factor alpha, amphiregulin and cripto-1 in human breast carcinomas. *Br. J. Cancer* 69, 903–910

27 Brandt, R. *et al.* (1994) Identification and biological characterization of an epidermal growth factor-related protein: cripto-1. *J. Biol. Chem.* 269, 17320–17328

28 Kannan, S. *et al.* (1997) Cripto enhances the tyrosine phosphorylation of Shc and activates mitogen-activated protein kinase (MAPK) in mammary epithelial cells. *J. Biol. Chem.* 272, 3330–3335

29 Groenen, L.C. *et al.* (1994) Structure-function relationships for the EGF/TGF-α family of mitogens. *Growth Factors* 11, 235–257

30 Bianco, C. *et al.* (1999) Cripto-1 indirectly stimulates the tyrosine phosphorylation of erbB-4 through a novel receptor. *J. Biol. Chem.* 274, 8624–8629

31 Ebert, A.D. *et al.* (1999) Cripto-1 induces phosphatidylinositol 3'-kinase-dependent phosphorylation of AKT and glycogen synthase kinase 3β in human cervical carcinoma cells. *Cancer Res.* 59, 4502–4505

32 Zhou, X. *et al.* (1993) Nodal is a novel TGF-β-like gene expressed in the mouse node during gastrulation. *Nature* 361, 543–547

33 Conlon, F.L. *et al.* (1994) A primary requirement for nodal in the formation and maintenance of the primitive streak in the mouse. *Development* 120, 1919–1928

34 Feldman, B. *et al.* (1998) Zebrafish organizer development and germ-layer formation require nodal-related signals. *Nature* 395, 181–185

35 Piccolo, S. *et al.* (1999) The head inducer Cerberus is a multifunctional antagonist of Nodal, BMP and Wnt signals. *Nature* 397, 707–710

36 Sampath, K. *et al.* (1998) Induction of the zebrafish ventral brain and floorplate requires cyclops/nodal signalling. *Nature* 395, 185–189

37 Rebagliati, M.R. *et al.* (1998) cyclops encodes a nodal-related factor involved in midline signaling. *Proc. Natl. Acad. Sci. U. S. A.* 95, 9932–9937

38 Levin, M. *et al.* (1995) A molecular pathway determining left–right asymmetry in chick embryogenesis. *Cell* 82, 803–814

39 Collignon, J. *et al.* (1996) Relationship between asymmetric *nodal* expression and the direction of embryonic turning. *Nature* 381, 155–158

40 Lowe, L.A. *et al.* (1996) Conserved left–right asymmetry of nodal expression and alterations in murine situs inversus. *Nature* 381, 158–161

41 Sampath, K. *et al.* (1997) Functional differences among *Xenopus* nodal-related genes in left–right axis determination. *Development* 124, 3293–3302

42 Oh, S.P. and Li, E. (1997) The signaling pathway mediated by the type IIB activin receptor controls axial patterning and lateral asymmetry in the mouse. *Genes Dev.* 11, 1812–1826

43 Varlet, I. *et al.* (1997) *nodal* expression in the primitive endoderm is required for specification of the anterior axis during mouse gastrulation. *Development* 124, 1033–1044

44 Jing, S. *et al.* (1996) GDNF-induced activation of the ret protein tyrosine kinase is mediated by GDNFR-alpha, a novel receptor for GDNF. *Cell* 85, 1113–1124

45 Treanor, J.J. *et al.* (1996) Characterization of a multicomponent receptor for GDNF. *Nature* 382, 80–83

46 Hirano, T. (1998) Interleukin-6. In *The Cytokine Handbook* (3rd edn) (Thomson, A., ed.), pp. 197–228, Academic Press

47 de Caestecker, M.P. *et al.* (1998) Smad2 transduces common signals from receptor serine-threonine and tyrosine kinases. *Genes Dev.* 12, 1587–1592

48 Kretzschmar, M. *et al.* (1999) A mechanism of repression of TGFβ/ Smad signaling by oncogenic Ras. *Genes Dev.* 13, 804–816

49 Massagué, J. (1998) TGF-β signal transduction. *Ann. Rev. Biochem.* 67, 753–791

50 Peyrieras, N. *et al.* (1998) Conversion of zebrafish blastomeres to an endodermal fate by TGF-β-related signaling. *Curr. Biol.* 8, 783–786

DEPARTMENT OF THE ARMY
US ARMY MEDICAL RESEARCH AND MATERIEL COMMAND AND FORT DETRICK
810 SCHRIEDER STREET, SUITE 218
FORT DETRICK, MARYLAND 21702-5000

REPLY TO
ATTENTION OF:

MCMR-RMI-S   (70-1y)   17 Oct 01

MEMORANDUM FOR Administrator, Defense Technical Information
Center (DTIC-OCA), 8725 John J. Kingman Road, Fort Belvoir,
VA   22060-6218

SUBJECT: Request Change in Distribution Statement

1.   The U.S. Army Medical Research and Materiel Command has
reexamined the need for the limitation assigned to technical
reports written for grants.   Request the limited distribution
statements for the Accession Document Numbers listed at enclosure
be changed to "Approved for public release; distribution
unlimited."   These reports should be released to the National
Technical Information Service.

2.   Point of contact for this request is Ms. Judy Pawlus at
DSN 343-7322 or by e-mail at judy.pawlus@det.amedd.army.mil.

FOR THE COMMANDER:

                              PHYLIS M. RINEHART
                              Deputy Chief of Staff for
                                 Information Management

Enclosure